Receptor Modeling of Transport of Acidic Air Pollutants and Oxidants to Forested Regions in the Sierra Nevada

Final Report

Contract No. A932-140

Prepared for:

California Air Resources Board
Research Division
2020 L Street
Sacramento, California 95814

Prepared by:
Alan W. Gertler
Robert F. Harrington
Roger L. Tanner
Judith C. Chow
Zhiqiang Lu
John G. Watson

Desert Research Institute
University and Community College System of Nevada
P. O. Box 60220
Reno, Nevada 89506

Ronald C.Henry
Department of Civil Engineering
USC-BHE
Rm 213, University Park
Los Angeles, California 90089

Daniel Grosjean
DGA, Inc.
4526 Telephone Road, Suite 205
Ventura, California 93003

December 1993

DISCLAIMER

The statements and conclusions in this report are those of the contractor and not necessarily those of the California Air Resources Board. The mention of commercial products, their source or their use in connection with material reported herein is not to be construed as either an actual or implied endorsement of such products.

ABSTRACT

The major source area of acidic species and their precursors which has the potential for impact in the Sierra Nevada is the San Joaquin Valley (SJV). During the summer of 1990, the San Joaquin Valley Air Quality Study (SJVAQS) and Atmospheric Utility Signatures, Predictions and Experiments (AUSPEX) studies, two major, integrated field studies, were performed. These studies provided a basis for extending our knowledge of air pollution effects to regions outside the study area which are affected by emissions from that region. By taking the approach of "piggy-backing" on to the SJVAQS/AUSPEX studies, it was possible to determine the relationship between acidic species and their precursors emitted in the SJV source region and their eventual deposition at susceptible, forested receptor sites in the Sierra Nevada.

There were two main facets to the study. The first involved field measurements that are required as input for the receptor modeling task. The second involved the application of receptor models to apportion sources of atmospheric acidity. Sites included SJVAQS/AUSPEX sites at Sequoia and Yosemite, a site in the vicinity of Tehachapi, and a site on the western slope of the northern Sierra Nevada near Lake Tahoe (Blodgett Experimental Forest). Measurements of gaseous and fine particulate inorganic and organic acidic species were made on 14 days corresponding to the SJVAQS/AUSPEX intensive measurement days.

Observed $PM_{2.5}$ concentrations were generally low, with a median concentration of 8 to 10 $\mu g/m^3$. Organic carbon and sulfate were the major components, accounting for more than 25% of the $PM_{2.5}$ mass.

Formic acid concentrations ranged from approximately 1 ppb to 40 ppb; those of acetic acid ranged from approximately 0.5 ppb to 13 ppb. Mean formic acid concentrations were 18 ppb at Tehachapi and between 12 and 13 ppb at the three other sites. Mean acetic acid concentrations ranged from 3.9 ppb at Blodgett to 8.0 ppb at Yosemite. Comparison of these results with previous studies indicate that carboxylic acid levels measured in the Sierra Nevada are higher than those measured in past studies and, in many cases, average concentrations of both formic and acetic acids observed during this study were greater than the maxima observed in other studies. Compared to levels of strong acids previously measured at Sierra Nevadan sites, organic acids appear to be significant contributors to the overall acidity. The high levels of organic acids measured during this program led to questions being raised regarding the current state of sampling and analysis methods for organic acids. The results of a review of the literature led to the conclusions that sampling is simple but preservation may be a problem, analytical methods are well developed but resolution problems remain, sources of primary emissions of organic acids are still not well characterized in most areas, and improvements in sampling and analysis methods are required before a monitoring network for gaseous- and hydrometeor-phase formic and acetic acids can be established.

The majority of the chemical species required for the model input of the Chemical Mass Balance (CMB) receptor model are well above the detection limits, with the sum of the species over $PM_{2.5}$ mass ratios above 0.5 in most cases. Contributions to the average apportionments were different for all four sites. Local sources had the greatest impact on Blodgett with primary geological material contributing 28% ($1.6 \pm 0.7\ \mu g/m^3$) and primary motor vehicles contributing 22% ($1.4 \pm 0.8\ \mu g/m^3$). Yosemite was dominated by vegetative burning (from both campfires

and forest fires) with results from the CMB calculation showing 6.8 $\pm$ 9.8 $\mu g/m^3$ (43% of $PM_{2.5}$ mass) vegetative burning for the 24 hr average. Motor vehicles contributed 15% of $PM_{2.5}$ mass during the same period. The mid-valley regional and secondary organic carbon sources are the major contributors at the Sequoia Lower Keweah site, which accounts for 55% of the $PM_{2.5}$ mass. Tehachapi appeared to be impacted by emissions both from the SJV and SoCAB. The lower valley regional profile along with primary motor vehicle exhaust were the major contributors at the Tehachapi site, accounting for 31% and 20% of the $PM_{2.5}$, respectively. Secondary ammonium sulfate contributions are high, and vary from 15 to 25 $\mu g/m^3$ depending on the sampling period and day. Unlike any of the other sites, secondary ammonium nitrate accounted for 8% of the $PM_{2.5}$ mass. For the PM_{10} averages at Sequoia and Yosemite, the major difference was the increased contribution of primary geological material. This source accounted for 43% of the mass at Sequoia and 40% of the mass at Yosemite.

The data were also analyzed by Principal Components Analysis (PCA) and the Source Apportionment by Factors with Explicit Restrictions (SAFER) multivariate receptor model. The data sets from each of the four sites showed five major principal components; two related to soil dust and wood smoke, and three related to secondary species: sulfate, nitrate, and nitric acid. The SAFER model was then used to determine the range of possible source compositions of the sources of airborne particles. For example, at the Sequoia site, the data set was found to have only three factors: wood smoke, soil dust, and a source of organic carbon presumably from transport. From the source compositions, it was determined that about 60% of the organic carbon was from transport.

ACKNOWLEDGEMENT

The authors wish to acknowledge the secretarial and technical staff from both DRI and other institutions without which the completion of this work would not have been possible. We thank Ms. Nancy Granata, Ms. Kim Snow, Ms. Bridget Ball, Ms. Dana Dondero, Ms. Barbara Hinsvark, Mrs. Beverly Finley, and Mrs. Ruth Tavernia for typing and editing the document. We would also like to thank William Pierson (DRI) for his helpful comments and Mr. Steve Anderson, Mr. Keith Freeburn, Mr. John Koos, Ms. Delores Lucero (all from ENSR), and Mr. Gary Jones (DRI) for their assistance in field operations, and Mr. Eric Grosjean (DGA) for organic acid analyses. The authors are grateful to the project officers Dr. Nehzat Motellebi, Dr. Praveen Amar, and Dr. Lowell Ashbaugh.

Table of Contents

Section		Page
Disclaimer		ii
Abstract		iii
Acknowledgement		vi
EXECUTIVE SUMMARY		S-1
S.1	Background	S-1
S.2	Project Overview	S-2
S.3	Monitoring Results	S-3
S.4	Organic Acid Results	S-4
S.5	Review of Organic Acid Measurement Methods	S-5
S.6	CMB Modeling Results	S-6
S.7	Multivariate Receptor Modeling	S-8
1.0	INTRODUCTION	1-1
1.1	Background	1-1
1.2	Objectives	1-3
1.3	Project Overview	1-3
1.4	Guide to Report	1-4
2.0	SAMPLER DESIGN AND ANALYTICAL METHODOLOGY	2-1
2.1	Sampling Methods	2-1
2.1.1	Filter Sampling for $PM_{2.5}$, PM_{10}, and Gaseous Species	2-1
2.1.2	Substrate Sampling for Inorganic Acids, Sulfur Dioxide, and Ammonia	2-7
2.2	Analytical Methods and Laboratory Operations	2-14
2.2.1	Substrate Preparation	2-14
2.2.2	Gravimetric Analysis	2-21
2.2.3	X-Ray Fluorescence Analysis for Elements	2-21
2.2.4	Thermal/Optical Carbon Analysis	2-28
2.2.5	Filter Extraction	2-34
2.2.6	Ion Chromatographic Analysis for Chloride, Nitrate, and Sulfate	2-35
2.2.7	Atomic Absorption Spectrophotometric Analysis for Sodium and Potassium	2-38
2.2.8	Automated Colorimetric Analysis for Ammonium	2-39
2.3	Quality Assurance	2-40
2.3.1	Standard Operating Procedures	2-41
2.3.2	Quality Audits	2-42
3.0	AEROSOL MEASUREMENTS	3-1
3.1	Precision	3-2
3.2	Accuracy	3-8
3.3	Data Validation	3-13
3.3.1	$PM_{2.5}/PM_{10}$ Ratios	3-18
3.3.2	Sum of Chemical Species versus Measured Mass	3-22

3.3.3 Physical Consistency 3-27
3.3.4 Ion Balances 3-28
3.4 Statistical Summary of 24-hour Mass and Chemical Concentrations 3-31
3.5 Temporal and Spatial Variations in $PM_{2.5}$ and PM_{10} 3-40
3.6 Temporal Variations of Particulate Nitrate, Nitric Acid, Particulate Ammonium, and Ammonia 3-43
3.7 Temporal Variations of Organic and Elemental Carbon 3-46

4.0 SAMPLING AND ANALYSIS OF ORGANIC ACIDS 4-1
4.1 Experimental Methods 4-1
4.1.1 Sampling Protocol 4-1
4.1.2 Liquid Chromatography Analysis 4-2
4.1.3 Method Performance 4-2
4.1.4 Sampling Periods 4-3
4.2 Results and Discussion 4-4
4.2.1 Ambient Levels of Formic Acid and Acetic Acid 4-4
4.2.2 Comparison with Other Studies 4-9
4.3 Summary 4-17

5.0 MEASUREMENT AND ANALYSIS OF ATMOSPHERIC ORGANIC ACIDS 5-1
5.1 Background 5-1
5.2 Summary of Collection Methods 5-4
5.2.1 Gas-Phase Collection 5-5
5.2.1.1 Impregnated Filters 5-5
5.2.2.2 Impregnated Cartridges and Sorbents 5-6
5.2.2.3 Coated Denuder Tubes 5-7
5.2.1.4 Other Sampling Methods 5-7
5.3 Particle-Phase Collection 5-8
5.4 Dew, Fog and Precipitation Collection 5-9
5.5 Sampling Method Deficiencies--A Summary 5-10
5.6 Summary of Analytical Methods for Organic Acids 5-11
5.6.1 Separation Methods for Organic Acids 5-11
5.6.2 Detection Methods 5-14
5.6.3 Gas Chromatographic Methods With and Without Derivatization 5-14
5.6.4 Other Analytical Methods 5-15
5.6.5 Analytical Method Deficiencies--A Summary 5-15
5.7 Sampling Method Deficiencies 5-16
5.7.1 Interferences During Collection 5-16
5.7.1.1 Peroxyacetyl Nitrate (PAN) Interference with Acetic Acid Determination 5-16
5.7.1.2 Aldehyde Interference with Formic Acetic Acid Determination 5-17
5.7.1.3 Other Potential Interferences 5-17
5.7.2 Collection Efficiencies and Their Variability 5-18
5.7.3 Storage Problems and the Use of Biocides 5-18
5.7.3.1 Gaseous and Particulate Samples 5-18
5.7.3.2 Hydrometeor Samples 5-19
5.8 Ambient Atmospheric Data for Organic Acids 5-20
5.8.1 Data on Formic, Acetic and Other Organic Acids in the Gas Phase 5-20
5.8.2 Data on Less Volatile Organic Acids Found in Particles 5-23

5.8.3 Data on Organic Acids in Dew, Fogs, Clouds and Precipitation 5-23
5.8.3.1 Dew, Fogwater and Cloudwater 5-23
5.8.3.2 Precipitation 5-24
5.8.4 Phase Distribution of Atmospheric Organic Acids 5-25
5.9 Primary and Secondary Sources of Organic Acids 5-27
5.9.1 Direct Emissions of Weak Acids 5-27
5.9.2 Mechanisms of Formation of Secondary Organic Acids 5-27
5.9.3 Source Apportionment of Organic Acids 5-28
5.10 Summary and Recommendations 5-29

6.0 CMB RECEPTOR MODELING 6-1
6.1 Source Profiles 6-1
6.1.1 Particulate Source Types 6-2
6.2 Particulate Source Apportionment 6-23
6.2.1 Chemical Mass Balance Receptor Model 6-23
6.2.2 CMB Application and Validation 6-25
6.2.3 Model Outputs and Performance Measures 6-29
6.2.4 Deviations from Model Assumptions 6-34
6.2.5 Identification and Correction of Model Input Errors 6-36
6.3 Average Source Contribution Estimates 6-36
6.4 Individual Source Contribution Estimates 6-42
6.5 Source Sub-Types 6-50

7.0 MULTIVARIATE ANALYSIS 7-1
7.1 Principal Component Analysis 7-1
7.2 Multivariate Receptor Modeling 7-7
7.3 SAFER Modelling Results 7-10
7.4 Inter-Site Correlations 7-16

8.0 SUMMARY AND CONCLUSIONS 8-1

9.0 REFERENCES 9-1

APPENDIX A - Sierra Nevada Data Base A-1
APPENDIX B - Summary of Sierra Nevada $PM_{2.5}$ and PM_{10} Source Contribution Estimates B-1

List of Tables

		Page
Table 2-1	Sierra Nevada Aerosol Measurements	2-2
Table 2-2	Excitation Conditions of Kevex/DRI X-Ray Fluorescence Analyzer	2-24
Table 2-3	Summary of Standard Operating Procedures Applied in the Sierra Nevada Study	2-43
Table 3-1	Field Blank Concentrations and Precisions (μg/filter) for the $PM_{2.5}$ Front and Backup Filter and Gaseous Samples Collected at the Blodgett Site	3-4
Table 3-2	Field Blank Concentrations and Precisions (μg/filter) for $PM_{2.5}$ Front and Backup Filter and Gaseous Samples Collected at the Tehachapi Site	3-6
Table 3-3	Precision, Lower Quantifiable Limits, and Distribution Statistics for $PM_{2.5}$ Aerosol and Gaseous Species at the Blodgett and Tehachapi Sites	3-9
Table 3-4	Frequency of Occurrence of Field Flags for the $PM_{2.5}$ Aerosol and Gaseous Samples at the Blodgett and Tehachapi Sites	3-14
Table 3-5	Frequency of Occurrence of Laboratory Chemical Analysis Flags for the $PM_{2.5}$ Aerosol and Gaseous Samples at the Blodgett and Tehachapi Sites	3-16
Table 3-6	Linear Regression Statistics of $PM_{2.5}$ and PM_{10} Mass and Chemical Species	3-20
Table 3-7	Statistical Summary of 24-hour $PM_{2.5}$ Measurements Between 7/13/90 and 8/24/90 During the Fourteen SJVAQS/AUSPEX Episode Days	3-32
Table 3-8	Statistical Summary of 24-hour PM_{10} Measurements Between 7/13/90 and 8/24/90	3-36
Table 4-1	Summary of ambient concentrations (ppbv).	4-5
Table 4-2	Ratios of acetic to formic acid concentrations, and daytime to nighttime ratios for formic and acetic acid	4-5
Table 4-3	Summary of previous studies of atmospheric formic and/or acetic acids.	4-10
Table 4-4	Spearman's rank-order correlation coefficients for formic (for) and acetic (ace) acid at Forest Study sites. A small significance level in parentheses indicates a significant correlation.	4-13
Table 4-5	Spearman's rank-order correlation coefficients for daytime and nighttime formic and acetic acids. In parentheses is the probability that the correlation coefficient would have been larger in the event of uncorrelated data, thus, a small probability indicates a significant correlation.	4-14
Table 4-6	Description of sampling locations.	4-16
Table 5-1	Organic Acids Commonly Found in Atmospheric Samples	5-3
Table 5-2	Summary of Measurement Methods for Atmospheric Organic Acids	5-12
Table 5-3	Ambient Gaseous Concentrations of Atmospheric Organic Acids	5-30
Table 6-1	Source Profiles Applied in Sierra Nevada $PM_{2.5}$ and PM_{10} Receptor Modeling	6-4
Table 6-2A	Geological Source Profile SOIL10 - $PM_{2.5}$	6-5
Table 6-2B	Geological Source Profile SOIL10 - PM_{10} and $PM_{2.5}$	6-6
Table 6-3	Motor Vehicle Source Profile PHRD - $PM_{2.5}$	6-12
Table 6-4	Marine Aerosol Source Profile MARO - $PM_{2.5}$	6-14
Table 6-5A	Secondary Sulfate Source Profile AMSUL - $PM_{2.5}$	6-16
Table 6-5B	Secondary Ammonium Nitrate Profile AMNIT - $PM_{2.5}$	6-17
Table 6-5C	Secondary Organic Carbon Source Profile OC - $PM_{2.5}$	6-18
Table 6-6A	Woodsmoke Source Profile BAMAJC - $PM_{2.5}$	6-19
Table 6-6B	Woodsmoke Source Profile WFIREC - $PM_{2.5}$	6-20

Table 6-7A	Regional SJV Source Profile ACA1 - $PM_{2.5}$	6-21
Table 6-7B	Regional SJV Source Profile EDI4 - $PM_{2.5}$	6-22
Table 6-8	Example CMB Output forPM_{10} Collected at Sequoia on August 8, 1990 Between 0000 and 0700 PST	6-30
Table 6-9	Example CMB Output for $PM_{2.5}$ Collected at Sequoia on August 8, 1990 Between 0000 and 0700 PST	6-31
Table 6-10	CMB $PM_{2.5}$ Source Contribution Estimates ($\mu g/m^3$)	6-38
Table 6-11	CMB PM_{10} Source Contribution Estimates ($\mu g/m^3$)	6-39
Table 7-1	Variables Included in the Data Sets	7-3
Table 7-2	Correlations of Sequoia PM_{10} Data	7-4
Table 7-3	Principal Component Analysis of the Correlation Matrix of Yosemite PM_{10} Data	7-5
Table 7-4	Principal Component Analysis of Correlation Matrix of Sequoia PM_{10} Data	7-6
Table 7-5	Range of Source Compositions Determined by SAFER for Sequoia	7-11
Table 7-6	Range of Source Compositions Determined by SAFER for Yosemite	7-11
Table 7-7	Average Chemical Mass Balance Results Using the Perferred Source Profiles	7-12
Table 7-8	Inter-site Correlations for Selected Species	7-17

List of Figures

		Page
Figure 1-1	Locations of sampling sites.	1-5
Figure 2-1	Modified DRI/ERT Sequential Filter Sampler with Bendix 240 Cyclone Preseparator and Aluminum Oxide Coated Nitric Acid Denuders for $PM_{2.5}$ and Sierra Andersen SA-254I Medium Volume PM_{10} Inlet.	2-6
Figure 2-2	Flow Diagram for the PM_{10} Sequential Filter Sampler.	2-8
Figure 2-3	Flow Diagram for the $PM_{2.5}$ Sequential Filter Sampler	2-9
Figure 2-4	Schematic of the Multistage Savillex Filter Holder	2-12
Figure 2-5	Filter Processing and Chemical Activities for Particle Mass, Ammonia, and Nitric Acid Samples.	2-15
Figure 2-6	Major Components of Kevex 700/8000 XRF System (Kevex, 1985).	2-23
Figure 2-7	Example XRF Spectrum.	2-25
Figure 2-8	Block Diagram of DRI/OGC Thermal/Optical Reflectance Carbon Analyzer.	2-30
Figure 2-9	Example Thermal/Optical Reflectance Thermogram.	2-32
Figure 2-10	Example Ion Chromatogram.	2-36
Figure 3-1	Scatterplots of $PM_{2.5}$ Versus PM_{10} Mass Sulfur, and Silicon Concentrations at the Sequoia Lower Research and Yosemite Sites.	3-19
Figure 3-2	Scatterplots of $PM_{2.5}$ Sum of Species Versus Mass, Sulfate Versus Sulfur, Front Versus BAckup Filter Nitrate and Carbon, and Calculated Versus Measured Ammonium at the Blodgett Site.	3-23
Figure 3-3	Scatterplots of $PM_{2.5}$ Sum of Species Versus Mass, Sulfate Versus Sulfur, Front Versus Backup Filter Nitrate and Carbon, and Calculated Versus Measured Ammonium at the Yosemite Site.	3-24
Figure 3-4	Scatterplots of $PM_{2.5}$ Sum of Species Versus Mass, Sulfate Versus Sulfur, Front Versus Backup Filter Nitrate and Carbon, and Calculated Versus Measured Ammonium at the Sequoia Lower Keweah Site.	3-25
Figure 3-5	Scatterplots of $PM_{2.5}$ Sum of Species Versus Mass, Sulfate Versus Sulfur, Front Versus Backup Filter Nitrate and Carbon, and Calculated Versus Measured Ammonium at the Tehachapi Site.	3-26
Figure 3-6a	Time Series Plot pf $PM_{2.5}$ and PM_{10} Mass at the Blodgett and Yosemite Sites.	3-41
Figure 3-6b	Time Series Plot of $PM_{2.5}$ and PM_{10} Mass at the Sequoia Lower Keweah and Techachapi Sites.	3-42
Figure 3-7a	Time Series Plot of $PM_{2.5}$ Nitrate, Volatidized Nitrate, and Nitric Acid at the Blodgett and Yosemite sites.	3-44
Figure 3-7b	Time Series Plot of $PM_{2.5}$ Nitrate, Volatidized Nitrate, and Nitric Acid at the Sequoia Lower Keweah and Tehachapi Sites.	3-45
Figure 3-8a	Time Series Plot of $PM_{2.5}$ Ammonium and Ammonia at the Blodgett and Yosemite Sites.	3-47
Figure 3-8b	Time Series Plot of $PM_{2.5}$ Ammonium and Ammonia at the Sequoia Lower Keweah and Tehachapi Sites	3-48
Figure 3-9a	Time Series of $PM_{2.5}$ Organic and Elemental Carbon at the Blodgett and Yosemite Sites.	3-49

Figure 3-9b	Time Series of $PM_{2.5}$ Organic and Elemental Carbon at the Sequoia Lower Keweah and Tehachapi Sites.	3-50
Figures 4-1a	Daytime formic acid level at sampling sites. Sample period durations indicated at bottom.	4-6
Figure 4-1b	Nighttime formic acid level at sampling sites. Sample period durations indicated at bottom.	4-6
Figure 4-2a	Daytime acetic acid levels at sampling sites. Sample interval durations indicated at bottom.	4-7
Figure 4-2b	Nighttime acetic acid levels at sampling sites. Sample interval durations indicated at bottom.	4-7
Figure 4-3	Histogram of formic acid concentrations for all sites.	4-8
Figure 4-4	Histogram of acetic acid concentrations for all sites.	4-8
Figure 6-1	Pie charts of 24-hour $PM_{2.5}$ source contributions for Sierra Nevada forest sites.	6-40
Figure 6-2	Pie charts of 24-hour PM_{10} source contributions for Sierra Nevada forest sites.	6-41
Figure 6-3	Diurnal source contributions to $PM_{2.5}$ at Sierra Nevada forest sites.	6-43
Figure 6-4	Diurnal source contributions to PM_{10} at Yosemite and Sequoia.	6-45
Figure 6-5	Pie charts of diurnal $PM_{2.5}$ source contribution estimates for Blodgett.	6-46
Figure 6-6	Pie charts of diurnal $PM_{2.5}$ source contribution estimates for Sequoia.	6-47
Figure 6-7	Pie charts of diurnal $PM_{2.5}$ source contribution estimates for Tehachapi.	6-48
Figure 6-8	Pie charts of diurnal $PM_{2.5}$ source contribution estimates for Yosemite.	6-49
Figure 6-9	Pie charts of diurnal PM_{10} source contribution estimates for Sequoia.	6-51
Figure 6-10	Pie charts for diurnal PM_{10} source contribution estimates for Yosemite.	6-52
Figure 7-1	Two-dimensional SAFER plot of Sequoia PM_{10} data for EC, OC, and soil elements.	7-8
Figure 7-2	Predicted versus observed Sequoia PM_{10} reduced total mass	7-14
Figure 7-3	Predicted versus observed Sequoia PM_{10} organic carbon.	7-15
Figure 7-4	Predicted versus observed elemental carbon for Sequoia PM_{10}.	7-15

S.0 EXECUTIVE SUMMARY

This report summarizes the results and findings of DRI's study A932-140 under contract to the California Air Resources Board (ARB) entitled "Receptor Modeling of Acidic Air Pollutants and Oxidants to Forested Regions in the Sierra Nevada."

S.1 Background

The problem of wet and dry acid deposition is one of the primary environmental issues currently being addressed. Most of the studies to date have, however, been performed in the Eastern United States (e. g., the National Acid Precipitation Assessment Program, National Dry Deposition Network, Acid Model Evaluation Study, and Clean Air Status and Trends Network), and little is known about the potential for impact in the highly sensitive mountainous regions of the West. Based on many factors, including soil characteristics, potential buffering capacity, surface water alkalinity, climate, and steepness the Sierra Nevada has been identified as one of the areas with great potential for suffering adverse effects due to acid deposition.

The major source area of acidic species and their precursors which has the potential for impact in the Sierra Nevada is the San Joaquin Valley (SJV). The elements leading to this conclusion were: proximity, lack of topographical barriers, prevailing winds and relatively high emission rates of NO_x and SO_2. During the summer of 1990 (July to September), the San Joaquin Valley Air Quality Study (SJVAQS) and Atmospheric Utility Signatures, Predictions and Experiments (AUSPEX) studies, two major, integrated field studies, were performed. These studies provided a basis for extending our knowledge of air pollution effects to regions outside the study area which are affected by emissions from that region. By taking the approach of

"piggy-backing" on to the SJVAQS/AUSPEX studies, it was possible to determine the relationship between acidic species and their precursors emitted in the SJV source region and their eventual deposition at susceptible, forested receptor sites in the Sierra Nevada.

In order to determine the relationship between sources of atmospheric acidic species and their precursors and the deposition of these species at receptor locations, the scope of work of this study included the following objectives:

- To develop a generalized methodology for estimating the contribution of sources to acid deposition at receptor sites.
- To apportion inorganic and organic acids at selected sites in the Sierra Nevada to sources in the SJV using receptor models.
- To quantify, using receptor models, the day/night differences between sources affecting forest receptor sites.
- To extend the capabilities of receptor models to evaluating the sources of secondary pollutants by determining the chemical profiles of acidic species emitters and estimating how these profiles change from source to receptor.

S.2 Project Overview

There were two main facets to the study. The first involved obtaining the required chemical and meteorological data through field measurements that are required as input for the receptor modeling task. The second involved the application of receptor models to apportion sources of atmospheric acidity. The approach taken is briefly outlined below.

FIELD MEASUREMENTS:

Use was made of existing sites and facilities in order to obtain concurrent ozone and meteorological data. Sites included SJVAQS/AUSPEX sites at Sequoia and Yosemite, a site in the vicinity of Tehachapi, and a site on the western slope of the northern Sierra

Nevada near Lake Tahoe (Blodgett Experimental Forest). Measurements of gaseous and fine particulate inorganic and organic acidic species were made on 14 days corresponding to the SJVAQS/AUSPEX intensive measurement days. The sampling periods were 7/13 - 7/14/90, 7/21 - 7/22/90, 7/27 - 7/29/90, 8/3 - 8/6/90, and 8/22 - 8/24/90. In order to quantify day/night (and the resultant upslope/downslope flow) differences, day/night samples were collected, one from 0700 to 1700 and the other from 1700 to 0700 PDT.

The great majority of gas, aerosol, and meteorological data required for the modeling phase of this study was obtained from the SJVAQS/AUSPEX data base. Measurements made primarily for this study included gas and aerosol sampling at Blodgett and Tehachapi and organic acid measurements at all four sites.

MODELING APPROACH:

Since many of the acidic species of interest in assessing ecological effects such as SO_2, HNO_3, formic acid, and acetic acid are secondary in nature, the corresponding source profile ratios will change during transport from source to receptor. Under these conditions, traditional receptor models which assume nonreactivity of source components fail. To perform the apportionment using receptor modeling changes in the profiles due to reactivity and loss were estimated and both the initial and "aged" profiles used in the Chemical Mass Balance (CMB) receptor model to apportion the sources of acidic species measured at the receptor sites. Principal Components Analysis (PCA) was employed to estimate the balance of chemical sources versus sinks in the SJV using meteorological data. Multivariate Receptor Modeling (MVR) using the Source Apportionment by Factors with Explicit Restrictions (SAFER) model was applied in conjunction with applicable physical constraints to the model predictions.

S.3 Monitoring Results

The four sampling locations were, from north to south, Blodgett Experimental Forest, Yosemite, Giant Forest (Sequoia), and Tehachapi. The sites are roughly equidistant from each other along a line parallel to the axis of the Sierra Nevada at elevations ranging from about 670 m to 1900 m. The elevation, topography, and vegetation are variable between sites. Variability of local environmental conditions between sites raises the question of whether the data recorded at each site reflect local conditions at each site, or regional air pollution patterns. For example, local mobile source emissions (i.e., from within a 5 km radius of the site) were probably

greatest at Tehachapi, and least at Blodgett. The Giant Forest site was situated on an exposed ridge, and may therefore have been affected by topographically controlled thermal convection. The Blodgett site was situated under a 20 m forest canopy, while all other sites were situated in openings.

Observed $PM_{2.5}$ concentrations were generally low, with a median concentration of 8 to 10 $\mu g/m^3$. Organic carbon and sulfate were the major components, accounting for more than 25% of the $PM_{2.5}$ mass.

The majority of the chemical species required for the model input of the Chemical Mass Balance (CMB) receptor model are well above the detection limits, with the sum of the species over $PM_{2.5}$ mass ratios above 0.5 in most cases. Descriptive data analysis to characterize the temporal and spatial variations of $PM_{2.5}$ mass and chemical compositions at the four sampling sites was also performed for the study.

S.4 Organic Acid Results

Formic acid concentrations ranged from approximately 1 ppb to 40 ppb; those of acetic acid ranged from approximately 0.5 ppb to 13 ppb. Mean formic acid concentrations were 18 ppb at Tehachapi and between 12 and 13 ppb at the three other sites. Mean acetic acid concentrations ranged from 3.9 ppb at Blodgett to 8.0 ppb at Yosemite. Formic acid was more abundant at all sites except Yosemite. The August 3 to 6 sampling interval was a period of particularly high carboxylic acid levels throughout the region. The greater diurnal fluctuation of formic acid is reflected in a bimodal appearance of the data, with a lower peak around 9 ppb

consisting mainly of nighttime measurements, and a higher peak around 15 ppb consisting mainly of daytime measurements. The acetic acid histogram did not show bimodality.

Comparison of these results with previous studies indicated that carboxylic acid levels measured in the Sierra Nevada are higher than those measured in past studies. In many cases, average concentrations of both formic and acetic acids observed during this study were greater than the maxima observed in other studies.

In relation to levels of strong acids previously measured at Sierra Nevadan sites, organic acids appear to be significant contributors to the overall acidity. Statistical analysis of the data suggests that formic acid and acetic acid levels are influenced by regional emissions possibly coupled to additional local inputs. The contribution of biogenic and local emissions to the observed levels of formic acid and acetic acid needs to be determined and suggests that further work is warranted to better understand the role of organic acids in the atmospheric environment and their effects on the Sierra Nevada.

S.5 Review of Organic Acid Measurement Methods

The high levels of organic acids measured during this program led to questions being raised regarding the current state of sampling and analysis methods for organic acids. How reliable are the existing ambient air and precipitation data? Can existing methods be improved to the point where network monitoring can be introduced? How well can primary and secondary sources of organic acids be identified with the current information base? Based on these questions, a review of the literature was performed to assess the current state of knowledge regarding measurements of organic acids in ambient air.

The results of this review of the literature led to the following general statements:

- Existing data sets for formic and acetic acids in air and precipitation for rural and remote areas vary widely, e.g.; marine boundary layer gaseous formic acid levels at Mauna Loa Observatory in the range of 0.1-1.0 ppbv have been observed, compared with 0.5-3 ppbv in boundary layer measurements in Austria and Germany, 1-10 ppbv in California's South Coast Air Basin, and levels averaging up to nearly 20 ppbv at elevated sites in the Sierra Nevada. This suggests that, in some cases at least, their wet and dry deposition is significant relative to inorganic acids.

- Sampling of common organic acids on alkaline filters, cartridges, denuders, etc. is relatively simple. Preserving the samples until analysis, and demonstrating the absence of interferences for specific acids is still difficult and problematical.

- Analytical methods using ion exchange, ion exclusion, and related chromatographic techniques are well developed, but issues concerning the resolution of common organic acids on existing columns (hence potential interferences) remain.

- Sources of primary emissions of organic acids are still not well characterized in most areas. Mechanisms of secondary acid formation are generally known but not quantified for given atmospheric conditions.

- Improvements in sampling and analysis methods are required before a monitoring network for gaseous- and hydrometeor-phase formic and acetic acids can be established.

S.6 CMB Modeling Results

The Chemical Mass Balance (CMB) receptor model was applied to this data set to estimate the source contributions to $PM_{2.5}$ using the source profiles identified as follows. No source-specific source profiles were measured for this study.

The potential source types in the study area are: 1) primary geological material; 2) primary motor vehicle exhaust; 3) primary marine aerosol (including NaCl and $NaNO_3$); 4) primary vegetative burning; 5) secondary ammonium sulfate; 6) secondary ammonium nitrate;

7) secondary organic carbon; and 8) regional SJV profiles developed from analysis of SJVAQS/AUSPEX particulate samples.

Contributions to the average apportionments were different for all four sites. Local sources had the greatest impact on Blodgett with primary geological material contributing 28% ($1.6 \pm 0.7\ \mu g/m^3$) and primary motor vehicles contributing 22% ($1.4 \pm 0.8\ \mu g/m^3$). Secondary ammonium sulfate contributed 18% ($1.2 \pm 0.8\ \mu g/m^3$).

Yosemite was dominated by vegetative burning (from both campfires and forest fires). Results from the CMB calculation showed $6.8 \pm 9.8\ \mu g/m^3$ (43% of $PM_{2.5}$ mass) vegetative burning for the 24 hr average. Motor vehicles contributed $2.4 \pm 1.1\ \mu g/m^3$ (15% of $PM_{2.5}$ mass) during the same period. Primary geological material, secondary organic carbon, and secondary ammonium sulfate are other significant sources, contributing 11% to 14% (1.7 to 2.3 $\mu g/m^3$) of the $PM_{2.5}$ mass.

The mid-valley regional and secondary organic carbon sources are the major contributors at the Sequoia Lower Keweah site, which accounts for 55% of the $PM_{2.5}$ mass. Secondary ammonium sulfate contributed $1.4 \pm 0.7\ \mu g/m^3$, primary motor vehicle and vegetative burning both contributed approximately 1 $\mu g/m^3$, whereas primary geological material contributed $0.2 \pm 0.4\ \mu g/m^3$, with $PM_{2.5}$ mass being 10.9 $\mu g/m^3$ over the sampling period.

Tehachapi appeared to be impacted by emissions both from the SJV and SoCAB. The lower valley regional profile along with primary motor vehicle exhaust were the major contributors at the Tehachapi site, accounting for 31% and 20% of the $PM_{2.5}$, respectively. Secondary ammonium sulfate contributions are high, and vary from 15 to 25 $\mu g/m^3$ depending

on the sampling period and day. Unlike any of the other sites, secondary ammonium nitrate accounted for 8% of the $PM_{2.5}$ mass.

For the PM_{10} averages at Sequoia and Yosemite, the major difference was the increased contribution of primary geological material. This source accounted for 43% of the mass at Sequoia and 40% of the mass at Yosemite.

Detailed CMB source contribution estimates for each sampling period at each of the four sampling sites are reported as an appendix of the report. To summarize the CMB results, the major sources of particulates at Blodgett were of local origin (geological and motor vehicle), Yosemite and Sequoia were best described by a regional (SJV) source profile and secondary organic carbon, while Tehachapi was impacted by both regional and local (motor vehicle) sources. The highest loadings occurred at Yosemite during a forest fire and for that sampling period the results were dominated by the vegetative burning contribution.

S.7 Multivariate Receptor Modeling

The data were also analyzed by Principal Components Analysis (PCA) and the Source Apportionment by Factors with Explicit Restrictions (SAFER) multivariate receptor model. All types of multivariate analysis require two things: data from as many sampling periods as possible, and all the air quality variables be present for each sampling period in the analysis. Thus, to meet these two somewhat contradictory goals, the data were screened to eliminate variables with too many missing values. The selection of variables which gives the largest number of complete time periods, while retaining the most variables was determined for each site. The final data sets contained between 18 and 25 variables and about 50 sampling periods

for each site. Experience has shown that for air quality data, 60-100 sampling periods is preferable; with fewer data points, the influence of error becomes greater and the results are less certain.

Air quality particulate and gas data are typically highly intercorrelated. The purpose of the PCA was to determine the overall structure of the data; i.e., to look for intercorrelations and relationships between the variables which can be explained by transport, common sources, chemical transformation, or other processes. The PCA identified those groups of correlated air quality variables that were statistically independent and explain the majority of the co-variation seen in the data. The data sets from each of the four sites showed five major principal components; two related to soil dust and wood smoke, and three related to secondary species: sulfate, nitrate, and nitric acid.

The SAFER model was then used to determine the range of possible source compositions of the sources of airborne particles. For example, at the Sequoia site, the data set was found to have only three factors. A graphical version of the SAFER model was applied to determine the range of composition of the three sources: wood smoke, soil dust, and a source of organic carbon presumably from transport. From the source compositions, it was determined that about 60% of the organic carbon was from transport. This is a significant amount, since at least 50% of the fine particle mass is from organic carbon at Sequoia.

1.0 INTRODUCTION

This report summarizes the results and findings of DRI's study #A932-140 under contract to the California Air Resources Board (ARB) entitled "Receptor Modeling of Acidic Air Pollutants and Oxidants to Forested Regions in the Sierra Nevada."

1.1 Background

The problem of wet and dry acid deposition is one of the primary environmental issues currently being addressed. Most of the studies to date have, however, been performed in the Eastern United States (e.g., the National Acid Precipitation Assessment Program, National Dry Deposition Network, Acid Model Evaluation Study, and Clean Air Status and Trends Network) and little is known about the potential for impact in the highly sensitive mountainous regions of the West. Based on many factors, including soil characteristics, potential buffering capacity, surface water alkalinity, climate, and steepness Roth, et al. (1985) identified the Sierra Nevada as one of the areas with great potential for suffering adverse effects due to acid deposition.

The major source area of acidic species and their precursors that has the potential for impact in the Sierra Nevada is the San Joaquin Valley (Daly, 1989). The elements leading to this conclusion were: proximity, lack of topographical barriers, prevailing winds and relatively high emission rates of NO_x and SO_2.

During the summer of 1990 (July to September) the San Joaquin Valley Air Quality Study (SJVAQS) and Atmospheric Utility Signatures, Predictions and Experiments (AUSPEX) studies, two major, integrated field studies, were performed. The study region included the San Joaquin Valley (SJV) and surrounding areas. These studies were designed to determine the causes of

exceedances of ozone air quality standards in the SJV and to provide a data base for the evaluation of air quality models for assessing not only ozone but also PM_{10}, visibility, and acid deposition (Blumenthal et al., 1989) in the area. The measurements and subsequent analyses provided by these studies were designed to increase our fundamental understanding of the sources, chemistry, meteorology, and deposition of gaseous and particulate pollutants in the SJV. Through this understanding it is hoped to achieve the eventual goal of improving air quality management strategies in the area.

These studies obtained a tremendous amount of air quality data that were the necessary input for use in air quality models. The measurement and management approach along with technical background for the studies are described in volume of collected papers edited by Solomon (1993). The data are available from the Air Resources Board SARMAP data manager.

In gathering these data and developing a modeling plan for the region (Solomon, 1993), these studies provided a basis for extending our knowledge of air pollution effects to regions outside the study area that are affected by emissions from that region. By carrying out this proposed study, it was possible to determine the relationship between acidic species and their precursors emitted in the SJV source region and their eventual deposition at susceptible, forested receptor sites in the Sierra Nevada.

The approach of "piggy backing" this study on the much larger SJVAQS and AUSPEX programs enabled one to use the extensive meteorological and chemical data bases and modeling results obtained from these studies to achieve the proposed objectives at minimal cost.

1.2 Objectives

Among the goals and objectives contained in ARB's Five-Year Research Plan for acid deposition research is to figure out the relationship between sources of atmospheric acidic species and their precursors and the deposition of these species at receptor locations. This source attribution is critical if decisions are to be made on how to regulate the emission of acidic species and those that lead to their formation in the atmosphere.

In order to address this goal and others that are used for assessing the sources, transport, transformation, deposition, and effects of atmospheric acidity, the scope of work included the following objectives:

- To develop a generalized methodology for estimating the contribution of sources to acid deposition at receptor sites.
- To apportion inorganic and organic acids at selected sites in the Sierra Nevada to sources in the SJV using receptor models.
- To quantify, using receptor models, the day/night differences between sources affecting forest receptor sites.
- To extend the capabilities of receptor models to evaluating the sources of secondary pollutants by determining the chemical profiles of acidic species emitters and estimating how these profiles change from source to receptor.

1.3 Project Overview

There were two main facets to the study. The first involved obtaining the required chemical and meteorological data through field measurements that are required as input for the receptor modeling task. The second involved the application of receptor models to apportion sources of atmospheric acidity. What was the technical approach required to accomplish this

and achieve the objectives of this study? The approach taken is briefly outlined below and in greater detail in the sections that follow.

FIELD MEASUREMENTS:
Use was made of existing sites and facilities to obtain concurrent ozone and meteorological data. Sites, shown in Figure 1-1, included SJVAQS/AUSPEX sites at Sequoia and Yosemite, a site near Tehachapi, and a site on the western slope of the northern Sierra Nevada near Lake Tahoe (Blodgett Experimental Forest). Measurements of gaseous and particulate inorganic and organic acidic species were made on fourteen days corresponding to the SJVAQS/AUSPEX intensive measurement days. To quantify day/night (and the resultant upslope/downslope flow) differences, day/night samples were collected.

The great majority of gas, aerosol, and meteorological data required for the modeling phase of this study was obtained from the SJVAQS/AUSPEX data base. Measurements made primarily for this study included gas and aerosol sampling at Blodgett and Tehachipi and organic acid measurements at all four sites.

MODELING APPROACH:
Since many of the acidic species of interest in assessing ecological effects such as HNO_3, formic acid, and acetic acid are secondary in nature, the corresponding source profile ratios will change during transport from source to receptor. Under these conditions, traditional receptor models that assume nonreactivity of source components fail (Malm et al., 1989). To perform the apportionment using receptor modeling changes in the profiles due to reactivity and loss were estimated and both the initial and "aged" profiles used in the Chemical Mass Balance (CMB) receptor model to apportion the sources of acidic species measured at the receptor sites. Multivariate Receptor Modeling (MVR) (Henry et al., 1984) using the Source Apportionment by Factors with Explicit Restrictions (SAFER) model (Henry and Kim (1989) were applied in conjunction with applicable physical constraints to the model predictions to determine the sources of ambient particulates and gaseous species observed at the four sites.

1.4 Guide to Report

Section 1 presents a brief overview of the research performed in the "Receptor Modeling of Acidic Air Pollutants and Oxidants to Forested Regions in the Sierra Nevada" program. The design and operation of the ambient sampling equipment and analytical methodology are presented in Section 2. Section 3 contains a description of the network along with a descriptive

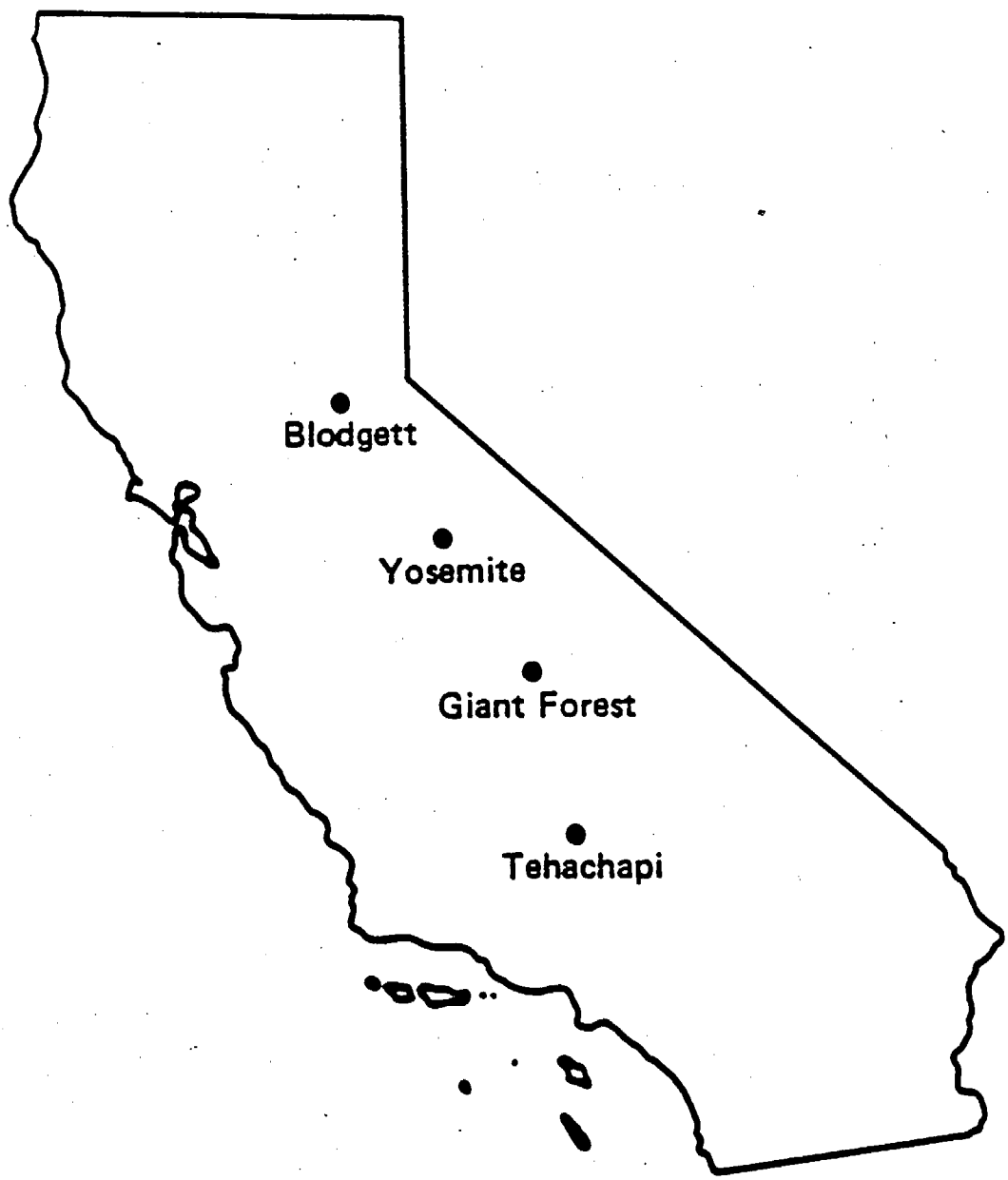

Figure 1-1 Locations of sampling sites.

analysis of the monitoring results. Sampling and analytical methods for the collection and analysis of organic acids are described in Section 4 along with a comparison of observed results from previous studies. A review of methods and procedures for determining ambient levels of organic acids is presented in Section 5. The results of CMB modeling of the observed particulate levels at the four sites is contained in Section 6, while Section 7 contains the results of multivarite analysis of the data. Section 8 summaries' the report and includes recommendations for future work. References are contained in Section 9. The data base structure for validated particulate and gas data and the data base structure for the particulate source profile library are outlined in Appendices A and B, respectively.

2.0 SAMPLER DESIGN AND ANALYTICAL METHODOLOGY

2.1 Sampling Methods

This section describes each of the sampling methods listed in Table 2-1. Watson et al. (1988a), in their planning for the SCENIC Denver visibility study, examined a large number of alternative methods for gas and aerosol sampling. These methods were applied in that study and, where they were successful, they are used in this study.

2.1.1 Filter Sampling for $PM_{2.5}$, PM_{10}, and Gaseous Species

Two types of sequential filter samplers were used in this study to collect $PM_{2.5}$ and PM_{10}. The primary difference between the two was the nature of the inlet. The $PM_{2.5}$ sampler used a Bendix 240 cyclone to separate the fine particulate fraction while the PM_{10} sampler used a Sierra Anderson SA-254 inlet to separate the coarse size fraction. The filter sampler is depicted in Figure 2-1. The sampler is very similar to the particle sampler use in CADMP.

The PM_{10} or $PM_{2.5}$ size fraction is transmitted through the size-selective inlet and into a plenum. The flow rate is controlled by maintaining a constant pressure across a valve with a differential pressure regulator. This flow rate can be adjusted from 5 to approximately 40 ℓ/min, while maintaining a total flow rate of 113 ℓ/min through the inlet. Flow rates of 20 ℓ/min are selected for this study because they provide adequate sample loadings for analysis without overloading the filters. This flow rate is drawn through each of the two filter packs simultaneously. The remaining flow rate of 73 ℓ/min needed by the inlet is drawn through a makeup air port. Flow rates are set with a calibrated rotameter and are monitored with the same

Table 2-1

Sierra Nevada Aerosol Measurements

Measurement	Sampling Sites	Averaging Time	Sample Frequency and Period	Measurement Method/Instrument
$PM_{2.5}$ Particles (0 to 2.5 μm)	Blodgett Yosemite[a] Sequoia Lower Keweah[a] Tehachapi	0001 to 0700 PDT. 0701 to 1200 PDT. 1201 to 1700 PDT. 1701 to 2400 PDT.	4 times/day for 14 episodic days from 7/13/90 through 8/24/90[b]	DRI Modified Sequential Filter Sampler (SFS) with Bendix 240 Cyclone and Aluminum Oxide HNO_3 Denuders
Ammonia (NH_3), Sulfur Dioxide (SO_2), and Nitric Acid (HNO_3)	Blodgett Yosemite[a] Sequoia Lower Keweah[a] Tehachapi	0001 to 0700 PDT. 0701 to 1200 PDT. 1201 to 1700 PDT. 1701 to 2400 PDT.	4 times/day for 14 episodic days from 7/13/90 through 8/24/90	DRI Modified Sequential Filter Pack Sampler with PFA-coated Bendix 240 Cyclone Inlet and Plenum using the Denuder Difference Method and Impregnated Filters
$PM_{2.5}$ Particle Mass	Blodgett Yosemite[a] Sequoia Lower Keweah[a] Tehachapi	0001 to 0700 PDT. 0701 to 1200 PDT. 1201 to 1700 PDT. 1701 to 2400 PDT.	4 times/day for 14 episodic days from 7/13/90 through 8/24/90	Gravimetric Analysis on Teflon Filters (Cahn 31 Electro-microbalance)
$PM_{2.5}$ Particle b_{abs}	Blodgett Yosemite[a] Sequoia Lower Keweah[a] Tehachapi	0001 to 0700 PDT. 0701 to 1200 PDT. 1201 to 1700 PDT. 1701 to 2400 PDT.	4 times/day for 14 episodic days from 7/13/90 through 8/24/90	Light Attenuation on Teflon Filters (TBX 10 Densitometer)

Table 2-1 (continued)

Sierra Nevada Aerosol Measurements

Sampling Measurement	Averaging Sites	Sample Frequency Time	Measurement and Period	Method/Instrument
$PM_{2.5}$ Particle Elements	Blodgett Yosemite[a] Sequoia Lower Keweah[a] Tehachapi	0001 to 0700 PDT. 0701 to 1200 PDT. 1201 to 1700 PDT. 1701 to 2400 PDT.	4 times/day for 14 episodic days from 7/13/90 through 8/24/90	X-ray Fluorescence Analysis on Teflon Filters (Kevex 0700/8000 XRF Analyzer)
$PM_{2.5}$ Particle Chloride (Cl^-), Nitrate (NO_3^-), and Sulfate ($SO_4^=$)	Blodgett Yosemite[a] Sequoia Lower Keweah[a] Tehachapi	0001 to 0700 PDT. 0701 to 1200 PDT. 1201 to 1700 PDT. 1701 to 2400 PDT.	4 times/day for 14 episodic days from 7/13/90 through 8/24/90	Ion Chromatographic Analysis on Quartz-fiber Filter Extracts and Nylon Backup Filter Extracts (Dionex 2020i Ion Chromatograph)
Water Soluble $PM_{2.5}$ Particle Sodium (Na^+) and Potassium (K^+) Ions	Blodgett Yosemite[a] Sequoia Lower Keweah[a] Tehachapi	0001 to 0700 PDT. 0701 to 1200 PDT. 1201 to 1700 PDT. 1701 to 2400 PDT.	4 times/day for 14 episodic days from 7/13/90 through 8/24/90	Atomic Absorption Spectrophotometry on Quartz-fiber Filter Extracts (Perkin-Elmer Model 2380)

Table 2-1 (continued)

Sierra Nevada Aerosol Measurements

Sampling Measurement	Averaging Sites	Sample Frequency Time	Measurement and Period	Method/Instrument
$PM_{2.5}$ Particle Ammonium (NH_4^+)	Blodgett Yosemite[a] Sequoia Lower Keweah[a] Tehachapi	0001 to 0700 PDT. 0701 to 1200 PDT. 1201 to 1700 PDT. 1701 to 2400 PDT.	4 times/day for 14 episodic days from 7/13/90 through 8/24/90	Technicon Automatic Colorimetry on Quartz-fiber Filter Extracts (TRAACS 800 System)
$PM_{2.5}$ Particle Organic and Elemental Carbon (high and low temperature OC and EC)	Blodgett Yosemite[a] Sequoia Lower Keweah[a] Tehachapi	0001 to 0700 PDT. 0701 to 1200 PDT. 1201 to 1700 PDT. 1701 to 2400 PDT.	4 times/day for 14 episodic days from 7/13/90 through 8/24/90	Thermal/Optical Reflectance Carbon Analysis on Pre-fired Quartz-fiber and Quartz-fiber Back-up Filters (DRI/OGC Thermal/Optical Reflectance Carbon Analyzer)
Sulfur Dioxide (SO_2)	Blodgett Yosemite[a] Sequoia Lower Keweah[a] Tehachapi	0001 to 0700 PDT. 0701 to 1200 PDT. 1201 to 1700 PDT. 1701 to 2400 PDT.	4 times/day for 14 episodic days from 7/13/90 through 8/24/90	Ion Chromatographic Analysis on Potassium Carbonate (K_2CO_3) Impregnated Whatman 41 Cellulose-fiber Filter Extracts (Dionex 2020i Ion Chromatograph)

Table 2-1 (continued)

Sierra Nevada Aerosol Measurements

Sampling Measurement	Averaging Sites	Sample Frequency Time	Measurement and Period	Method/Instrument
Denuder Difference Nitric Acid (HNO_3)	Blodgett Yosemite[a] Sequoia Lower Keweah[a] Tehachapi	0001 to 0700 PDT. 0701 to 1200 PDT. 1201 to 1700 PDT. 1701 to 2400 PDT.	4 times/day 15 episodic days from 7/13/90 through 8/24/90	Ion Chromatographic Analysis on Nylon Back-up Filter Extracts (Dionex 2020i Ion Chromatograph)
Ammonia (NH_3)	Blodgett Yosemite[a] Sequoia Lower Keweah[a] Tehachapi	0001 to 0700 PDT. 0701 to 1200 PDT. 1201 to 1700 PDT. 1701 TO 2400 PDT.	4 times/day for 14 episodic days from 7/13/90 through 8/24/90	Automated Colorimetric Analysis on Citric Acid Impregnated Whatman 41 Cellulose-fiber Filter Extracts (TRAACS 800 System)

[a] Part of the SJVAQS/AUSPEX sites.

[b] The fourteen sampling days were:

- 7/13/90 and 7/14/90
- 7/21/90 and 7/22/90
- 7/27/90 to 7/29/90
- 8/3/90 to 8/6/90
- 8/22/90 to 8/24/90

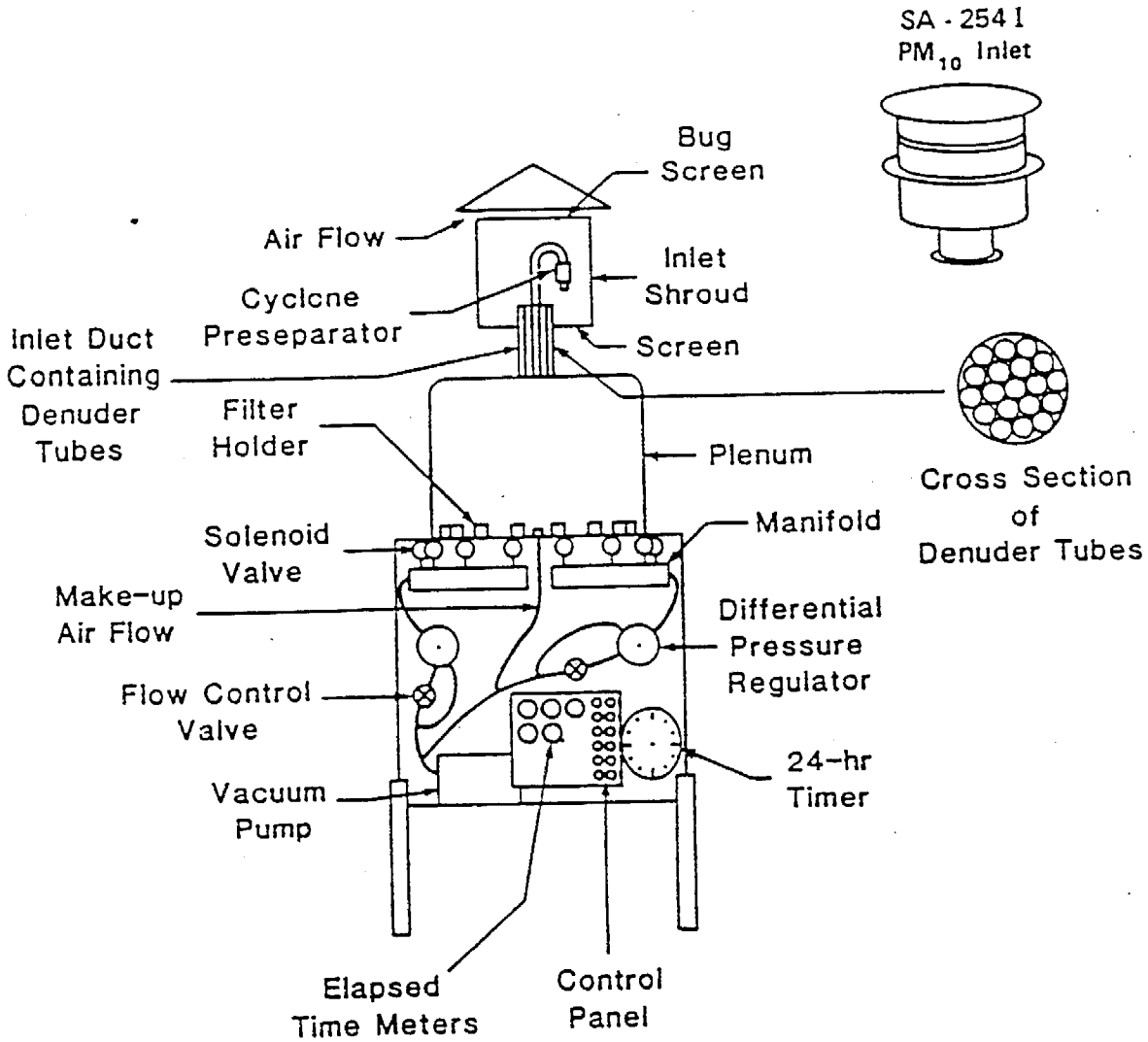

Figure 2-1. Modified DRI/ERT Sequential Filter Sampler with Bendix 240 Cyclone Preseparator and Aluminum Oxide Coated Nitric Acid Denuders for $PM_{2.5}$ and Sierra Andersen SA-254I Medium Volume PM_{10} Inlet.

rotameter at each sample changeout. The sequential sampling makes it unnecessary to have an operator present at every sample changing interval.

The PM_{10} and $PM_{2.5}$ filter configuration is illustrated in Figures 2-2 and 2-3, respectively. A Teflon-membrane filter backed by a drain disk (TT filter pack) is used for mass and elemental analysis. The deposit on the quartz filter (TQ filter pack) is submitted for ion and carbon analyses. The nylon filter allows the magnitude of volatilized particulate nitrate to be determined and added to the nitrate measurement on the front filter to obtain total particulate nitrate. A set of nitric acid denuder tubes removes gaseous nitric acid from the airstream. Watson et al. (1988b; 1988c) show that these tubes remove more than 95% of gaseous nitric acid from the airstream. With this measurement, coarse particle nitrate concentrations can be obtained.

Filter packs are loaded in the laboratory and shipped under refrigeration to and from the field. This minimizes contamination of filters which always occurs when they are loaded and unloaded from filter holders in the field.

Each sampler is serviced by: 1) verifying and recording post-sampling flow rates; 2) recording elapsed sample time; 3) removing exposed filters; 4) installing unexposed filters; 5) verifying and recording pre-sampling flow rates; and 6) resetting the timer. Inlets are cleaned every two weeks, and pump exhaust filters are changed every two months.

2.1.2 Substrate Sampling for Inorganic Acids, Sulfur Dioxide, and Ammonia

Nitric acid deposits on just about any surface and has a high reactivity with coarse, alkaline particles. Nitric acid is most commonly determined by the difference between total

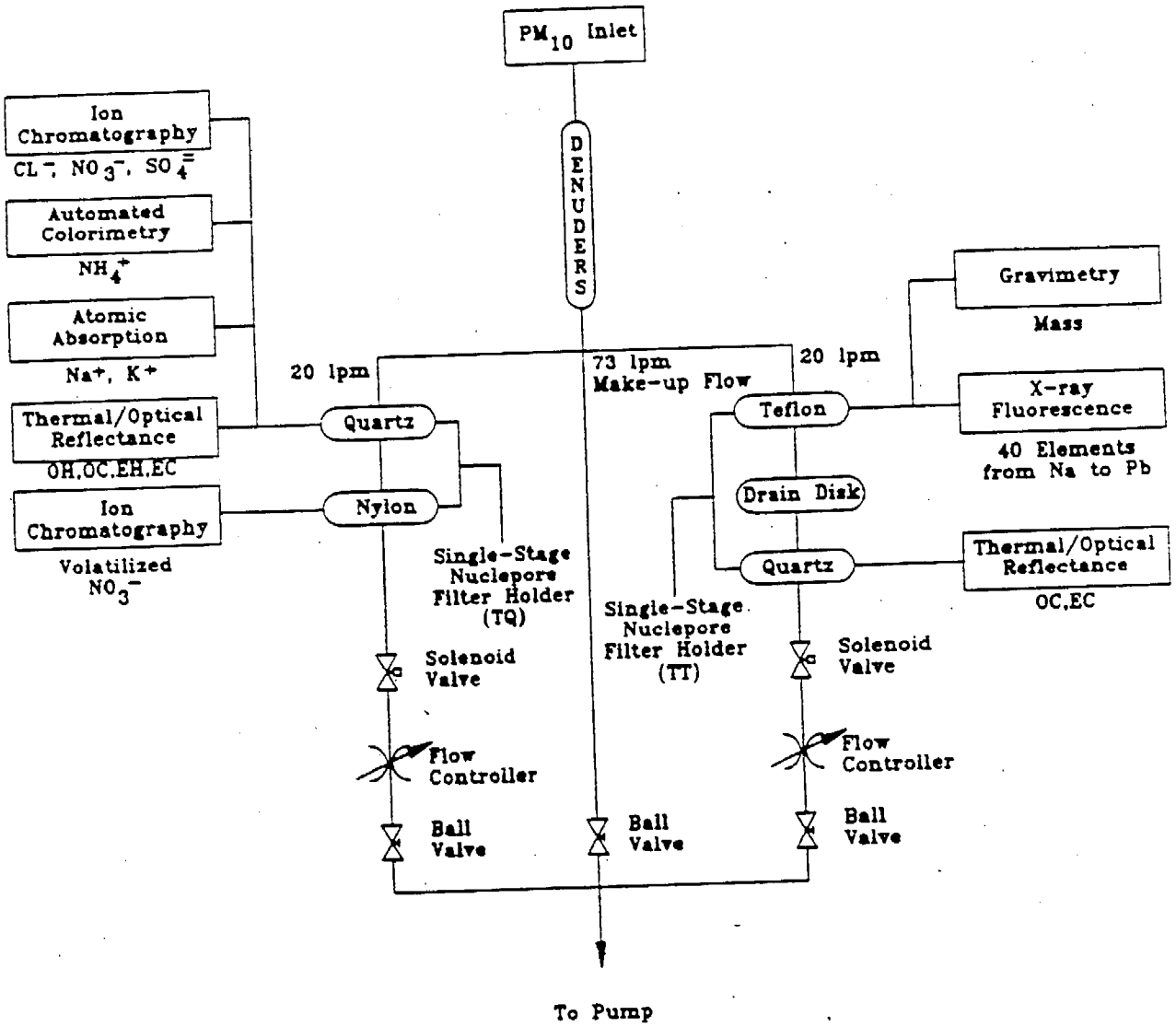

Figure 2-2. Flow Diagram for the PM_{10} Sequential Filter Sampler.

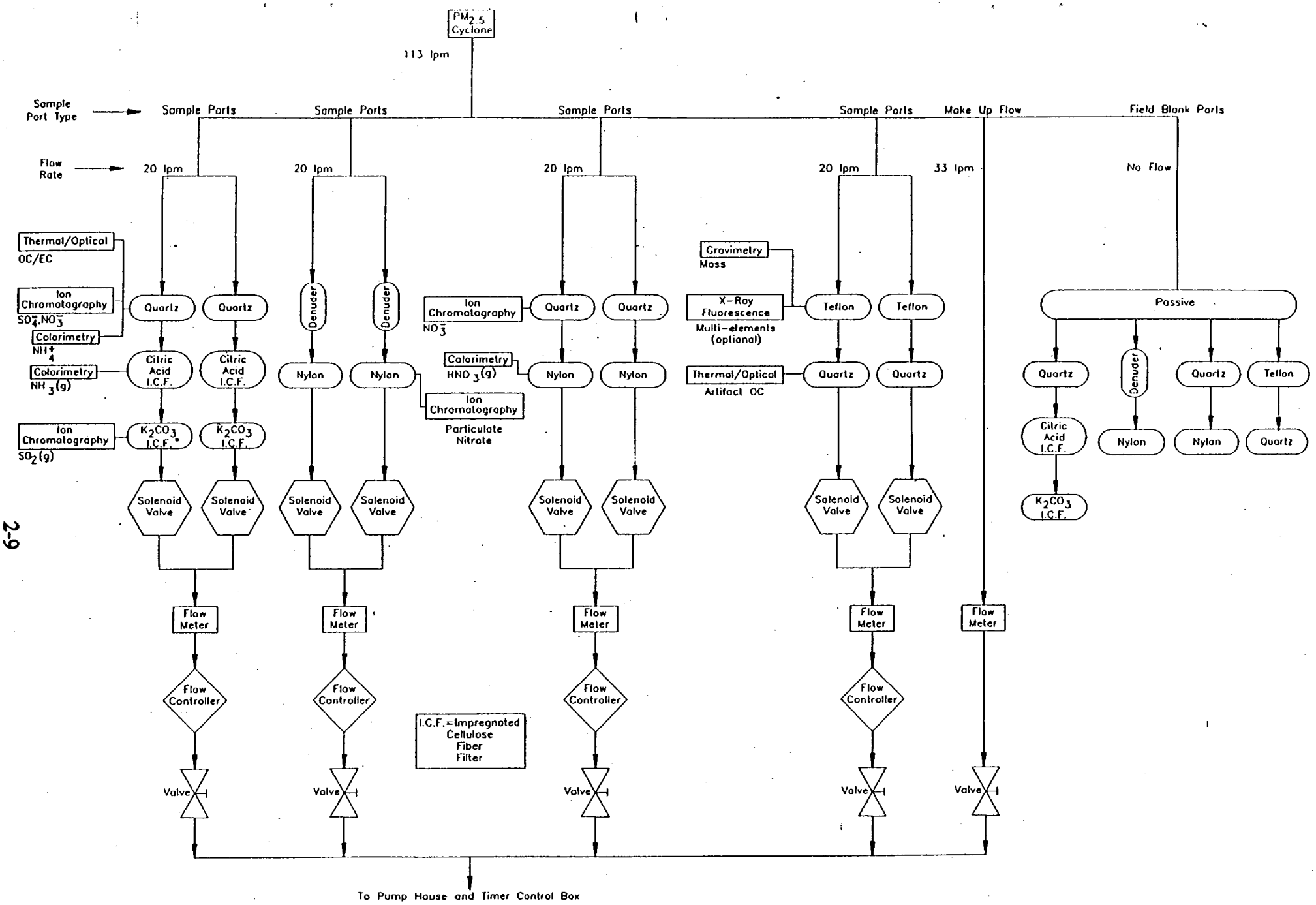

Figure 2-3. Flow Diagram for the $PM_{2.5}$ Sequential Filter Sampler.

nitrate (particulate and gaseous) and particulate nitrate. Since particulate nitrate is being measured by the unit, the challenge is to obtain an accurate measure of total nitrate. The technology developed by DRI for the CADMP (Watson et al., 1989a, 1989b, 1989c; Ashbaugh et al., 1989) is used to make these measurements.

It is well known that certain sampling surfaces absorb or react with gases and particles, thereby preventing their collection on sampling substrates (John et al., 1985; Mitchell, 1987; Hering et al., 1988). This is especially the case for nitric acid vapor, which sticks to nearly everything. In the case of denuders, a surface which does absorb nitric acid is desired. In the case of all other sampling components, a surface which does not absorb nitric acid is desired.

Drs. Bruce Appel and Walter John of the California Air and Industrial Hygiene Laboratory (AIHL) have tested different materials with respect to their affinity for nitric acid (Appel and Povard, 1987). These researchers have tested the transmission of nitric acid through an AIHL cyclone coated with PFA Teflon. The transmission, relative to a sample of the same atmosphere without passing through a size-selective inlet, was 28% for the first three hours of sampling, 54% for the second three-hour sampling period, and 74% for the third three-hour sampling period. Apparently the Teflon-coated surfaces become seasoned to the nitric acid content of the atmosphere.

Dr. John has also determined that denuders made of aluminum have an almost infinite capacity for absorbing nitric acid vapor while transmitting $PM_{2.5}$ size range particles with high efficiency.

For this project, a conical plenum and a Bendix 240 cyclone was coated with PFA Teflon following the procedures developed at AIHL. The coating process consists of washing and

sandblasting the metal surface, then spreading it with a mixture of TFE Teflon, chromic acid, and phosphoric acid. This coating is hardened by baking at 450 °C and serves as a primer to which the PFA Teflon will adhere. The TFE surface and a supply of PFA powder are then given opposite charges and the PFA powder is sprayed at the TFE surface where it is electrostatically deposited. The surface is then heated to 750 °C to melt the PFA powder onto the surface (Watson et al, 1989b).

Prior to use in sampling, these PFA surfaces are washed with a dilute solution of nitric acid which remains in contact with the surface for several hours. They are then washed in distilled-deionized water and dried. Laboratory tests at DRI have shown that this washing minimizes further absorption of nitric acid by the surface and that it does not act as a source of nitric acid when clean air is drawn over it.

Previous nitric acid measurements have shown that the choice of filter holder is critical. Much nitric acid can be lost on the holder itself. An adequate filter holder must: 1) mate to the sampler and to the flow system without leaks; 2) be composed of inert materials (e.g., no metals) which do not absorb acidic gases; 3) allow a uniformly distributed deposit to be collected; 4) have a low pressure drop across the empty holder; 5) accommodate the sizes of commonly available air sampling filters (e.g., 37 or 47 mm); and 6) be reasonably priced.

The Savillex 47mm filter holder is made of injection-molded PFA Teflon, a substance which has shown the lowest inclination to absorb nitric acid (Mitchell, 1987; Hering et al., 1988). These filter holders have a tapered extender section (called a receptacle) which can be mated to a sampler plenum with an O-ring in a retainer ring, as illustrated in Figure 2-4. Several grids and grid rings can be stacked within the holder to obtain series filtration. The cost

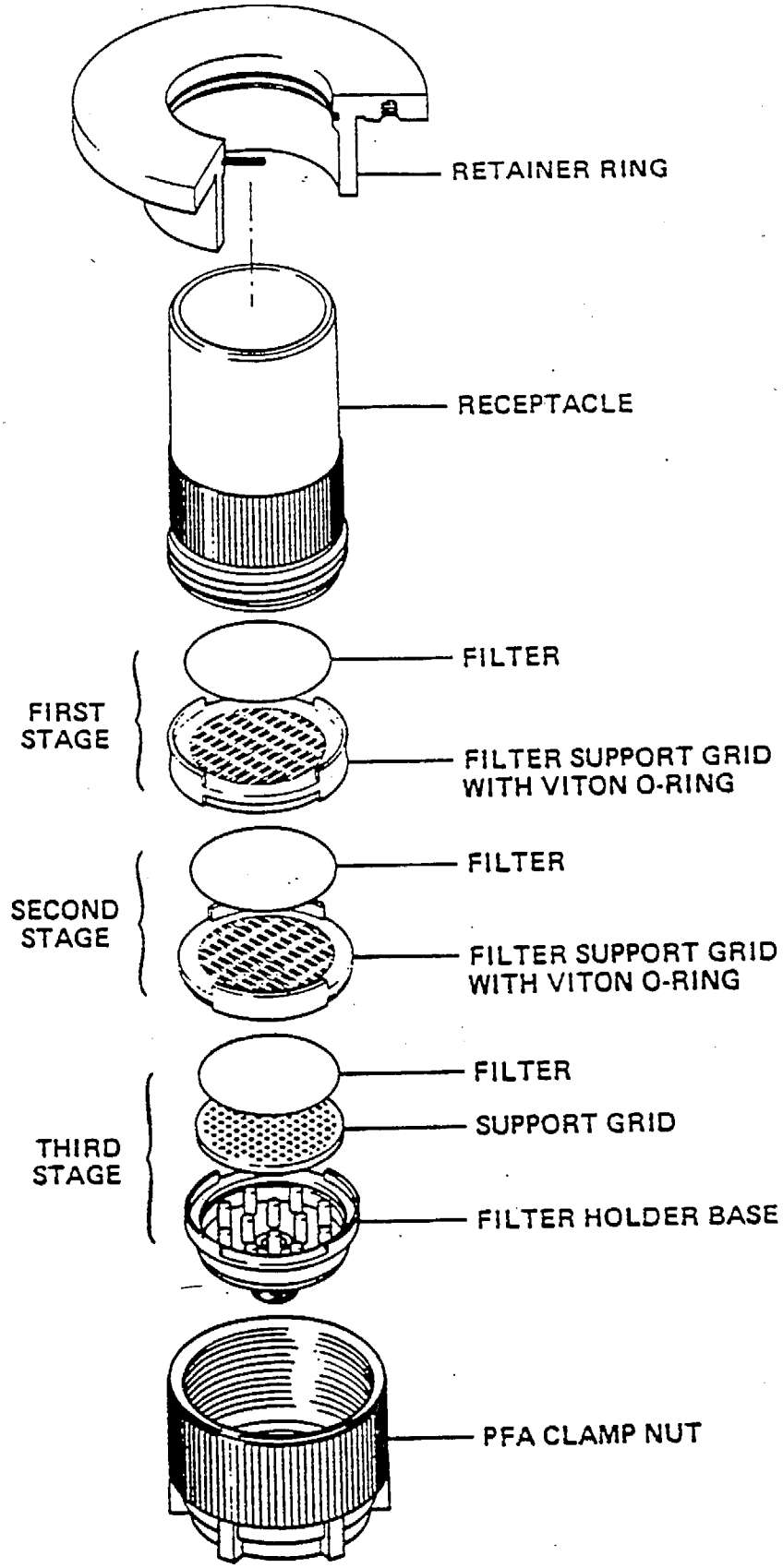

Figure 2-4. Schematic of the Multistage Savillex Filter Holder.

is reasonable. The major disadvantages of this holder are non-uniform manufacturing tolerances (diameters can be specified within a 0.01-inch tolerance), and non-uniform porosity of the support grid.

Specifications have been given to Savillex for the extender section dimensions, and these can be met within the tolerances allowed by a typical sampler retainer ring. Savillex support grid has been replaced with a grid manufactured by ATEC, Inc. which has been especially designed for dry deposition monitoring. This new support grid has a more uniform porosity which results in a uniform filter deposit. It also reduces the flow resistance across the filter holder.

The Electric Power Research Institute (EPRI) has sponsored tests of this filter holder under its Operational Evaluation Network (OEN) program which were performed by ENSR Consulting and Engineering (formerly ERT). Monodisperse fluorescent droplets of 9.2 μm diameter were submitted to a filter through an inlet which was longer and of smaller diameter than that proposed for this project. Slightly over 6% of the 9.2 μm particles were found to be deposited in the inlet, while fewer than 1% were found on the filter holder surfaces. Particle deposition in all parts of the holder summed to less than 1% of the test concentration for 5.2 μm particles.

These tests also show that the inline version of this filter holder causes particles to impact on the center of the sampling substrate, rather than being homogeneously distributed. The open-faced receptacle pictured in Figure 2-4 can be used in place of the in-line configuration in order to eliminate this impaction in the center of the filter.

EPRI/OEN also performed tests of filter sealing at temperatures ranging from -20 to 25°C and found that any shrinkage of the PFA Teflon components in response to temperature changes did not affect the sealing of the filters within the holder. No leaks were detected as a result of temperature changes.

2.2 Analytical Methods and Laboratory Operations

The chemical properties identified in Table 2-1 were selected for their roles in atmospheric acidity and its source apportionment. These species can be measured by a number of different methods. Watson et al. (1988a) provide a justification for the specific measurement methods described in this sub-section. Figure 2-5 shows the filter processing and chemical analysis activities for particulates, ammonia, sulfur dioxide, and nitric acid samples. The individual components of this figure are described in the following sub-sections.

2.2.1 Substrate Preparation

The choice of filter type results from a compromise among the following filter attributes: 1) mechanical stability; 2) chemical stability; 3) particle or gas sampling efficiency; 4) flow resistance; 5) loading capacity; 6) blank values; 7) artifact formation; 8) compatibility with analysis method; and 9) cost and availability. U.S. EPA filter requirements for PM_{10} sampling specify 0.3 μm DOP (dioctyl phthalate) sampling efficiency in excess of 99%, weight losses or gains due to mechanical or chemical instability of less than 5 $\mu g/m^3$ equivalent, and alkalinity of less than 25 microequivalents/gm to minimize sulfur dioxide (SO_2) and nitrogen oxides (NO_x) absorption (Federal Register, 1987a; 1987b; 1987c; 1987d; 1987e; 1987f). Summaries and

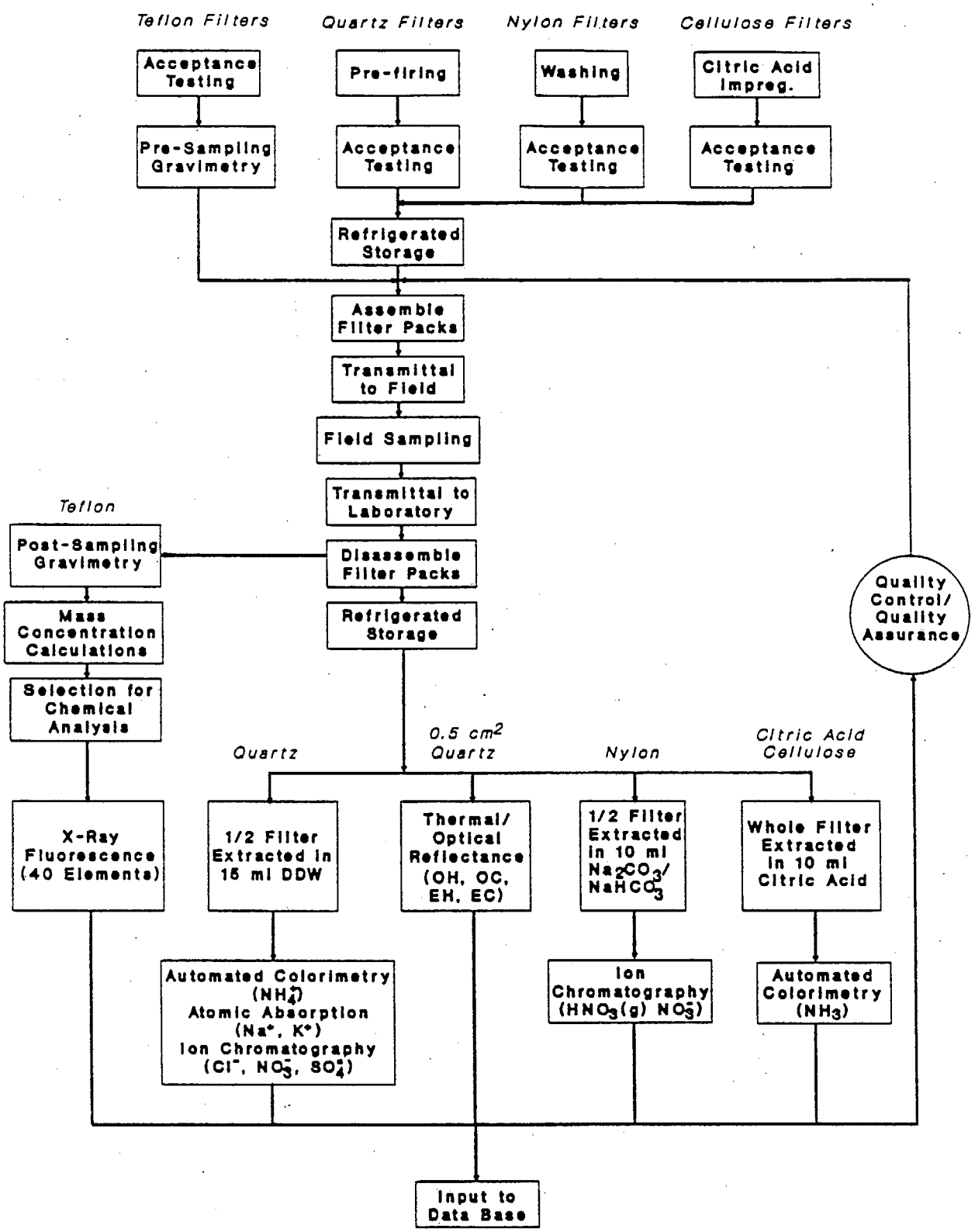

Figure 2-5. Filter Processing and Chemical Activities for Particle Mass, Ammonia, and Nitric Acid Samples.

experimental evaluations of several of these attributes for various filter media have been prepared by Lippman (1989).

The most commonly used filter media for atmospheric particle and gaseous sampling are cellulose-fiber, glass-fiber, Teflon-coated glass-fiber, Teflon-membrane, Nuclepore-membrane, quartz-fiber, and nylon-membrane. None of these materials is perfect for all purposes.

- **Cellulose-fiber** filters meet requirements in most categories with the exception of sampling efficiency and water vapor artifacts. Sampling efficiencies below 50% in the submicron region have been observed, but these are highly dependent on the filter weave. Cellulose fiber is hygroscopic and requires precise relative humidity control in the filter processing environment to obtain accurate mass measurements. This substrate has low elemental blanks and is commonly used for chemical speciation of the deposit. The hygroscopic properties of this medium make it especially amenable to filter impregnation for gaseous sampling.

- **Glass-fiber** filters meet requirements in most categories with the exception of artifact formation and blank levels (Witz et al., 1983). Sampling efficiency is very high for all particle sizes. The high alkalinity of these substrates causes sulfur dioxide, nitrogen oxides, and gaseous nitric acid to be absorbed. Blank levels for most elements of interest are extremely high and variable. Particulate nitrate and ammonium losses have been observed when these samples are stored at room temperature for long periods, but this is probably true of deposits on all types of filter media. Glass-fiber filters may exhibit volatilizable carbon artifacts.

- **Teflon-coated glass-fiber** filters meet requirements in all categories except blank element and carbon levels. Though a small nitric acid artifact has been observed, it is tolerable in most situations. These filters are excellent for ion analyses but not for carbon analyses owing to their Teflon coating.

- **Teflon-membrane** filters meet requirements in all categories except flow resistance and carbon blank levels. Because of their low porosity, it is not usually possible to attain the flow rates needed by the size-selective inlets in high volume sampling, though it is possible to obtain flow rates required for lo-vol and med-vol inlets. These filters cannot be analyzed for carbon because of its presence in the filter material, though they have very low blank levels for ions and elements. Most nondestructive multi-elemental analysis methods use Teflon-membrane filters. The deposit of particles on the filter surface makes these substrates especially amenable to XRF and PIXE analyses.

- **Nuclepore-membrane** filters have low sampling efficiencies, even for small pore sizes (Liu and Lee, 1976; Buzzard and Bell, 1980). They have low elemental blank levels. Nuclepore filters hold an electrostatic charge (Engelbrencht et al., 1980; Chow, 1985) which influences mass measurements unless substantial effort is invested in discharging them. Nuclepore filters are most appropriate for electron microscopic and elemental analyses. Ion analyses are also possible. Carbon analyses are not performed on these substrates because the filter material contains carbon.

- **Quartz-fiber** filters meet requirements in most categories and have artifact properties which are significantly lower than those for glass-fiber filters, though these substrates may absorb organic gases. Trace element blank levels are often too variable for most elemental analyses, though these filters are widely used for carbon analyses. The greatest drawback of quartz-fiber filters is their fragility, which requires extremely careful handling for accurate mass measurements. New formulations have been developed to minimize this drawback (Lundgren and Gunderson, 1975; Witz and Wendt, 1981; West, 1985; McMann, 1986). Various quartz filter formulations have been shown to have low carbon blank levels, though there is evidence that these substrates absorb organic vapors (McDow, 1986). This absorbed organic carbon can equal 10 to 50% of the organic carbon measured on these filters (McDow, 1986). Quartz-fiber filters have also been generally found to have low ionic blank levels and minimal absorption of gases such as SO_2, NO_x, and nitric acid (Mesorole et al., 1976, 1979; Pierson et al., 1976, 1983; Coutant, 1977; Appel et al., 1979, 1984; Spicer and Schumacher, 1979; Watson et al., 1981).

- **Nylon-membrane** filters are used almost exclusively for the collection of nitric acid, although these filters were not originally manufactured for this purpose. However, there is a substantial difference between the properties of filters from different manufacturers. Nylon filters have high flow resistances, which increase rapidly with filter loading. Nylon filters also absorb substantial quantities of SO_2 with variable efficiencies (Japar and Brachaczek, 1984).

The substrates used for this study are: 1) Gelman (Ann Arbor, MI) poly methyl pentane ringed, 2.0 μm pore size, 47 mm and 37 mm diameter PTFE Teflon-membrane filters (#R2PI047) for particle mass, and elements; 2) Schleicher and Schuell (Keene, NH) 1.2 μm pore size, grade 66, 47 mm diameter, nylon membrane filters (#00440) for volatilized particle nitrate as well as total nitrite); 3) Pallflex (Puttman, CT) 47 mm diameter quartz-fiber (#2500 QAT-UP) primary carbon as well as chloride, nitrate, sulfate, ammonium, sodium, and potassium

measurements; carbon backup filters for particulate carbon, and 4) Whatman No. 41 (Maldstone, England) 47 mm diameter cellulose-fiber filters (#1441047) impregnated with absorbing chemicals for sulfur dioxide and ammonia measurements.

The manufacturer's identification numbers are important specifications since only these have been found to acceptably meet the requirements for aerosol sampling. Watson et al. (1988a; 1988b) address concerns about artifact formation and contamination of these filter media and demonstrate that these substrates are the most appropriate for the prescribed measurements. All SFS filters are 47 mm diameter disks which are compatible with Nuclepore and Savillex filter holders used in the sequential filter samplers.

These filter substrates require treatment and representative chemical analyses before they can be used (Chow, 1987). Discoveries of excessive blank levels and filter interferences in several previous monitoring programs which have not included these measures have severely compromised the results of those studies.

At least one filter from each lot purchased from the specified manufacturers is analyzed for all species to verify that pre-established specifications have been met. Lots are rejected if they do not pass this acceptance test. Each filter is individually examined prior to labeling for discoloration, pinholes, creases, or other defects. Testing of sample media continues throughout the course of the project. In addition to laboratory blanks, 5 to 10% of all samples are designated as field blanks, and these follow all handling procedures except for actual sampling. Sample pre-treatment for this study includes:

- Pre-firing of Quartz-Fiber Filters. Quartz-fiber filters absorb organic vapors with time. Blank quartz-fiber filters are heated for at least three hours at 900 °C. A sample of each batch of 100 pre-fired filters is tested for carbon blank levels prior to sampling, and sets of filters with carbon levels exceeding 1 $\mu g/cm^2$ are re-fired

or rejected. All pre-fired filters are stored in a freezer prior to preparation for field sampling.

- Washing Nylon Filters. Nylon filters absorb nitric acid over time. Blank nylon filters are soaked for four hours in 0.015 M sodium carbonate (Na_2CO_3), then rinsed in distilled-deionized water (DDW) for 10 minutes, soaked overnight in DDW, rinsed three times in DDW, then dried in a vacuum oven at 60 °C for 5 to 10 minutes. Extraction efficiency tests have shown that the sodium carbonate ion chromatograph eluent is needed to remove nitrates from the active sites of the nylon filter. Sets of washed nylon filters with nitrate levels exceeding 1 μg/filter are rejected. All pre-washed nylon filters are sealed and refrigerated prior to preparation for field sampling.

- Equilibrating Teflon-Membrane Filters. On several occasions over the past 10 years, batches of Gelman ringed Teflon filters have yielded variable (by up to 100 μg/filter over a few days) blank masses. As the time from manufacture increases, this variability decreases. Since Gelman has minimized its long-term inventory of these filters, and is manufacturing them on an as-ordered basis, this variability is being observed with greater frequency. A one-month storage period in a controlled environment followed by one week of equilibration in the weighing environment is currently being applied to these filters at DRI, and this appears to have reduced the variability to acceptable (within ± 15 μg/filter for re-weights of 47 mm and 37 mm diameter filters) levels. Sets of Teflon-membrane filters which exceed twice XRF detection limits for elements are rejected. FEP Teflon sheets are equilibrated in a similar manner prior to gravimetric analysis.

The results of all filter treatments, chemical analyses, and visual inspections are recorded in a data base with the lot numbers. A set of filter IDs is assigned to each lot so that a record of acceptance testing can be associated with each sample.

Whatman 41 cellulose-fiber filters are impregnated with gas-absorbing solutions to collect gaseous ammonia (NH_3). Several impregnation solutions have been used to absorb gaseous ammonia. These solutions differ with respect to their reactive components and with respect to their formulations. The criteria which must be met by the impregnation solution are: 1) availability of pure reagents; 2) stability of the impregnation solution composition before and after impregnation; 3) low degree of hazard or toxicity; 4) lack of interferences with other

pollutants being sampled or with analytical methods; and 5) minimal effects of environmental factors such as temperature and water vapor content.

Sulfuric acid (Okita and Kanamori, 1971; Knapp et al., 1986), oxalic acid (Ohira et al., 1976; Shendrikar and Lodge, 1975), phosphoric acid, and citric acid (Stevens et al., 1985) have been used as the active agent in the sampling of ammonia on a variety of substrates. Citric acid impregnating solutions best meet the criteria described above.

Fung (1988) reports results of testing 47 mm diameter Whatman 41 cellulose-fiber filters impregnated with 0.13 μg of citric acid and 0.024 μg of glycerine were shown to absorb more than 4,000 μg of ammonia with better than 99% efficiency. Tests at temperatures ranging from -20 to 25 °C and at high and low relative humidities showed sampling efficiencies for ammonia in excess of 99%. The citric acid/glycerine mixture has been selected for ammonia impregnation in this study which consist of : 25% citric acid and 5% glycerol (balance being water).

To impregnate filters, 47 mm diameter Whatman 41 cellulose-fiber filter disks are immersed in the impregnating solution for approximately 30 minutes. These disks are then removed and placed in clean Petri slides for drying in a vacuum oven for five to ten minutes. One hundred impregnated filters are immediately sealed in polyethylene bags and placed under refrigeration for later loading into filter holders. One sample from each lot of citric acid filters is submitted to ammonium analysis prior to use. One sample from each lot of potassium carbonate filters is submitted to sulfate analysis before loading to identify sulfur dioxide contamination. The extract is also submitted to soluble potassium analysis to determine that a sufficient quantity of potassium carbonate remains on the filter. Lots are rejected when contamination or insufficient potassium carbonate is discovered.

2.2.2 Gravimetric Analysis

Unexposed and exposed Teflon-membrane filters are equilibrated at 20±5 °C temperature and 30±5% relative humidity for a minimum of 24 hours prior to weighing. Weighing is performed on a Cahn 31 electromicrobalance with ±0.001 mg sensitivity. The charge on each filter is neutralized by a polonium source for 30 seconds prior to being placed on the balance pan.

The balance is calibrated with a 20 mg Class M weight and the tare is set prior to weighing each batch of filters. After every 10 filters are weighed, the calibration and tare are re-checked. If the results of these performance tests deviate from specifications by more than ±5 μg, the balance is re-calibrated. If the difference exceeds ±0.015 mg, the previous 10 samples are re-weighed. At least 30% of all weights are checked by an independent technician and samples are re-weighed if these check-weights do not agree with the original weights within ±0.015 mg. Pre- and post-weights, check weights, and re-weights (if applied) are recorded on data sheets for later entry into the data base management system.

2.2.3 X-Ray Fluorescence Analysis for Elements

X-ray fluorescence (XRF) analysis is performed on Teflon-membrane filters for Na, Mg, Al, Si, P, S, Cl, K, Ca, Ti, V, Cr, Mn, Fe, Co, Ni, Cu, Zn, Ga, As, Se, Br, Rb, Sr, Y, Zr, Mo, Pd, Ag, Cd, In, Sn, Sb, Ba, La, Au, Hg, Tl, Pb, and U with an energy dispersive x-ray fluorescence (EDXRF) analyzer.

In XRF, inner shell electrons are removed from the atoms of the aerosol deposit. An x-ray photon with a wavelength characteristic of each element is emitted when an outer shell

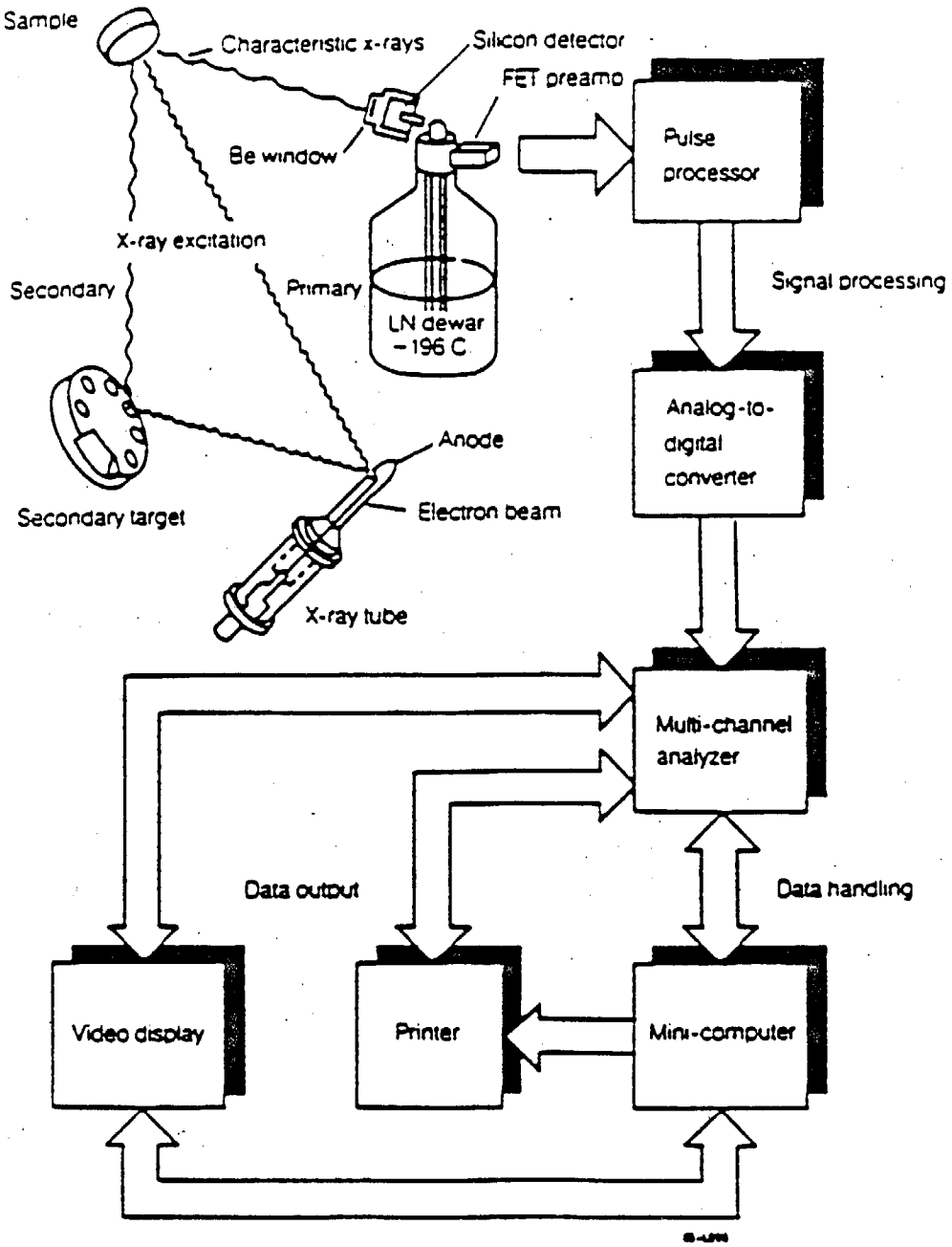

Figure 2-6. Major Components of Kevex 700/8000 XRF System (Kevex, 1985).

Table 2-2

Excitation Conditions of Kevex/DRI X-Ray Fluorescence Analyzer

Parameter	Condition Number				
	1	2	3	4	5
Tube Voltage	60 KV	35 KV	30 KV	30 KV	8 KV
Tube Current	0.4 mA	3.3 mA	3.3 mA	3.3 mA	1.0 mA
Direct Mod					
Filter	Mo	Rh	None	None	Whatman 41
Thickness	0.10 mm	0.13 mm	None	None	3 layers
Secondary Target	None	None	Ge	Ti	None
Filter	None	None	Whatman 41	Mylar	None
Thickness	None	None	1 layer	3.8 μm	None
Analysis Time	100 sec	400 sec	400 sec	100 sec	100 sec
Energy Range	0-40 KeV	0-20 KeV	0-10 KeV	0-10 KeV	0-10 KeV
Elements	Pd, Ag, Cd, In, Sn, Sb, Ba, La	Fe, Co, Ni, Cu, Zn, Ga, As, Se, Br, Rb, Sr, Y, Zr, Mo, Au, Hg, Tl, Pb, U	K, Ca, Ti, V, Cr, Mn, Fe, Co, Ni, Cu, Zn	Al, Si, P, S, Cl, K, Ca	Na, Mg, Al, Si, P, S

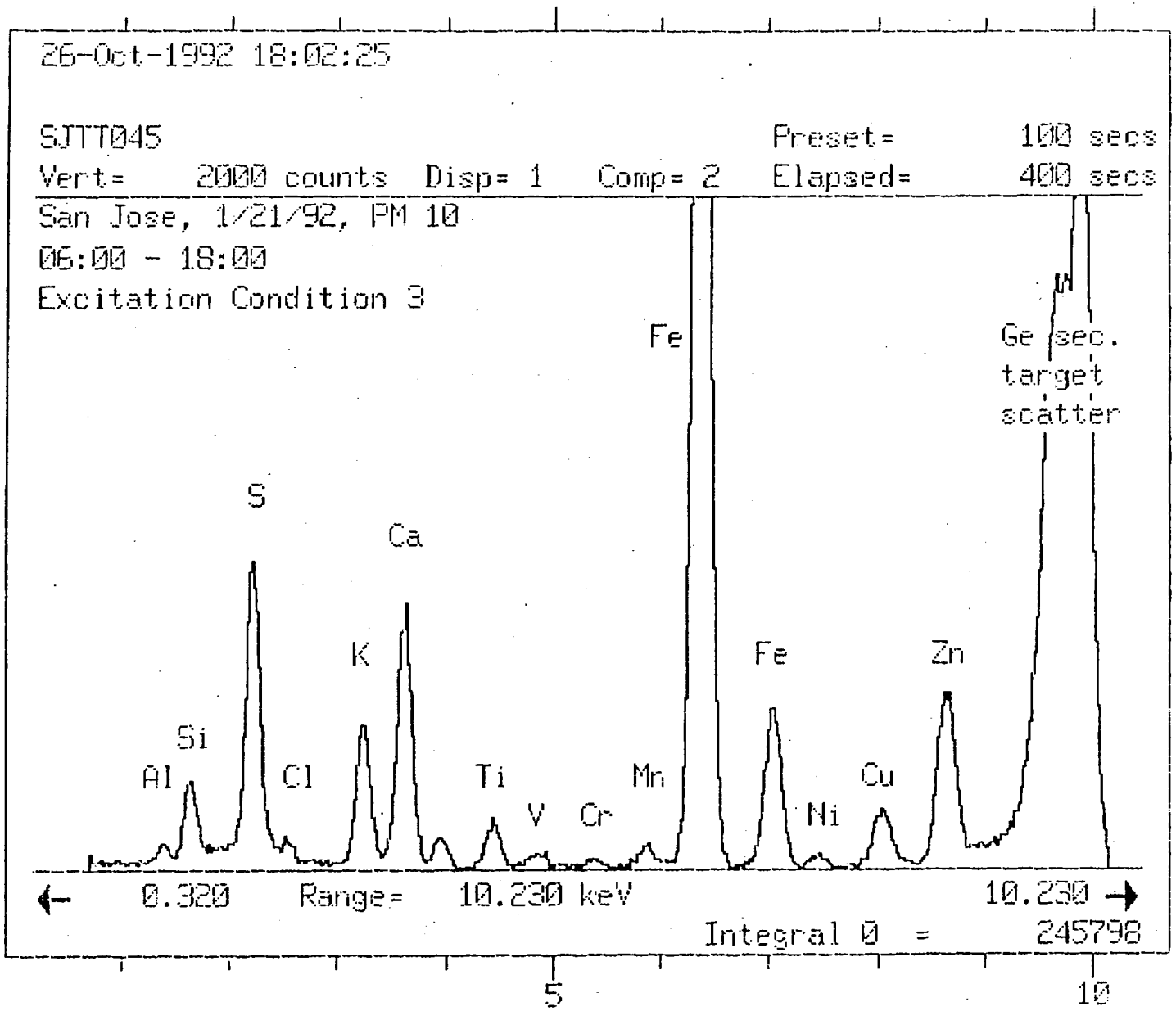

Figure 2-7. Example XRF Spectrum.

and Fe, Pb, K, Si, Ti, and Zn (SRM 1833). A separate micromatter thin-film standard is used to calibrate the system for each element.

Sensitivity factors (number of x-ray counts per $\mu g/cm^2$ of the element) are determined for each excitation condition. These factors are then adjusted for absorption of the incident and emitted radiation in the thin film. These sensitivity factors are plotted as a function of atomic number and a smooth curve is fitted to the experimental values. The calibration sensitivities are then read from these curves for the atomic numbers of each element in each excitation condition. The polymer film and NBS standards are analyzed on a periodic basis using these sensitivity factors to verify both the standards and the stability of the instrument response. When deviations from specified values are greater than $\pm 5\%$, the system is re-calibrated.

The sensitivity factors are multiplied by the net peak intensities yielded by ambient samples to obtain the $\mu g/cm^2$ deposit for each element. The net peak intensity is obtained by: 1) subtracting background radiation; 2) subtracting spectral interferences; and 3) adjusting for x-ray absorption.

The elemental x-ray peaks reside on a background of radiation scattered from the sampling substrate. A model background is formed by averaging spectra obtained from 10 filters of the same type used in ambient sampling. This model background has the same shape and features of the sample spectra (minus the elemental peaks) if the deposit mass is small relative to the substrate mass (Russ, 1977). This model background is normalized to an excitation radiation scatter peak in each sample spectrum to account for the difference in scatter intensity due to different masses. Experience has shown that use of a scatter peak for blank normalization from too low an energy region (e.g., the Ti secondary target scatter peak from

Condition 2) can lead to unreliable background estimation. Therefore, the Mo scatter peak is used for Conditions 1 and 2, and the Ge scatter peak is used for Conditions 3, 4, and 5.

The number and spacing of the characteristic x-ray lines relative to detector resolution are such that the peaks from one element can interfere with a peak from another element (Dzubay, 1986). A variety of methods has been used to subtract these peak overlaps (Arinc et al., 1977; Parkes et al., 1979; Drane et al., 1983), including least squares fitting to library spectra, Gaussian and other mathematical functions, and the use of peak overlap coefficients. Peak overlap coefficients are applied to aerosol deposits. The most important of these overlaps are the K-beta to K-alpha overlaps of elements from potassium (K) to zirconium (Zr), the lead (Pb) L-alpha to arsenic (As) K-alpha interference, and the lead (Pb) M line to sulfur (S) K line interference. The ratios of overlap peaks to the primary peak are determined from the thin film standards for each element for the spectral regions of the remaining elements. These ratios are multiplied by the net peak intensity of the primary peak and subtracted from the spectral regions of other elements.

The ability of an x-ray to penetrate matter depends on the energy of the x-ray and the composition and thickness of material. In general, lower energy x-rays, characteristic of light elements, are absorbed in matter to a much greater degree than higher energy x-rays. Larger particles collected during aerosol sampling have sufficient size to cause absorption of x-rays within the particles. Attenuation factors for fine particles (particles with aerodynamic diameter less than 2.5 μm) are generally negligible (Criss, 1976), even for the lightest elements, but these attenuations can be significant for coarse fraction particles (particles with aerodynamic diameter

from 2.5 to 10 μm). Correction factors have been derived using the theory of Dzubay and Nelson (1975) and will be applied to the particle measurements.

During XRF analysis, filters are removed from their Petri slides and placed with their deposit sides downward into polycarbonate filter cassettes. A polycarbonate retainer ring keeps the filter flat against the bottom of the cassette. These cassettes are loaded into a carousel in the x-ray chamber which contains 16 openings. The filter IDs are recorded on a data sheet to correspond to numbered positions in the carousel. The sample chamber is evacuated to 10^{-3} torr and a computer program controls the positioning of the samples and the excitation conditions. Complete analysis of 16 samples under five excitation conditions requires approximately six hours. The vacuum in the x-ray chamber and the heat induced by the absorption of x-rays can cause certain materials to volatilize. For this reason, labile species such as nitrate and organic carbon are measured on a quartz-fiber, rather than the Teflon-membrane, filter.

A quality control standard and a replicate from a previous batch are analyzed with each set of 14 samples. If the quality control values differ from specifications by more than $\pm 5\%$ or if the replicate concentrations differ from the original values (assuming they are at least 10 times detection limits) by more than $\pm 10\%$, the samples are re-analyzed. If further tests of standards show that the system calibration has changed significantly, the instrument is re-calibrated as described above.

2.2.4 Thermal/Optical Carbon Analysis

In the following discussion, carbonaceous species which absorb light are termed elemental carbon and those which do not are termed organic carbon. There has been much discussion

concerning the definition of elemental and organic carbon. The definition of importance to visibility source apportionment is that which classifies black carbon (whether or not it is in a graphitic or amorphous form) as elemental carbon. That is the definition adopted for this study.

The Thermal Optical Reflectance (TOR) method is based on the principle that carbon evolving under different temperature and oxidation conditions is determined separately and summed to obtain the light-absorbing and non-light-absorbing fractions (Chow et al. 1992). These fractions are useful for comparison with other methods which are specific to a single definition (which may differ from the visibility-related definition chosen for this project) for elemental and organic carbon. Seven carbon fractions are proposed: 1) the carbon evolved in a helium atmosphere at temperatures between ambient and 120 °C (OC1); 2) the carbon evolved in a helium atmosphere at temperatures between 120 and 250 °C (OC2); 3) the carbon evolved in a helium atmosphere at temperatures between 250 and 450 °C (OC3); 4) the carbon evolved in a helium atmosphere between 450 and 550 °C (OC4); 5) the carbon evolved in an oxidizing atmosphere at 550 °C (EC1); 6) the carbon evolved in an oxidizing atmosphere between 550 and 700 °C (EC2); and 7) the carbon evolved in an oxidizing atmosphere between 700 and 800 °C (EC3).

The thermal/optical reflectance carbon analyzer consists of a thermal system and an optical system which are diagrammed in Figure 2-8. The thermal system consists of a quartz tube placed inside a coiled heater. The current through the heater is controlled to attain and maintain pre-set temperatures for given time periods. A portion of a quartz filter is placed in the heating zone and heated to different temperatures under non-oxidizing and oxidizing atmospheres. The optical system consists of a He-Ne laser, a fiber optic transmitter and

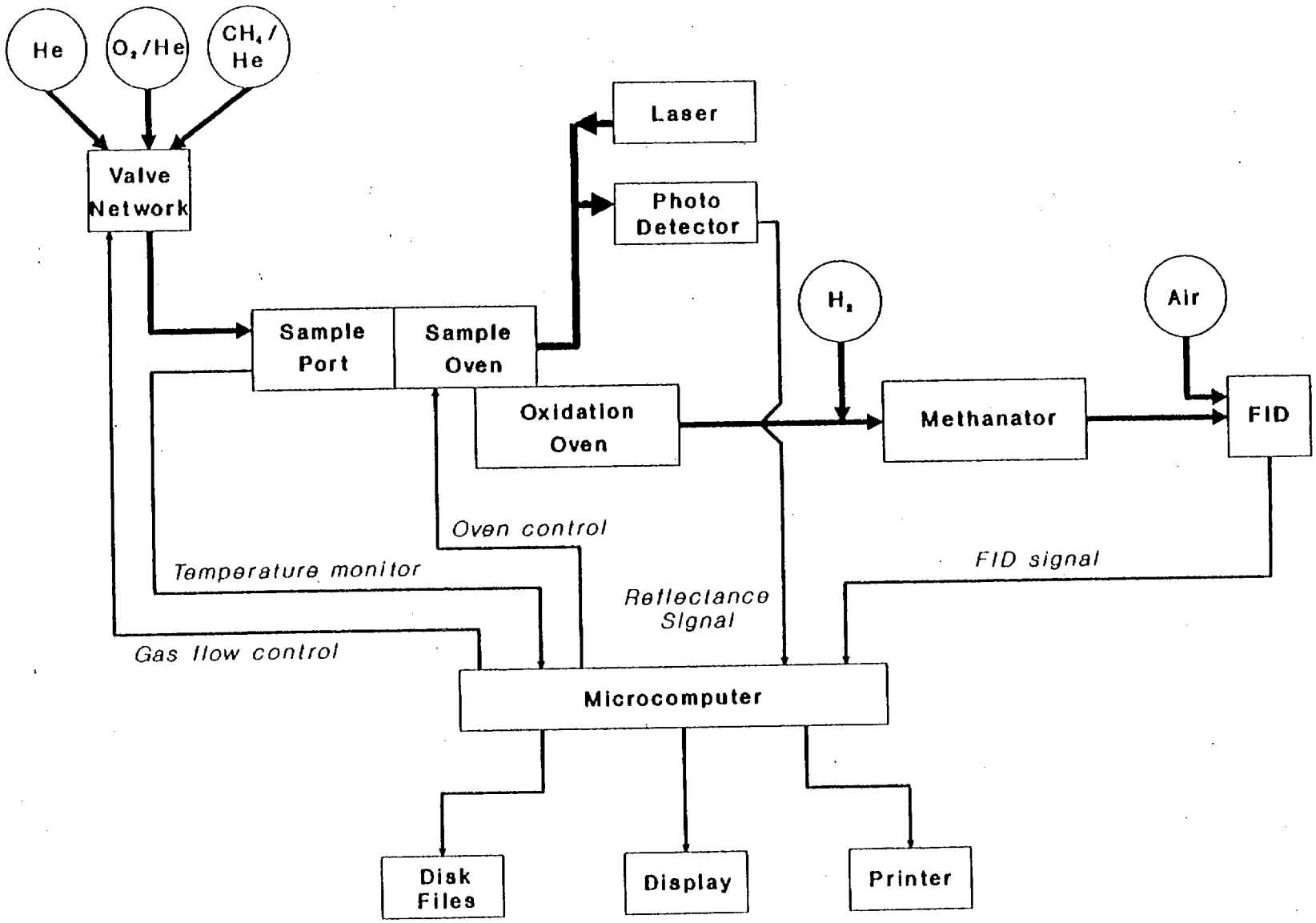

Figure 2-8. Block Diagram of DRI/OGC Thermal/Optical Reflectance Carbon Analyzer.

receiver, and a photocell. The filter deposit faces a quartz light tube so that the intensity of the reflected laser beam can be monitored throughout the analysis.

As the temperature increases from ambient (~25 °C) to 550 °C, organic compounds are volatilized from the filter in a non-oxidizing (He) atmosphere while elemental carbon is not oxidized. When oxygen is added to the helium at temperatures greater than 550 °C, the elemental carbon burns and enters the sample stream. The evolved gases pass through an oxidizing bed of heated manganese dioxide where they are oxidized to carbon dioxide, then across a heated nickel catalyst which reduces the carbon dioxide to methane (CH_4). The methane is then quantified with a flame ionization detector (FID).

The principal function of the laser reflectance system is to continuously monitor the filter reflectance throughout an analysis cycle. The negative change in reflectance is proportional to the degree of pyrolytic conversion from organic to elemental carbon which takes place during organic carbon analysis. After oxygen is introduced, the reflectance increases rapidly as the light-absorbing carbon is burned off the filter. The carbon measured after the reflectance attains the value which it had at the beginning of the analysis cycle is classified as elemental carbon. This adjustment for pyrolysis in the analysis is significant, as high as 25% of organic or elemental carbon, and it cannot be ignored. Johnson et al. (1981) reported that an average of 22% of the organic carbon in the samples they analyzed was pyrolytically converted to elemental carbon as evidenced by reflectance corrections. The precision of the pyrolytic conversion has been found to be ±10% in both organic and elemental carbon (Johnson et al., 1981).

An example thermal/optical reflectance output is shown in Figure 2-9. This figure identifies the different temperatures and oxidizing conditions which are achieved during the

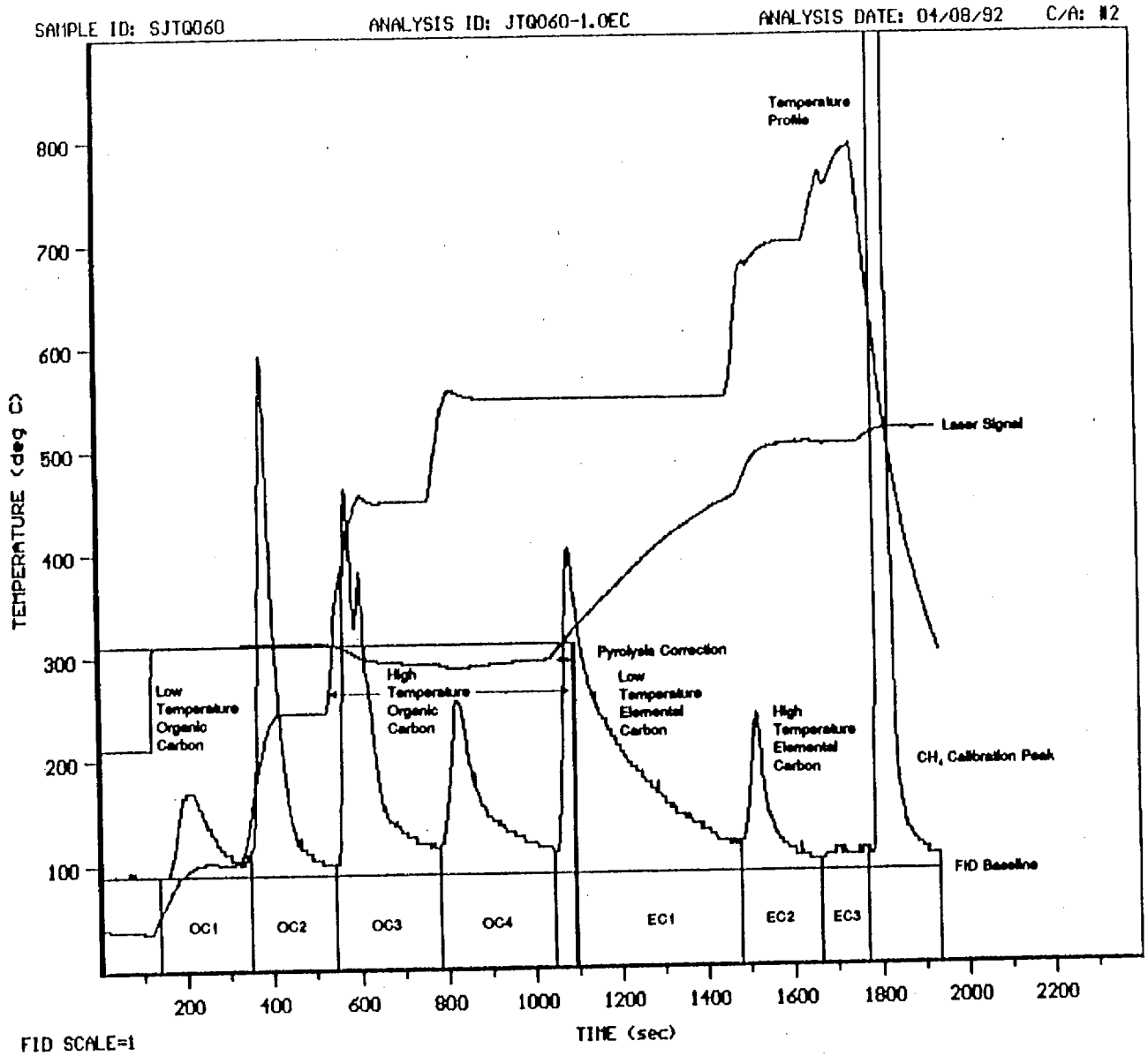

Figure 2-9. Example Thermal/Optical Reflectance Thermogram.

analysis. The fractions of carbonaceous material which evolve at the different temperatures are shown as is the fraction which represents the organic carbon pyrolized during the analysis. The rapid increase in reflectance after oxygen is added demonstrates that this method classifies most of the light-absorbing material as total elemental carbon (EC1+EC2+EC3). The fraction which evolves after the temperature reaches 700 °C is that which should be compared with TMO elemental carbon. Since the reflectance has decreased substantially by the time this temperature is reached, it is evident that this fraction cannot be related to particulate light absorption. For routine analysis, a 0.5 cm^2 circular punch is removed from a quartz-fiber filter. This punch is placed vertically into a quartz boat which is inserted into the oven area with a thermocouple pushrod. The atmosphere flowing through the oven at this stage is pure helium. The temperature ramps from ~25 °C to 120 °C, 250 °C, to 450 °C, to 550 °C and the FID output is recorded every second on a microcomputer data acquisition system. A 2% oxygen (O_2) in helium (He) atmosphere is introduced at 550 °C, followed by temperature increases to 700 °C, then 800 °C. The microcomputer controls the time intervals, monitors the temperatures, FID output, and reflectance, and integrates the FID response over the pre-specified temperature, oxidation, and reflectance intervals. The fractions in the intervals corresponding to reflectances less than or equal to the initial value are summed to yield organic carbon, and fractions in the intervals with reflectances greater than the initial value in the oxidizing atmosphere are summed to yield elemental carbon.

The system is calibrated by analyzing samples of known amounts of methane, carbon dioxide, and potassium hydrogen phthalate (KHP). The FID response is ratioed to a reference level of methane injected at the end of each sample analysis. Performance tests of instrument

calibration are conducted at the beginning and end of daily operation, as well as at the end of each sample run. All intervening samples are re-analyzed if calibration changes of more than $\pm 10\%$ are found.

Known amounts of American Chemical Society (ACS) certified reagent grade crystal sucrose and potassium hydrogen phthalate (KHP) are combusted as a verification of the organic carbon fractions. A total of 15 different standards are used for each calibration. Widely accepted primary standards for elemental and/or organic carbon are still lacking. Establishment of such standards is in progress.

2.2.5 Filter Extraction

Water-soluble chloride, nitrate, sulfate, ammonium, sodium, and potassium are obtained by extracting half of the quartz-fiber particle filter in 10 ml of deionized-distilled water (DDW). Teflon sheets are also extracted in 15 ml of DDW for ion analysis of MOUDI samples. The entire potassium carbonate impregnated cellulose-fiber filter is extracted in 5 ml 0.1% of H_2O_2 to ensure oxidation of sulfite to sulfate and followed by a 1:21 dilution with DDW to determine sulfur dioxide by ion chromatography. The entire citric acid impregnated cellulose-fiber filter is extracted in 10 ml of citric acid to determine ammonia by automated colorimetry. Half of the nylon backup filter is extracted in 10 ml of potassium carbonate solution for nitrate measurements to determine the degree of particle volatilization from the quartz-fiber filter.

Each filter is first cut in half with a precision positioning jig attached to a paper cutter. The blade is cleaned between each filter cutting. One filter half is placed in a Falcon (#2045) 16 x 150 mm polystyrene extraction vial. Each vial is labeled with a bar code sticker

containing the filter ID code. The extraction tubes are placed in tube racks, and the extraction solutions are added.

The extraction vials are capped and sonicated for 60 minutes, shaken for 60 minutes, then aged overnight to assure complete extraction of the deposited material in the solvent. The bath water is continually replaced to prevent temperature increases from the dissipation of ultrasonic energy in the water. After extraction, these solutions are stored under refrigeration prior to analysis. The unused filter is placed back to the original Petri slide and archived.

2.2.6 Ion Chromatographic Analysis for Chloride, Nitrate, and Sulfate

Anion chromatography for chloride (Cl^-), nitrate (NO_3^-), and sulfate ($SO_4^=$) is performed with the Dionex 2020i (Sunnyvale, CA) ion chromatograph. In IC, an ion-exchange column separates the sample ions in time for individual quantification by a conductivity detector. Prior to detection, the column effluent enters a suppressor column where the chemical composition of one element is altered, resulting in a matrix of low conductivity. The ions are identified by their elution/retention times and are quantified by the conductivity peak area. Figure 2-10 shows an example ion chromatogram.

Approximately 2 ml of the filter extract are injected into the ion chromatograph. The resulting peaks are integrated and the peak integrals are converted to concentrations using calibration curves derived from solution standards. The system for the analysis of Cl^-, NO_3^-, and $SO_4^=$ contains a guard column (AG4a column, Cat. No. #37042) and an anion separator column (AS4a column, Cat. No. #37041) with a strong basic anion exchange resin, and an anion micro membrane suppressor column (250 x 6 mm ID) with a strong acid ion exchange resin. The

Sample Name: SJTQ060 Date: Fri Apr 03 13:22:51 [illegible]
Data File : A:\04038A21.D57
Method : C:\DX\METHOD\ANION2.met
ACI Address: 1 System : 2 Injects: 57 Detector: [illegible]

REPORT	VOLUME	DILUTION	POINTS	RATE	START	STOP	AREA	REJ
External	1	1	3010	10Hz	[illegible]	[illegible]	[illegible]	

Pk. Num	Ret Time	Component Name	Concentration	Height	Area	Bl. Code	[illegible]
1	1.20		0.000	107221	373380	1	
2	1.40	CHLORIDE	0.068	560110	2307928	1	[illegible]
3	2.28	NITRATE	5.411	23992483	170048927	[illegible]	[illegible]
4	3.35	SULFATE	0.740	3540839	30094311	1	[illegible]
5	4.27		0.000	134802	1424495	1	

File: A:\04038A21.D57 Sample: SJTQ060

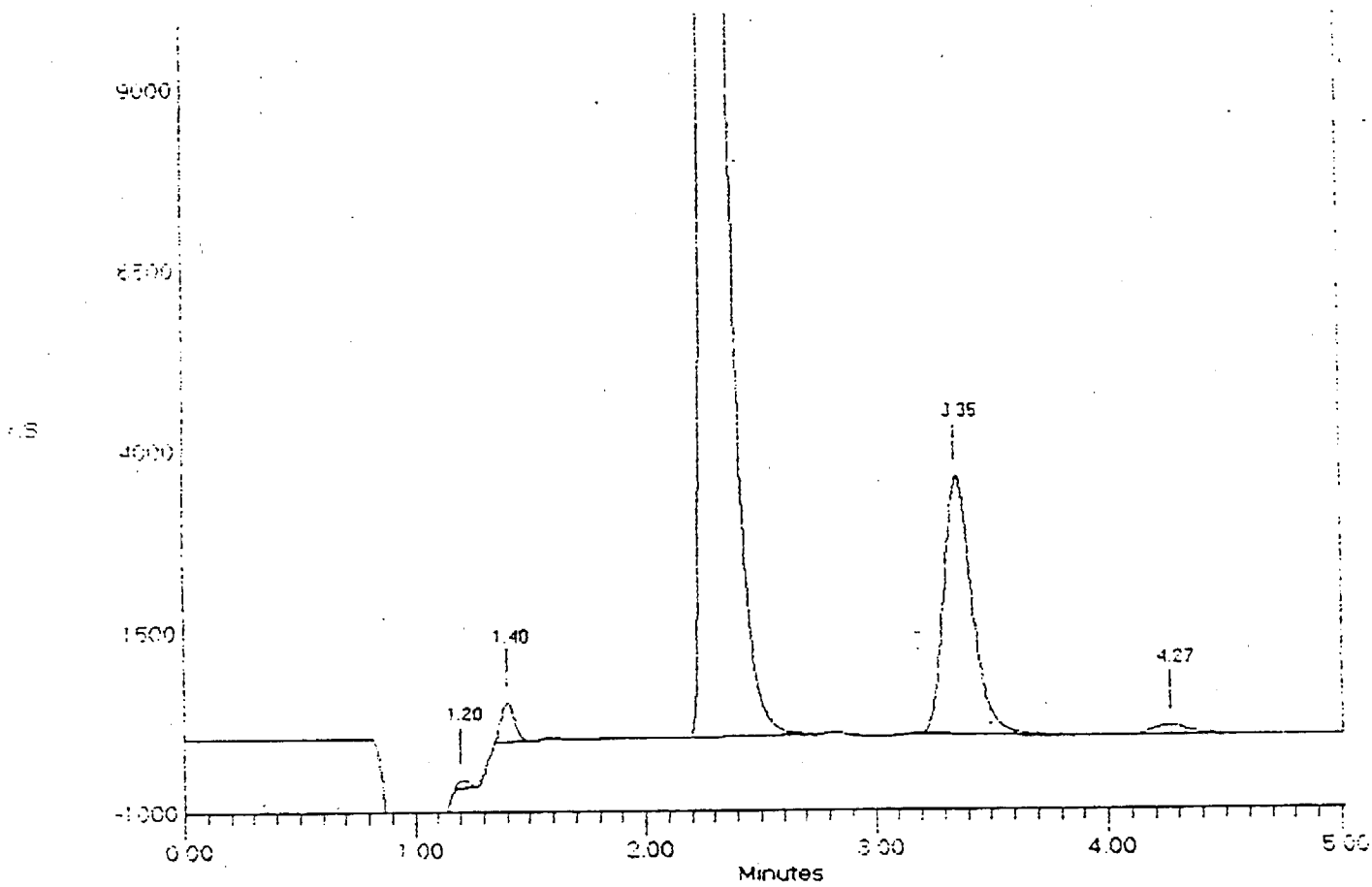

Figure 2-10. Example Ion Chromatogram.

anion eluent consists of Na_2CO_3 and $NaHCO_3$ prepared in DDW. The DDW is verified to have a conductivity of less than 10^{-5} ohm^{-1} cm^{-1} prior to preparation of the eluent. For quantitative determinations, the ion chromatograph is operated at a flow rate of 2.0 l/min.

Standard solutions of NaCl, $NaNO_3$ and $(Na)_2SO_4$ are prepared with reagent grade salts which are dehydrated in a desiccator several hours prior to weighing. These anhydrous salts are weighed to the nearest 0.010 mg on a regularly calibrated analytical balance under controlled temperature (~20 °C) and relative humidity (±30%) conditions. These salts are diluted in precise volumes of eluent. A standard solution is prepared monthly and stored in a refrigerator. Calibration solutions are prepared weekly by diluting the standard solution to concentrations covering the range of concentrations expected in the filter extracts. The calibration concentrations prepared are at 0.1, 0.2, 0.5, 1.0, 2.0, and 5.0 μg/ml for each of the analysis species. These transfer standards are also be traceable to National Institute of Standards and Technology (NIST),formerly National Bureau of Standards (NBS), weights and volumes via the mass and volume measurements from which the standardized values were derived.

Calibration is required before the sample run. The ions are identified by matching the retention times of each peak in the unknown sample with each peak in the chromatogram of the standard.

An eluent blank is tested after every 20 samples and a performance test standard is analyzed after every 10 samples as quality control checks on baseline and calibration, respectively. Both the NIST (NBS) traceable simulated rain water standards (Standard Reference Materials: SRM 2694-I and SRM 2694-II) and the Environmental Research Associates (ERA) standard solution are used daily as an independent quality control check. If the values obtained

for these standards do not coincide within a pre-specified uncertainty level (typically three standard deviations of the baseline level or ±5%), all of the samples between that standard and the previous performance test standard are re-analyzed. The Dionex IC is capable of measuring ions with 5 to 10 ppb detection limits for small sample volumes.

After analysis, the printout for each sample in the batch is reviewed for: 1) proper operational settings; 2) correct peak shapes and integration windows; 3) peak overlaps; 4) correct background substraction; and 5) quality control sample comparisons. When values for replicates differ by more than ±10% or values for standards differ by more than ±5%, all samples before and after these quality control checks are designated for re-analysis in a subsequent batch. Individual samples with unusual peak shapes, background subtractions, or operating parameters are also designated for re-analysis.

2.2.7 Atomic Absorption Spectrophotometric Analysis for Sodium and Potassium

A Perkin-Elmer Model 2380 Double Beam Atomic Absorption Spectrometer is used to analyze quartz filter extracts for soluble potassium and sodium. A dual hollow cathode lamp emits wavelengths appropriate for sodium and potassium analyses. For potassium, the monochrometer is set at 766.5 nm with a 2.0 nm bandpass. For sodium, the monochrometer is set at 589.0 nm with a 0.7 nm bandpass.

Approximately one to two milliliters of the extract are aspirated into an air/acetylene flame at approximately 0.5 ml/min. The output of the photomultiplier is recorded on an IBM/XT at a rate of two readings per second. These are averaged over a 30-second interval and

compared with standards using custom software developed at DRI's Environmental Analysis Facility.

For routine analysis, 50 sample vials containing 2 ml of solution are loaded into the autosampler. The first six vials contain standards and a DDW blank. Four sets of 11 vials follow which contain 9 ambient extracts, 1 standard, and 1 replicate from a previous batch. Samples are re-analyzed when quality control standards differ from specifications by more than ±5% or when replicates (at levels exceeding 10 times detection limits) differ by more than ±10%.

The ACS reagent grade potassium standard is used as stock standard solution. The dilutions of the stock solution to be used as calibration standards are prepared daily prior to sample analysis. Ionization interference is eliminated by addition of cesium chloride (CsCl) to samples and standard solutions.

2.2.8 Automated Colorimetric Analysis for Ammonium

The Technicon (Tarrytown, NY) TRAACS 800 Automated Colorimetric System is used to measure ammonium concentrations by the indophenol method. Ammonium in the extract is reacted with phenol and alkaline sodium hypochlorite to produce indophenol, a blue dye. The reaction is catalyzed by the addition of sodium nitroprusside. The absorbance of the solution is measured at 630 nm.

Approximately two milliliters of extract are placed in an autosampler which is controlled by a computer. Five standard concentrations are prepared from ACS reagent-grade $(NH_4)_2SO_4$ following the same procedure as that for IC standards. Each set of samples consists of 2 distilled

water blanks to establish a baseline, 5 calibration standards and a blank, then sets of 10 samples followed by analysis of one of the standards and a replicate from a previous batch. The computer control allows additional analysis of any filter extract to be repeated without the necessity of loading the extract into more than one vial.

The system determines carry-over by analysis of a low concentration standard following a high concentration. The percent carry-over is then automatically calculated and can be applied to the samples analyzed during the run. Technicon software operating on an IBM/XT microcomputer controls the sample throughput, calculates concentrations, and records data with dBASE II software.

Formaldehyde has been found to interfere when present in an amount which exceeds 20% of the ammonium content and hydrogen sulfide interferes in concentrations which exceed 1 mg/ml. Nitrate and sulfate are also potential interferents when present at levels which exceed 100 times the ammonium concentration. These levels are rarely exceeded in ambient samples. The precipitation of hydroxides of heavy metals such as calcium and magnesium is prevented by the addition of disodium ethylenediamine-tetracetate (EDTA) to the sample stream (Chow, 1981).

2.3 Quality Assurance

Every measurement consists of a value, a precision, an accuracy, and a validity (Mueller et al., 1979; Mueller and Watson, 1981; Hidy, 1985). Quality control (QC) and quality auditing establish the precision, accuracy, and validity of measured values (Watson et al., 1983). Quality assurance integrates quality control and quality auditing to determine these four attributes of each

environmental measurement. Quality assurance (QA) and QC activities include calibration, performance test, and auditing activities.

QA is a project management responsibility which integrates quality control, quality auditing, measurement method validation, and sample validation into the measurement process. The results of quality assurance are data values with specified precisions, accuracies, and validities. Quality auditing is performed by personnel who are independent of those performing the procedures. A separate quality assurance manager performed these audits as part of the SJVAQS/AUSPEX study.

QC is the responsibility of each contractor. QC is intended to prevent, identify, correct, and define the consequences of difficulties which might affect the precision, accuracy, and/or validity of the measurements. The QC activities included: 1) creating and modifying standard operating procedures (SOPs) to be followed during ambient and source sampling, analysis, and data processing; 2) equipment overhaul, repair, acceptance testing, and spare parts; 3) operator training, supervision and support; 4) periodic calibrations and performance tests, which include blank and replicate analyses; and 5) quality auditing.

2.3.1 Standard Operating Procedures

Standard Operating Procedures (SOPs) codify the actions which are taken to implement a measurement process over a specified time period. State-of- the-art scientific information is incorporated into the SOP with each revision. SOPs include the following elements:

- A brief summary of the measurement method, its principles of operation, its expected accuracy and precision, and the assumptions which must be met for it to be valid.

- A list of materials, equipment, reagents, and suppliers. Specifications are given for each expendable item and its storage location.
- Designation of the individual to be responsible for each part of the procedure.
- A general traceability path, the designation of primary standards or reference materials, tolerances for transfer standards, and a schedule for transfer standard verification.
- Start-up, routine, and shut-down operating procedures and an abbreviated checklist.
- Copies of data forms with examples of filled out forms.
- Routine maintenance schedules, maintenance procedures, and troubleshooting tips.
- Internal calibration and performance testing procedures and schedules.
- External performance auditing schedules.
- References to relevant literature and related standard operating procedures.

The field operations, laboratory operations, and data processing/data validation procedures used in this study are specified in Table 2-3.

2.3.2 Quality Audits

The principal investigators work with the Quality Assurance task manager to define and conduct independent audits of the measurement processes. The quality auditing function consists of two components: 1) systems audits and 2) performance audits. Systems audits start with a review of the operational and QC procedures to assess whether they are adequate to assure valid data which meet the specified levels of accuracy and precision. After reviewing the procedures, the auditor examines all phases of the measurement or data processing activity to determine that the procedures are being followed and the operational people are properly trained. The systems

Table 2-3

Summary of Standard Operating Procedures Applied in the Sierra Nevada Study

Subject	Observable/ Method	DRI Standard Operating Procedure (SOP) Title[a]
I. FIELD OPERATIONS		
• Air Quality Sampling	$PM_{2.5}$ and PM_{10}	Sequential Filter Sampler Field Operations (DRI SOP # 1-207.2)
II. LABORATORY OPERATIONS		
• Sample Pretreatment	Potassium Carbonate Impregnation Citric Acid Impregnation	Impregnating, Drying, and Acceptance Testing of Filters for Sampling Gases in Air (DRI SOP #2-104.2)
	Nylon Filter Cleaning	Preparation of Nylon Filters for Nitric Acid or Total Nitrate Sampling (DRI SOP #2-105.2)
	Quartz Filter Pre-firing	Pre-firing of Quartz Fiber Filters for Carbonaceous Material Sampling (DRI SOP # 2-106.2)
	Sample Section	Filter Sectioning (DRI SOP #2-201.2)
	Filter Extraction	Extraction of Ionic Species from Filter Samples (DRI SOP #2-202.2)

Table 2-3 (continued)

Summary of Standard Operating Procedures Applied in the Sierra Nevada Study

Subject	Observable/ Method	DRI Standard Operating Procedure (SOP) Title[a]
II. LABORATORY OPERATIONS (continued)		
• Chemical Analysis (continued)	Mass	Gravimetric Analysis Procedures (DRI SOP #2-102.2)
	40 Elements (Na to Pb)	X-ray Fluorescence (XRF) Analysis of Aerosol Filter Samples (DRI SOP #2-205.2)
	Chloride (Cl^-) Nitrate (NO_3^-) Sulfate ($SO_4^=$)	Analysis of Filter Extracts and Precipitation Samples by Ion Chromatography (DRI SOP #2-203.2)
	Ammonium (NH_4^+) Ammonia (NH_3) as (NH_4^+)	Analysis of Filter Extracts and Precipitation Samples by Automated Colorimetric Analysis (DRI SOP #2-207.2)
	Soluble Sodium (Na^+) Soluble Potassium (K^+)	Analysis of Filter Extracts and Precipitation Samples by Atomic Absorption Spectroscopy (DRI SOP #2-206.2)

Table 2-3 (continued)

Summary of Standard Operating Procedures Applied in the Sierra Nevada Study

Subject	Observable/ Method	DRI Standard Operating Procedure (SOP) Title[a]
II. LABORATORY OPERATIONS (continued)		
• Chemical Analysis	High Temperature Organic Carbon (OH) Total Organic Carbon (OC) High Temperature Elemental Carbon (EH) Total Elemental Carbon (EC) Total Carbon (TC)	Thermal/Optical Reflectance Carbon Analysis of Aerosol Filter Samples (DRI SOP #2-204.3)
• Chain-of-Custody	Filter Pack Assembling and Disassembling	Filter Pack Assembling, Disassembling, and Cleaning Procedure (DRI SOP #2-208.2)
	Shipping and Receiving	Sample Shipping, Receiving, and Chain-of-Custody (DRI SOP #2-209.2)
III. DATA PROCESSING/DATA VALIDATION		
• Aerosol/Gas Data	Data Validation	Dry Deposition Field, Mass, and Chemical Data Processing and Data Validation (DRI SOP # 3-003.2)

audit is intended to be a cooperative assessment resulting in improved data, rather than a judgmental activity.

Performance audits establish whether the predetermined specifications are being achieved in practice. The performance audit challenges the measurement/analysis system with a known standard sample which is traceable to a primary standard. For data processing, the performance audit consists of independently processing sections of the data and comparing the results.

Auditing services were performed as part of the SJVAQS/AUSPEX study at the Yosemite and Sequioia sites, while DRI personnel independent of this study audited the Blodgett and Tehachapi sites.

The field performance audits test sampler flow rates. These flow rates are verified by measuring the flow through each port using a mass flow meter traceable to an National Institute of Standards and Technology (NIST) spirometer. The percent difference between the audit flow and the nominal flow is calculated. Elapsed times are verified using an audit stopwatch. Meteorological monitors are audited by verifying: 1) the direction of wind vanes using an accurate compass; 2) the wind speed recorded by the anemometer with a synchronous motor; 3) the temperature against a traceable thermometer; and 4) the relative humidity against a traceable sling psychrometer.

The laboratory performance audit consists of the submission of known standards to routine laboratory procedures and of an interlaboratory comparison of those standards. To audit the analysis of soluble species, a solution containing ammonium, chloride, nitrate, sulfate, sodium, and potassium is prepared and deposited in known amounts on quartz-fiber filters. Samples at three concentration levels are submitted to the routine chemical analyses for chloride,

nitrate, and sulfate by ion chromatography, soluble sodium and potassium by atomic absorption spectrophotometry, and ammonium by automated colorimetry. To audit the analysis of elements by XRF, six thin-film Micromatter pure-element deposits are submitted for routine XRF analysis.

3.0 AEROSOL MEASUREMENTS

Every measurement consists of four attributes: 1) a value; 2) a precision; 3) an accuracy; and 4) a validity (Hidy, 1985; Watson *et al.*, 1989a). The measurement methods described by Egami *et al.* (1991b) are used to obtain the value. Performance testing via regular submission of standards, blank analysis, and replicate analysis are used to estimate precision. These precisions are reported within the SJVAQS/AUSPEX data base so that they can be propagated through air quality models and used to evaluate how well different values compare with one another. The submission and evaluation of independent standards through quality audits are used to estimate accuracy. Validity applies both to the measurement method and to each measurement taken with that method. The validity of each measurement is indicated by appropriate flagging within the data base, while the validity of the methods has been evaluated in this study by a number of tests.

The precision, accuracy, and validity of the aerosol measurements are defined as follows:

- A measurement is an observation at a specific time and place which possesses four attributes: 1) value--the center of the measurement interval; 2) precision--the width of the measurement interval; 3) accuracy--the difference between measured and reference values; and 4) validity--the compliance with assumptions made in the measurement method.

- A measurement method is the combination of equipment, reagents, and procedures which provide the value of a measurement. The full description of the measurement method requires substantial documentation. For example, two methods may use the same sampling systems and the same analysis systems. These are not identical methods, however, if one performs acceptance testing on filter media and the other does not. Seemingly minor differences between methods can result in major differences between measurement values.

- Measurement method validity is the identification of measurement method assumptions, the quantification of effects of deviations from those assumptions, the ascertainment that deviations are within reasonable tolerances for the specific application, and the creation of procedures to quantify and minimize those

deviations during a specific application. A substantial effort was expended in SJVAQS/AUSPEX to establish the validity of measurement methods, especially for the measurements of elemental carbon, light absorption, and particle nitrate. Some of the method validity will be addressed in detail as part of the SARMAP data analysis tasks (Watson *et al.*, 1993b).

- Sample validation is accomplished by procedures which identify deviations from measurement assumptions and the assignment of flags to individual measurements for potential deviations from assumptions.

- The comparability and equivalence of sampling and analysis methods are established by the comparison of values and precisions for the same measurement obtained by different measurement methods. Interlaboratory and intralaboratory comparisons are usually made to establish this comparability. Simultaneous measurements of the same observable are considered equivalent when more than 90% of the values differ by no more than the sum of two one-sigma precision intervals for each measurement.

- Completeness measures how many environmental measurements with specified values, precisions, accuracies, and validities were obtained out of the total number attainable. It measures the practicality of applying the selected measurement processes throughout the measurement period. Data bases which have excellent precision, accuracy, and validity may be of little utility if they contain so many missing values that data interpretation is impossible.

A data base with numerous data points such as that in this study requires detailed documentation of precision, accuracy, and validity of the measurements. This section addresses the procedures followed to define these quantities and presents the results of those procedures.

3.1 Precision

Dynamic field blanks were periodically placed in each sampling system without air being drawn through them to estimate the magnitude of passive deposition for the period of time which filter packs remained in a sampler (typically 24 hours). Three to four field blanks were obtained per site per sampler. No significant inter-site differences in field blank concentrations were found between sites for any species after removal of outliers (i.e., concentration exceeding three

times the standard deviations of the field blanks). The average field blank concentrations (with outliers removed) were calculated for each species on each substrate ($PM_{2.5}$, PM_{10}, backup filter, gas). With only three or four field blank samples per site, inter-site differences are not statistically significant.

Blank precisions (σ_{Bi}) are defined as the larger of the standard deviation of the blank measurements, STD_{Bi}, or the square root of the averaged squared uncertainties of the blank concentrations, SIG_{Bi}. If the average blank for a species was less than its precision, the blank was set to zero. Dynamic field blank concentrations are given in Tables 3-1 and 3-2 for $PM_{2.5}$ and gaseous samples in μg/filter at the Blodgett and Tehachapi sites. Dynamic field blanks for the Yosemite and Sequoia Lower Keweah sites are reported by Chow *et al.* (1992) as part of the SJVAQS/AUSPEX aerosol measurements.

The precisions (σ_{Mi}) for x-ray fluorescence (XRF) analysis were determined from counting statistics unique to each sample. Hence, the σ_{Mi} is a function of the energy-specific peak area, the background, and the area under the baseline. These precisions were compared with the calculated precisions and were found to be equivalent for equivalent concentrations. Precisions for species concentrations obtained from other analytical methods were calculated for different concentration ranges. These precisions (σ_{Mi}) were determined separately for $PM_{2.5}$, PM_{10}, backup filter, and gaseous species. Where fractional uncertainties ($\bar{D}_{Mij}$) were found to vary with concentration, $\bar{D}_{Mij}$ were calculated for up to two concentration ranges to provide a reasonable statistical distribution. Ranges were selected to overestimate, rather than underestimate, measurement precision.

Table 3-1
Field Blank Concentrations and Precisions (μg/filter) for the $PM_{2.5}$ Front and Backup Filter and Gaseous Samples Collected at the Blodgett Site

Species[a]	Blank[b] Subtracted (B_i)	Blank[c] Precision (σ_{Bi})	Average Field Blank	Field Blank Std. Dev. (STD_{Bi})	Root Mean Squared Blank Precision (σ_{RMSi})	Total No. of Blank in Average
Mass	0.00	6.34	3.33	6.34	4.77	3
CLIC	1.3050	0.2762	1.3050	0.2762	0.1098	4
N3IC	1.4025	0.2318	1.4025	0.2318	0.0258	4
S4IC	2.1975	0.9775	2.1975	0.9775	0.0210	4
N4CC	0.5693	0.2215	0.5693	0.2215	0.0251	4
NAAC	0.6815	0.1266	0.6815	0.1266	0.1039	4
KPAC	0.9397	0.2973	0.9397	0.2973	0.1174	4
OCTC	56.2250	6.2203	56.2250	6.2203	4.4764	4
O1TC	22.7250	9.1921	22.7250	3.1204	9.1921	4
O2TC	10.1000	1.9757	10.1000	0.5701	1.9757	4
O3TC	19.0000	3.2688	19.0000	3.2688	2.3080	4
O4TC	4.4000	0.6806	4.4000	0.6745	0.6806	4
OPTC	0.0000	13.8000	0.0000	0.0000	13.8000	4
ECTC	8.0250	3.2782	8.0250	3.2782	1.2320	4
E1TC	4.0000	3.2272	4.0000	3.2272	1.5950	4
E2TC	4.0250	2.9936	4.0250	2.9936	0.4955	4
E3TC	0.0000	13.8000	0.0000	0.0000	13.8000	4
BKN3IC	2.2200	0.3262	2.2200	0.3262	0.0082	3
BKOCTC	52.9667	18.7265	52.9667	18.7265	5.5979	3
BKO1TC	4.9000	2.6420	4.9000	2.6420	0.6968	3
BKO2TC	5.9667	2.5382	5.9667	2.5382	0.5471	3
BKO3TC	24.0667	6.5652	24.0667	6.5652	4.6895	3
BKO4TC	8.5000	3.6914	8.5000	3.6914	3.3937	3
BKOPTC	9.5333	6.2804	9.5333	3.7026	6.2804	3
BKECTC	3.1333	0.9145	3.1333	0.2055	0.9145	3
BKE1TC	8.1333	4.0446	8.1333	0.7364	4.0446	3
BKE2TC	3.7333	2.2867	3.7333	2.2867	0.6320	3
BKE3TC	0.8000	7.9767	0.8000	0.6164	7.9767	3
ALXC	0.0000	0.1746	0.0227	0.0442	0.1746	3
SIXC	0.0000	0.1139	-0.0087	0.0390	0.1139	3
PHXC	0.0000	0.9900	0.0063	0.0194	0.9900	3
SUXC	0.0000	0.0961	-0.0545	0.0288	0.0961	3
CLXC	0.0000	0.1838	0.0029	0.0928	0.1838	3
KPXC	0.0000	0.1439	-0.0747	0.0593	0.1439	3
CAXC	0.0000	0.1313	0.0087	0.0415	0.1313	3
TIXC	0.0000	0.4229	-0.0243	0.0372	0.4229	3
VAXC	0.0000	0.2057	-0.0316	0.0522	0.2057	3
CRXC	0.0000	0.0582	-0.0097	0.0144	0.0582	3

Table 3-1 (continued)
Field Blank Concentrations and Precisions (μg/filter) for the $PM_{2.5}$ Front and Backup Filter and Gaseous Samples Collected at the Blodgett Site

Species[a]	Blank[b] Subtracted (B_i)	Blank[c] Precision (σ_{Bi})	Average Field Blank	Field Blank Std. Dev. (STD_{Bi})	Root Mean Squared Blank Precision (σ_{RMSi})	Total No. of Blank in Average
MNXC	0.0000	0.0329	-0.0069	0.0126	0.0329	3
FEXC	0.0259	0.0235	0.0259	0.0042	0.0235	3
COXC	0.0033	0.0171	0.0033	0.0020	0.0171	3
NIXC	0.0065	0.0167	0.0065	0.0020	0.0167	3
CUXC	0.0035	0.0200	0.0035	0.0026	0.0200	3
ZNXC	0.0268	0.0181	0.0268	0.0149	0.0181	3
GAXC	0.0170	0.0371	0.0170	0.0017	0.0371	3
ASXC	0.0000	0.0479	-0.0049	0.0103	0.0479	3
SEXC	0.0121	0.0241	0.0121	0.0060	0.0241	3
BRXC	0.0000	0.0222	-0.0101	0.0045	0.0222	3
RBXC	0.0000	0.0201	-0.0018	0.0024	0.0201	3
SRXC	0.0060	0.0218	0.0060	0.0022	0.0218	3
YTXC	0.0000	0.0262	0.0062	0.0102	0.0262	3
ZRXC	0.0000	0.0333	-0.0042	0.0004	0.0333	3
MOXC	0.0065	0.0541	0.0065	0.0049	0.0541	3
PDXC	0.0256	0.2085	0.0256	0.0235	0.2085	3
AGXC	0.1275	0.2378	0.1275	0.0781	0.2378	3
CDXC	0.0000	0.2393	0.0400	0.0562	0.2393	3
INXC	0.0000	0.2716	-0.0826	0.0193	0.2716	3
SNXC	0.0000	0.3360	0.0192	0.0621	0.3360	3
SBXC	0.0000	0.3601	-0.0610	0.0229	0.3601	3
BAXC	0.0000	1.0518	-0.4421	0.0837	1.0518	3
LAXC	0.0000	1.2510	0.0654	0.5094	1.2510	3
AUXC	0.0395	0.0598	0.0395	0.0021	0.0598	3
HGXC	0.0171	0.0524	0.0171	0.0058	0.0524	3
TLXC	0.0000	0.0503	-0.0114	0.0092	0.0503	3
PBXC	0.0180	0.0602	0.0180	0.0106	0.0602	3
URXC	0.0000	0.0472	0.0017	0.0097	0.0472	3
GSN3IC	2.5267	0.7285	2.5267	0.7285	0.0229	3
GSS4IC	6.5250	2.0828	6.5250	2.0828	0.0617	4
GSN4CC	4.5385	1.1233	4.5385	1.1233	0.0711	4

[a] See Table A-2 and Table A-3 from Appendix A for species identification.
[b] Values used in data processing. Non-zero average blank concentrations are subtracted when the average blank exceeds its standard deviation.
[c] Larger of either the analytical precision or standard deviation from the field.

Table 3-2
Field Blank Concentrations and Precisions (μg/filter) for $PM_{2.5}$ Front and Backup Filter and Gaseous Samples Collected at the Tehachapi Site

Species[a]	Blank[b] Subtracted (B_i)	Blank[c] Precision (σ_{Bi})	Average Field Blank	Field Blank Std. Dev. (STD_{Bi})	Root Mean Squared Blank Precision (σ_{RMSI})	Total No. of Blank in Average
MTGC	0.0000	17.5729	4.8333	17.5729	5.0900	6
CLIC	1.0500	0.2001	1.0500	0.2001	0.0540	4
N3IC	0.6675	0.0249	0.6675	0.0249	0.0248	4
S4IC	1.0575	0.1348	1.0575	0.1348	0.0784	4
N4CC	0.8205	0.1391	0.8205	0.1391	0.0084	4
NAAC	0.8588	0.2598	0.8588	0.2598	0.0124	4
KPAC	0.2054	0.1214	0.2054	0.1214	0.0390	4
OCTC	51.7000	5.5396	51.7000	2.4809	5.5396	4
O1TC	5.9000	3.6756	5.9000	1.2369	3.6756	4
O2TC	10.0000	3.3786	10.0000	0.7036	3.3786	4
O3TC	25.7750	4.5675	25.7750	1.5833	4.5675	4
O4TC	6.9250	2.0278	6.9250	2.0278	1.6179	4
OPTC	3.1000	0.4658	3.1000	0.4301	0.4658	4
ECTC	1.4750	0.6379	1.4750	0.6379	0.2883	4
E1TC	2.9000	0.9000	2.9000	0.9000	0.8312	4
E2TC	1.5750	0.2586	1.5750	0.2586	0.2057	4
E3TC	0.0000	11.9513	0.1000	0.1732	11.9513	4
BKN3IC	0.5367	0.1339	0.5367	0.1339	0.0069	6
BKOCTC	46.7000	6.6783	46.7000	6.6783	4.5618	6
BKO1TC	8.6500	1.4818	8.6500	1.4818	1.4632	6
BKO2TC	9.7167	1.4713	9.7167	1.4713	0.7729	6
BKO3TC	21.7667	3.8012	21.7667	3.8012	2.2112	6
BKO4TC	5.3000	0.9309	5.3000	0.9309	0.9082	6
BKOPTC	1.2667	8.3544	1.2667	1.2351	8.3544	6
BKECTC	2.0750	1.4940	2.0750	0.8757	1.4940	4
BKE1TC	1.3333	0.7180	1.3333	0.7180	0.5467	6
BKE2TC	1.2667	0.7157	1.2667	0.7157	0.5550	6
BKE3TC	0.0000	11.2677	0.0333	0.0471	11.2677	6
ALXC	0.0506	0.1739	0.0506	0.0487	0.1739	6
SIXC	0.0000	0.4532	0.1780	0.4532	0.1088	6
PHXC	0.0000	0.9931	0.0103	0.0400	0.9931	6
SUXC	0.0000	0.0901	0.0320	0.0375	0.0901	6
CLXC	0.0000	0.1939	-0.0904	0.0848	0.1939	6
KPXC	0.0000	0.1605	-0.0341	0.0775	0.1605	6
CAXC	0.0000	0.1327	-0.0353	0.0374	0.1327	6
TIXC	0.0000	0.4325	-0.0558	0.0576	0.4325	6
VAXC	0.0000	0.2074	-0.0523	0.0366	0.2074	6
CRXC	0.0000	0.0596	-0.0323	0.0254	0.0596	6
MNXC	0.0000	0.0349	-0.0059	0.0061	0.0349	6

Table 3-2 (continued)
Field Blank Concentrations and Precisions (μg/filter) for $PM_{2.5}$ Front and Backup Filter and Gaseous Samples Collected at the Tehachapi Site

Species[a]	Blank[b] Subtracted (B_i)	Blank[c] Precision (σ_{Bi})	Average Field Blank	Field Blank Std. Dev. (STD_{Bi})	Root Mean Squared Blank Precision (σ_{RMSi})	Total No. of Blank in Average
FEXC	0.0000	0.0277	0.0064	0.0169	0.0277	6
COXC	0.0000	0.0186	-0.0053	0.0044	0.0186	6
NIXC	0.0000	0.0175	0.0014	0.0036	0.0175	6
CUXC	0.0000	0.0211	0.0031	0.0149	0.0211	6
ZNXC	0.0000	0.0223	0.0013	0.0109	0.0223	6
GAXC	0.0000	0.0386	-0.0082	0.0228	0.0386	6
ASXC	0.0000	0.0493	-0.0124	0.0176	0.0493	6
SEXC	0.0040	0.0247	0.0040	0.0024	0.0247	6
BRXC	0.0000	0.0201	0.0039	0.0050	0.0201	6
RBXC	0.0000	0.0199	-0.0012	0.0021	0.0199	6
SRXC	0.0000	0.0224	-0.0079	0.0081	0.0224	6
YTXC	0.0000	0.0265	-0.0020	0.0052	0.0265	6
ZRXC	0.0000	0.0334	-0.0021	0.0067	0.0334	6
MOXC	0.0000	0.0546	-0.0183	0.0139	0.0546	6
PDXC	0.0000	0.2237	-0.0800	0.0907	0.2237	6
AGXC	0.0000	0.2507	0.0543	0.9900	0.2507	6
CDXC	0.0919	0.2514	0.0919	0.0873	0.2514	6
INXC	0.0000	0.2797	0.0382	0.0958	0.2797	6
SNXC	0.0000	0.3494	0.0188	0.1488	0.3494	6
SBXC	0.0000	0.3729	0.0111	0.1814	0.3729	6
BAXC	0.0000	1.0858	-0.0436	0.2011	1.0858	6
LAXC	0.0000	1.2959	-0.0035	0.3958	1.2959	6
AUXC	0.0000	0.0637	-0.0443	0.0397	0.0637	6
HGXC	0.0000	0.0530	-0.0073	0.0175	0.0530	6
TLXC	0.0000	0.0505	-0.0067	0.0084	0.0505	6
PBXC	0.0000	0.0622	-0.0018	0.0347	0.0622	6
URXC	0.0000	0.0480	-0.0009	0.0126	0.0480	6
GSN3IC	0.7700	0.1075	0.7700	0.1075	0.0182	6
GSS4IC	2.8640	0.4771	2.8640	0.4771	0.0651	5
GSN4CC	3.1713	0.3507	3.1713	0.3507	0.0182	6

[a] See Table A-2 and Table A-3 in Appendix A for species identification.
[b] Values used in data processing. Non-zero average blank concentrations are subtracted when the average blank exceeds its standard deviation.
[c] Larger of either the analytical precision or standard deviation from the field.

The root mean squared (RMS) precision, lower quantifiable limits (LQL), field blank levels, and concentration distribution is given in Table 3-3 for $PM_{2.5}$ aerosol and gaseous species for the Blodgett and Tehachapi sites. Similar statistical summaries were made by Chow *et al.* (1992) for the Yosemite and Sequoia Lower Keweah sites. The LQL is defined as a concentration corresponding to two times the precision of the dynamic field blank. The LQLs in Table 3-3 were divided by 8.5 m^3, the average volume of a 7-hour $PM_{2.5}$ sample. Actual volumes varied from sample to sample. These tables indicate that the RMS precisions are comparable in magnitude to the LQL calculated for the typical sample volume. Statistical distributions of chemical concentrations (i.e., the median, 5th percentile, and 95th percentile concentrations) for the entire data set are also given in these tables.

The number of reported (non-void, non-missing) concentrations for each species and the number of reported concentrations greater than the LQLs are also summarized in Table 3-3. $PM_{2.5}$ mass, sulfate (and sulfur), nitrate, and ammonium were detected in most cases. Several XRF elements were not detected very frequently, which is typical for regionally representative sites without influences from heavy industry. Al, Si, S, K, Ca, Mn, and Fe, were detected frequently, and most of these are abundant in resuspended dust.

3.2 Accuracy

Two performance audits of field operations were performed as part of the quality assurance (Gertler *et al.*, 1992). Both system and performance audits are performed during field measurements. Auditors acquired and reviewed the standard operating procedures and

Table 3-3

Precision, Lower Quantifiable Limits, and Distribution Statistics for $PM_{2.5}$ Aerosol and Gaseous Species at the Blodgett and Tehachapi Sites

Species[a] Code	RMS Precision[b] ($\mu g/m^3$)	LQL[c] ($\mu g/m^3$)	No.[d] Values	No. >LQL	Median ($\mu g/m^3$)	5th Percentile ($\mu g/m^3$)	95th Percentile ($\mu g/m^3$)
MTGC	5.9798	3.4882	101	65	8.7146	0.0000	19.8517
CLIC	0.0795	0.0642	101	15	0.0000	0.0000	0.2856
N3IC	0.0976	0.0948	101	99	0.3821	0.1606	3.1293
S4IC	0.2127	0.2120	101	101	1.5472	0.4429	3.4131
N4CC	0.0695	0.0526	101	97	0.5422	0.0640	1.3802
NAAC	0.0917	0.0524	101	62	0.0844	0.0000	0.2928
KPAC	0.0626	0.1016	101	10	0.0040	0.0000	0.1499
OCTC	2.5135	1.2348	85	35	0.8811	0.0000	6.1580
O1TC	3.1218	2.0567	85	3	0.0000	0.0000	1.3128
O2TC	1.5222	0.6512	85	20	0.2430	0.0000	2.0828
O3TC	1.7805	1.0002	85	23	0.6052	0.0000	1.7907
O4TC	0.8303	0.4633	85	50	0.5453	0.0000	1.3420
OPTC	4.3564	2.2973	85	0	0.7046	0.0000	1.4939
ECTC	0.6005	0.9500	85	32	0.6186	0.0000	2.8097
E1TC	0.6805	0.5723	85	40	0.5327	0.0000	2.0759
E2TC	0.4287	0.5771	85	40	0.5504	0.0305	1.5428
E3TC	5.6086	3.0374	85	0	0.2505	0.0835	0.5294
BKOCTC	3.5104	2.9327	101	5	0.0000	0.0000	2.7414
BKO1TC	0.8028	0.6188	101	36	0.2673	0.0000	1.6602
BKO2TC	0.6193	0.6098	101	35	0.3943	0.0000	1.3419
BKO3TC	1.6527	1.1806	101	7	0.0000	0.0000	1.4117
BKO4TC	0.6486	0.6399	101	4	0.0000	0.0000	0.4844
BKOPTC	4.8329	1.8177	101	2	0.0000	0.0000	0.9217
BKECTC	1.0197	0.3008	101	70	0.6319	0.0000	1.6254
BKE1TC	0.6997	0.7733	101	5	0.0000	0.0000	0.7424
BKE2TC	0.5026	0.4362	101	27	0.2569	0.0000	1.0572
BKE3TC	5.1452	2.4208	101	0	0.2021	0.0000	0.3842

Table 3-3 (continued)

Precision, Lower Quantifiable Limits, and Distribution Statistics for $PM_{2.5}$ Aerosol and Gaseous Species at the Blodgett and Tehachapi Sites

Species[a] Code	RMS Precision[b] ($\mu g/m^3$)	LQL[c] ($\mu g/m^3$)	No.[d] Values	No. >LQL	Median ($\mu g/m^3$)	5th Percentile ($\mu g/m^3$)	95th Percentile ($\mu g/m^3$)
ALXC	0.0772	0.0410	101	79	0.1264	0.0423	0.4063
SIXC	0.1496	0.0896	101	85	0.3258	0.0812	0.7468
PHXC	0.0576	0.0233	101	1	0.0000	0.0000	0.0148
SUXC	0.0571	0.0217	101	100	0.7119	0.2927	1.5892
CLXC	0.0865	0.0448	101	1	0.0000	0.0000	0.0242
KPXC	0.0531	0.0365	101	84	0.1125	0.0340	0.2443
CAXC	0.0475	0.0311	101	84	0.0859	0.0238	0.5606
TIXC	0.1895	0.1010	101	0	0.0088	0.0000	0.0267
VAXC	0.0858	0.0487	101	0	0.0017	0.0000	0.0080
CRXC	0.0239	0.0139	101	0	0.0000	0.0000	0.0027
MNXC	0.0149	0.0081	101	1	0.0026	0.0000	0.0072
FEXC	0.0132	0.0062	101	100	0.1363	0.0374	0.2933
COXC	0.0090	0.0043	101	1	0.0005	0.0000	0.0028
NIXC	0.0077	0.0041	101	0	0.0015	0.0000	0.0035
CUXC	0.0092	0.0049	101	3	0.0021	0.0000	0.0067
ZNXC	0.0076	0.0049	101	19	0.0019	0.0000	0.0159
GAXC	0.0171	0.0090	101	0	0.0008	0.0000	0.0037
ASXC	0.0219	0.0115	101	0	0.0000	0.0000	0.0022
SEXC	0.0109	0.0058	101	0	0.0011	0.0000	0.0027
BRXC	0.0089	0.0049	101	15	0.0035	0.0003	0.0120
RBXC	0.0091	0.0047	101	0	0.0000	0.0000	0.0009
SRXC	0.0099	0.0052	101	0	0.0009	0.0000	0.0030
YTXC	0.0118	0.0062	101	0	0.0000	0.0000	0.0016
ZRXC	0.0149	0.0079	101	0	0.0004	0.0000	0.0033
MOXC	0.0242	0.0128	101	0	0.0000	0.0000	0.0015

Table 3-3 (continued)

Precision, Lower Quantifiable Limits, and Distribution Statistics for $PM_{2.5}$ Aerosol and Gaseous Species at the Blodgett and Tehachapi Sites

Species[a] Code	RMS Precision[b] ($\mu g/m^3$)	LQL[c] ($\mu g/m^3$)	No.[d] Values	No. >LQL	Median ($\mu g/m^3$)	5th Percentile ($\mu g/m^3$)	95th Percentile ($\mu g/m^3$)
PDXC	0.0994	0.0515	101	0	0.0000	0.0000	0.0189
AGXC	0.1108	0.0580	101	0	0.0054	0.0000	0.0249
CDXC	0.1117	0.0582	101	0	0.0069	0.0000	0.0285
INXC	0.1235	0.0652	101	0	0.0000	0.0000	0.0150
SNXC	0.1558	0.0812	101	0	0.0101	0.0000	0.0463
SBXC	0.1657	0.0867	101	0	0.0010	0.0000	0.0333
BAXC	0.4802	0.2528	101	1	0.0000	0.0000	0.1018
LAXC	0.5774	0.3014	101	1	0.0000	0.0000	0.0992
AUXC	0.0281	0.0147	101	0	0.0006	0.0000	0.0065
HGXC	0.0235	0.0124	101	0	0.0000	0.0000	0.0032
TLXC	0.0226	0.0119	101	1	0.0000	0.0000	0.0012
PBXC	0.0274	0.0145	101	0	0.0050	0.0000	0.0099
URXC	0.0215	0.0112	101	1	0.0003	0.0000	0.0039
BKN3IC	0.0776	0.1936	101	53	0.2357	0.0000	1.9566
GSN3IC	0.2860	0.2195	101	97	2.0927	0.3667	10.2139
GSS4IC	0.2353	0.5449	100	59	0.9537	0.0000	4.6584
GSN4CC	0.2269	0.2385	100	80	0.6245	0.1076	6.6941

[a] See Table A-2 and A-3 of Appendix A for species identifications.

[b] RMS or root mean squared error is the square root of the average of the squared uncertainties of the individual uncertainties of the observations divided by the number of observations.

[c] LQL or lower quantifiable limit is equal to two times the uncertainty of the field blank. The LQL is expressed here in terms of mass per cubic meter, after dividing by 8.5 m^3, the nominal volume of a 7-hour sample.

[d] Number of non-voided (with -99) values reported.

examined all phases of measurement activities to assure that procedures were being followed and that operators were properly trained. Overall, all procedures reviewed by the auditors were acceptable and proved to be adequate for the study .

Performance audits establish whether the predetermined specifications are being achieved in practice. For field performance audits, the auditor used a flow meter traceable to a primary calibrator and verified the flow rates for each of the sampling systems. The results of this performance audit are summarized by Gertler *et al.* (1992).

Laboratory operations audits were performed in cooperation with the Navajo Generating Station Visibility Impairment Contribution Study (Gertler *et al.*, 1990).

Interlaboratory comparisons of over 100 filter-based samples, as well as laboratory spiked filters were submitted to four independent laboratories for gravimetric, x-ray fluorescence, ion chromatographic, automated colorimetric, and carbon analyses. Analysis of audit standards were within approximately 10% of the standard value for most species. It was concluded that the measurements acquired from these analyses were valid, accurate, and precise to the extent which can be determined by audit. Detailed audit results are documented by Gertler *et al.* (1990).

Interlaboratory measurements of particle absorption were performed between DRI and the University of California, Davis, as part of the SCENIC Denver Study (Watson *et al.*, 1988b). Light transmission measurements used to quantify particle absorption were precise, typically within $\pm 5\%$.

3.3 Data Validation

Level I validation consists of verifying field sampling parameters and ensuring that all samples collected were subjected to the specified chemical analyses. Field flags were assigned which indicate: 1) sampler malfunction and lost samples; 2) sample duration and flow rates outside of the specified ($\pm 10\%$) ranges; and 3) filter appearance (e.g., filter integrity, insects, discoloration). Comments by the field technicians noted on the field data sheets aided in assigning field data validation flags. Samples which were not collected because of power failures, machine malfunction, or operator error were voided at Level I. Similar flags were assigned during laboratory analysis. Various comparisons were made to determine the internal consistency of the data. Analytical flags indicate: 1) damaged filters or unusual material deposited on filters; 2) re-analysis; and/or 3) replacement of concentrations subsequent to re-analysis.

Frequency of occurrence of field flags for $PM_{2.5}$, PM_{10}, and gaseous samples at each site are summarized in Table 3-4. Field validation flags are presented in Table A-6 of Appendix A. These initially assigned field flags were further investigated as part of the Level II data validation.

Frequencies of laboratory chemical analysis validation flags are summarized in Table 3-5. Several of the samples were re-weighed and species were re-analyzed in the laboratory when inconsistencies were found during the data validation process. For example, some abnormal deposit area (e.g., possible leakage) was noted at the Tehachapi site. These laboratory validation flags are explained in Table A-7 of Appendix A.

Table 3-4
Frequency of Occurrence of Field Flags for the $PM_{2.5}$ Aerosol and Gaseous Samples at the Blodgett and Tehachapi Sites

Field Flags[a]	Blodgett		Tehachapi	
	$PM_{2.5}$	Gas	$PM_{2.5}$	Gas
F1	0	11	0	0
F2	0	0	0	0
F3	0	0	0	0
F4	0	0	0	0
F5	4	0	0	0
F6	0	0	2	0
G1	0	0	0	0
G2	0	0	0	0
G3	0	0	0	0
G4	0	0	0	0
G5	0	0	0	0
G6	0	0	0	0
H1	0	1	0	0
H2	0	0	0	0
H3	0	0	0	0
H4	0	0	0	0
I1	0	0	0	0
I2	0	0	0	0
I3	0	0	0	0
I4	0	0	0	0
I5	0	0	0	0
M	0	0	0	0
N1	2	0	1	0
N2	0	1	0	0
N3	0	0	0	0
P	0	0	0	0
Q1	0	4	0	0
Q2	0	0	0	0
Q3	0	0	0	0
Q4	0	0	0	0
Q5	0	0	0	0
Q6	0	0	0	0
R1	3	0	0	0
R2	0	0	0	0
S1	0	0	0	0
S2	0	0	0	0

Table 3-4 (continued)
Frequency of Occurrence of Field Flags for the $PM_{2.5}$ Aerosol and Gaseous Samples at the Blodgett and Tehachapi Sites

Field Flags[a]	Blodgett		Tehachapi	
	$PM_{2.5}$	Gas	$PM_{2.5}$	Gas
T1	0	0	6	7
T2	0	0	6	6
T3	0	0	0	0
T4	0	0	0	0
T5	1	1	1	2
T6	0	0	0	0
V	4	3	2	22
X	4	3	0	01
Z1	0	0	0	0
Z2	0	0	0	0

[a] See Table A-6 of Appendix A for field flags identification.

Table 3-5
Frequency of Occurrence of Laboratory Chemical Analysis Flags for the $PM_{2.5}$ Aerosol and Gaseous Samples at the Blodgett and Tehachapi Sites

Field Flags[a]	Blodgett		Tehachapi	
	$PM_{2.5}$	Gas	$PM_{2.5}$	Gas
c6	0	0	2	0
e1	0	0	0	0
e2	0	0	0	0
f1	0	0	0	0
f2	1	0	6	0
f3	1	0	0	0
f4	2	0	0	0
f5	0	0	0	0
f6	3	0	7	0
i1	0	0	1	0
i2	1	0	0	0
i3	0	0	0	0
i4	1	0	12	0
i5	0	0	0	0
i6	0	0	1	0
i7	0	0	0	0
i8	0	0	0	0
i9	0	0	0	0
j	0	0	0	0
l	0	0	0	0
y	0	0	0	0
n0	0	0	0	0
n1	0	0	0	0
n2	0	0	0	0
n3	0	0	0	0
n4	0	0	0	0
n5	0	0	0	0
n6	0	0	0	0
n7	0	0	0	0
n8	0	0	0	0
n9	0	0	0	0

Table 3-5 (continued)
Frequency of Occurrence of Laboratory Chemical Analysis Flags for the $PM_{2.5}$ Aerosol and Gaseous Samples at the Blodgett and Tehachapi Sites

Field Flags[a]	Blodgett		Tehachapi	
	$PM_{2.5}$	Gas	$PM_{2.5}$	Gas
n10	0	0	0	0
r1	0	0	0	0
r2	0	0	0	0
r3	0	0	0	0
r4	0	0	0	0
r5	0	0	0	0
r6	0	0	0	0
r7	0	0	0	0
r8	0	0	0	0
s	0	1	0	0
v	0	0	0	0
w3	4	0	0	0
w4	1	0	0	0
w5	0	0	0	0
x	0	0	0	0

[a] See Table A-6 of Appendix A for chemical analysis flags identification.

Level II validation evaluates the chemical data for internal consistency and for consistency with expected environmental behavior. Various comparisons were made for: 1) $PM_{2.5}/PM_{10}$ (ratios for the Yosemite and Sequoia Lower Keweah sites only); 2) sum of chemical species versus measured mass; 3) sulfate versus sulfur; 4) $PM_{2.5}$ particulate nitrate versus nitric acid denuded nitrate; and 5) ion balances. The comparisons were made for the Blodgett, Yosemite, Sequoia Lower Keweah, and Tehachapi sites.

3.3.1 $PM_{2.5}/PM_{10}$ Ratios

Both the $PM_{2.5}$ mass and chemical species concentrations should be less than or equal to the corresponding PM_{10} concentrations. The analysis of the $PM_{2.5}$ to PM_{10} ratios provides insight into the validity of the data base. Samples for which the $PM_{2.5}/PM_{10}$ ratio is greater than unity within three propagated precision intervals have been identified and summarized by Chow *et al.* (1992). Outliers are defined for which the difference between the $PM_{2.5}$ and PM_{10} species is greater than three times the square root of the sum of the square uncertainties (i.e., $PM_{2.5} - PM_{10} > 3 \times [\sigma^2_{PM2.5} + \sigma^2_{PM10}]^{1/2}$). Figure 3-1 displays scatterplots of PM_{10} versus $PM_{2.5}$ mass, sulfur, and silicon, at the Yosemite and Sequoia Lower Keweah sites. These chemical species were selected because they are measured on both the $PM_{2.5}$ and PM_{10} samples. Linear regression statistics (excluding the outliers) are also reported in Table 3-6 for each of these scatterplots with PM_{10} as the independent variable and $PM_{2.5}$ as the dependent variable.

The $PM_{2.5}$ to PM_{10} mass ratios are generally below the one-to-one lines as shown in Figure 3-1. Approximately 80% of the PM_{10} is in the $PM_{2.5}$ fraction at the Yosemite site with good ($r^2 = 0.94$) correlation. The Sequoia Lower Keweah site experienced a very low

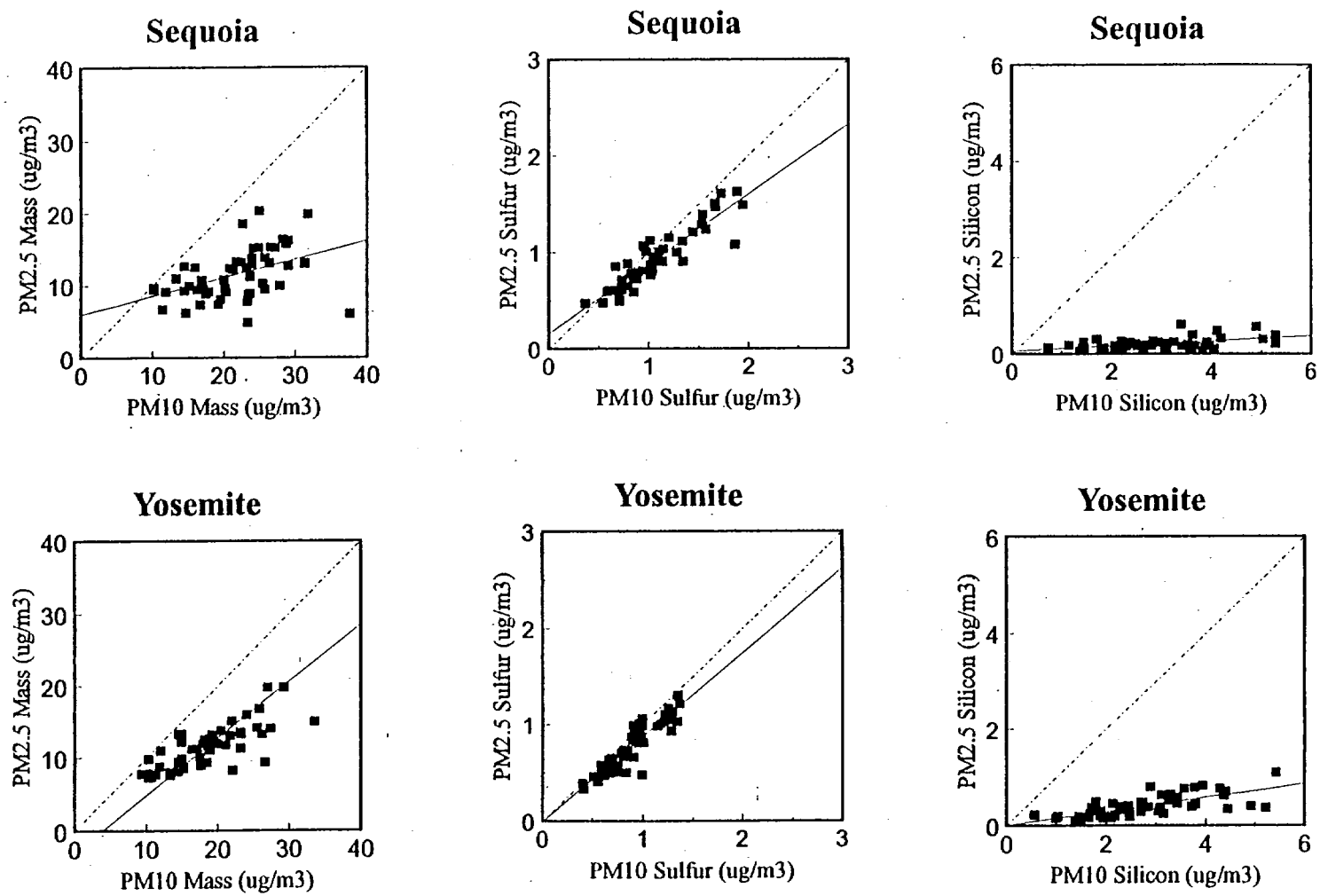

Figure 3-1. Scatterplots of $PM_{2.5}$ Versus PM_{10} Mass Sulfur, and Silicon Concentrations at the Sequoia Lower Research and Yosemite Sites.

Table 3-6
Linear Regression Statistics of $PM_{2.5}$ and PM_{10} Mass and Chemical Species

	Sum of Species vs. Mass				Mesured vs. Calculated Sulfate vs. Sulfur				Measured vs. Calculated Front NO_3 vs. Total NO_3				Front OC vs. Backup OC				NH_4 (w/o correction)				NH_4 (w/correction)			
	b[a]	a[b]	r^2	n	b	a	r^2	n	b	a	r^2	n	b	a	r^2	n	b	a	r^2	n	b	a	r^2	n
$PM_{2.5}$ Species																								
Blodgett	0.39	1.78	0.55	49	1.86	0.03	0.73	49	0.58	0.10	0.90	36	0.42	-0.11	0.41	50	0.86[c]	0.24[c]	0.65[c]	49[c]	0.76[c]	0.20[c]	0.76[c]	12[c]
																	0.44[c]	0.18[c]	0.45[c]	49[c]	0.37[c]	0.15[c]	0.62[c]	11[c]
Yosemite	0.66	7.57	0.86	55	2.16	0.02	0.90	55	0.65	-0.00	0.62	43	0.11	6.65	0.12	54	0.94[c]	0.30[c]	0.75[c]	55[c]	0.95[c]	0.19[c]	0.79[c]	30[c]
																	0.49[d]	0.18[d]	0.68[d]	55[d]	0.46[d]	0.10[d]	0.72[d]	29[d]
Sequoia	0.48	5.39	0.32	51	1.94	0.21	0.78	52	0.33	0.06	0.43	50	0.19	2.46	0.08	37	0.97[c]	0.14[c]	0.94[c]	52[c]	0.85[c]	0.11[c]	0.88[c]	34[c]
																	0.49[d]	0.11[d]	0.86[d]	52[d]	0.36[d]	0.08[d]	0.61[d]	34[d]
Tehachapi	0.45	5.54	0.44	54	1.92	0.20	0.92	110	0.71	-0.43	0.82	42	0.56	0.30	-1.45	27	1.02[c]	0.24[c]	0.78[c]	115[c]	0.95[c]	0.16[c]	0.75[c]	25[c]
																	0.69[d]	0.15[d]	0.58[d]	115[d]	0.51[d]	0.21[d]	0.45[d]	96[d]

	$PM_{2.5}$ vs. PM_{10} Mass				$PM_{2.5}$ vs. PM_{10} Sulfur				$PM_{2.5}$ vs. PM_{10} Silicon			
	b[a]	a[b]	r^2	n	b	a	r^2	n	b	a	r^2	n
Yosemite	0.79	-3.0	0.94	54	0.88	-0.01	0.82	54	0.14	0.01	0.56	55
Sequoia	0.26	5.95	0.19	51	0.72	0.16	0.82	47	0.05	0.06	0.31	52

[a] b = slope
[b] a = intercept

correlation ($r^2 = 0.19$), even though the $PM_{2.5}$ mass are, in general, less than or equal to the PM_{10} mass.

Sulfur and silicon concentrations are acquired by x-ray fluorescence analysis on Teflon-membrane filters. Concentration ranges were generally low for the $PM_{2.5}$ and PM_{10} sulfur with median concentrations of ~ 1.0 $\mu g/m^3$. The slopes are approximately 20% higher at the Yosemite site with respect to the Sequoia Lower Keweah site, with correlations greater than 0.82. As expected, the majority of the sulfur are in the $PM_{2.5}$ fractions. Total sulfur concentrations were ~ 0.5 to 1.0 $\mu g/m^3$ higher at the Sequoia Lower Keweah site as compared to the Yosemite site.

Silicon is known to be enriched in coarse particle geological material. It is expected that PM_{10} silicon generally exceeds $PM_{2.5}$ silicon by large amounts. Poor correlations ($r^2 \leq 0.31$) were found for $PM_{2.5}$ versus PM_{10} silicon at the Sequoia Lower Keweah site. It is suspected that some of the coarse particles penetrated through the cyclone preseparator and were collected on the $PM_{2.5}$ samples. Chow *et al.* (1992b) flagged several of the suspect sample pairs at this site.

The examples given in Figure 3-1 show how the data validation process provides explanations for physical inconsistencies in the data set. Chow *et al.* (1992) documented the sampling site, date, period, and the suspect chemical species concentrations which have been discovered as inconsistent in the data base.

3.3.2 Sum of Chemical Species versus Measured Mass

The sum of the individual chemical concentrations for $PM_{2.5}$ and PM_{10} should be less than or equal to the corresponding mass loadings measured by gravimetric analysis. The sum of chemical species is calculated as a direct sum of Teflon and front quartz filter species concentrations. Chemical species measured more than once by different chemical analyses methods such as soluble sodium, chloride, and potassium, and total sulfur are excluded from the sum. No weighting was applied in these calculations since weighting the sum by converting metals to their respective oxides and organic carbon to some "typical" molecular weight compound imposes unnecessary assumptions for validation purposes. PM_{10} size fractions were not acquired at the Blodgett and Tehachapi sites and no such comparison were made. Therefore, Figures 3-2 to 3-5 show the scatterplots of $PM_{2.5}$ sum of species versus mass at all sites. Each plot contains a line indicating the 1:1 relationship as well as regression statistics with mass as the independent variable and sum of species as the dependent variable. The sum of chemical species is expected to be less than total mass since several important species (e.g., oxygen, hydrogen) have not been measured.

These figures show that the majority of the sum of species are less than the corresponding mass at the Blodgett and Tehachapi sites. The correlations are high at the Yosemite ($r^2 = 0.86$), and low ($r^2 = 0.32$) at the Sequoia Lower Keweah site. The sum of species at these sites is consistently lower than the measured mass, particularly at higher concentrations, where organic carbon and crustal elements constitute a large fraction of the mass.

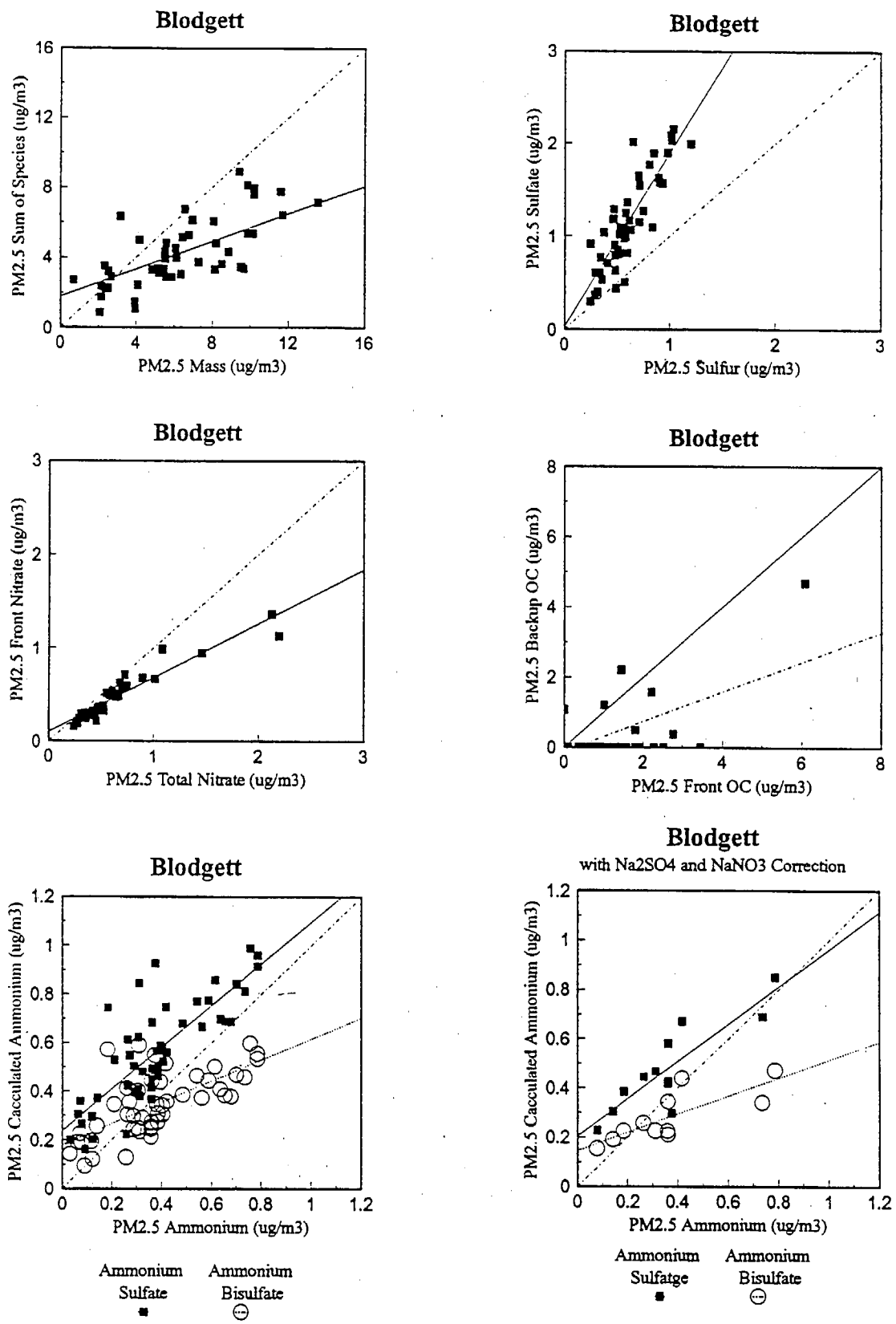

Figure 3-2. Scatterplots of $PM_{2.5}$ Sum of Species Versus Mass, Sulfate Versus Sulfur, Front Versus BAckup Filter Nitrate and Carbon, and Calculated Versus Measured Ammonium at the Blodgett Site.

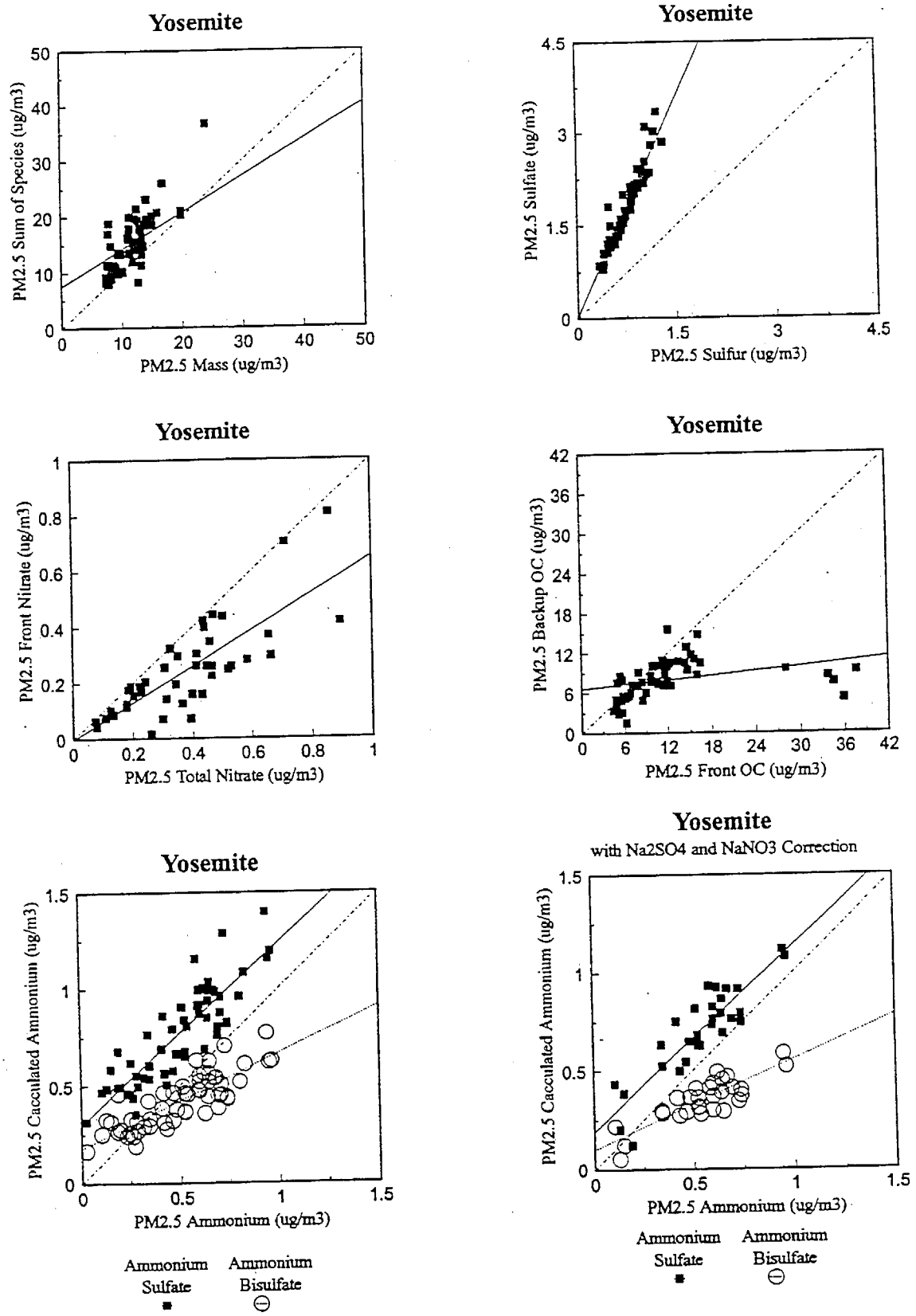

Figure 3-3. Scatterplots of $PM_{2.5}$ Sum of Species Versus Mass, Sulfate Versus Sulfur, Front Versus Backup Filter Nitrate and Carbon, and Calculated Versus Measured Ammonium at the Yosemite Site.

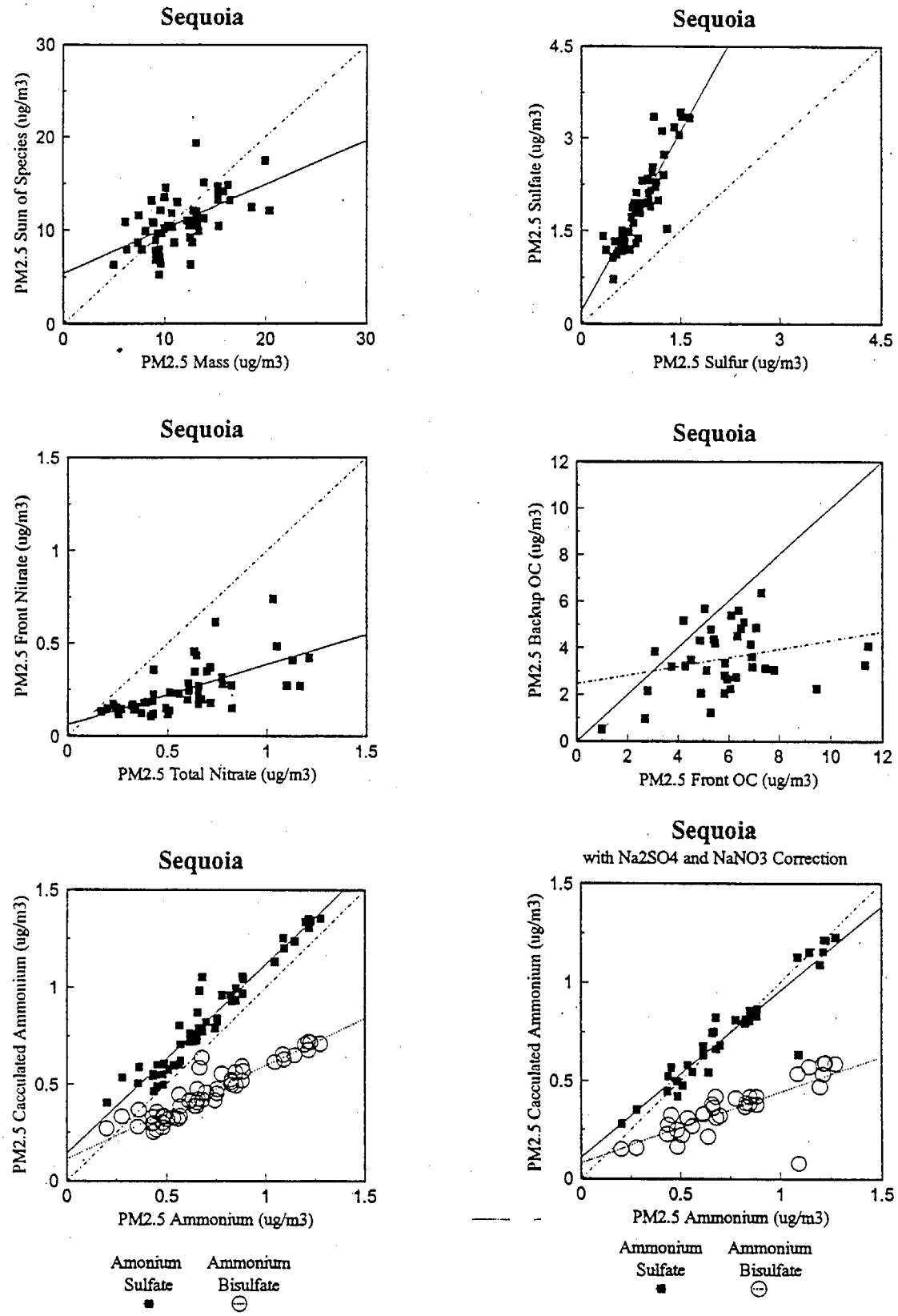

Figure 3-4. **Scatterplots of $PM_{2.5}$ Sum of Species Versus Mass, Sulfate Versus Sulfur, Front Versus Backup Filter Nitrate and Carbon, and Calculated Versus Measured Ammonium at the Sequoia Lower Keweah Site.**

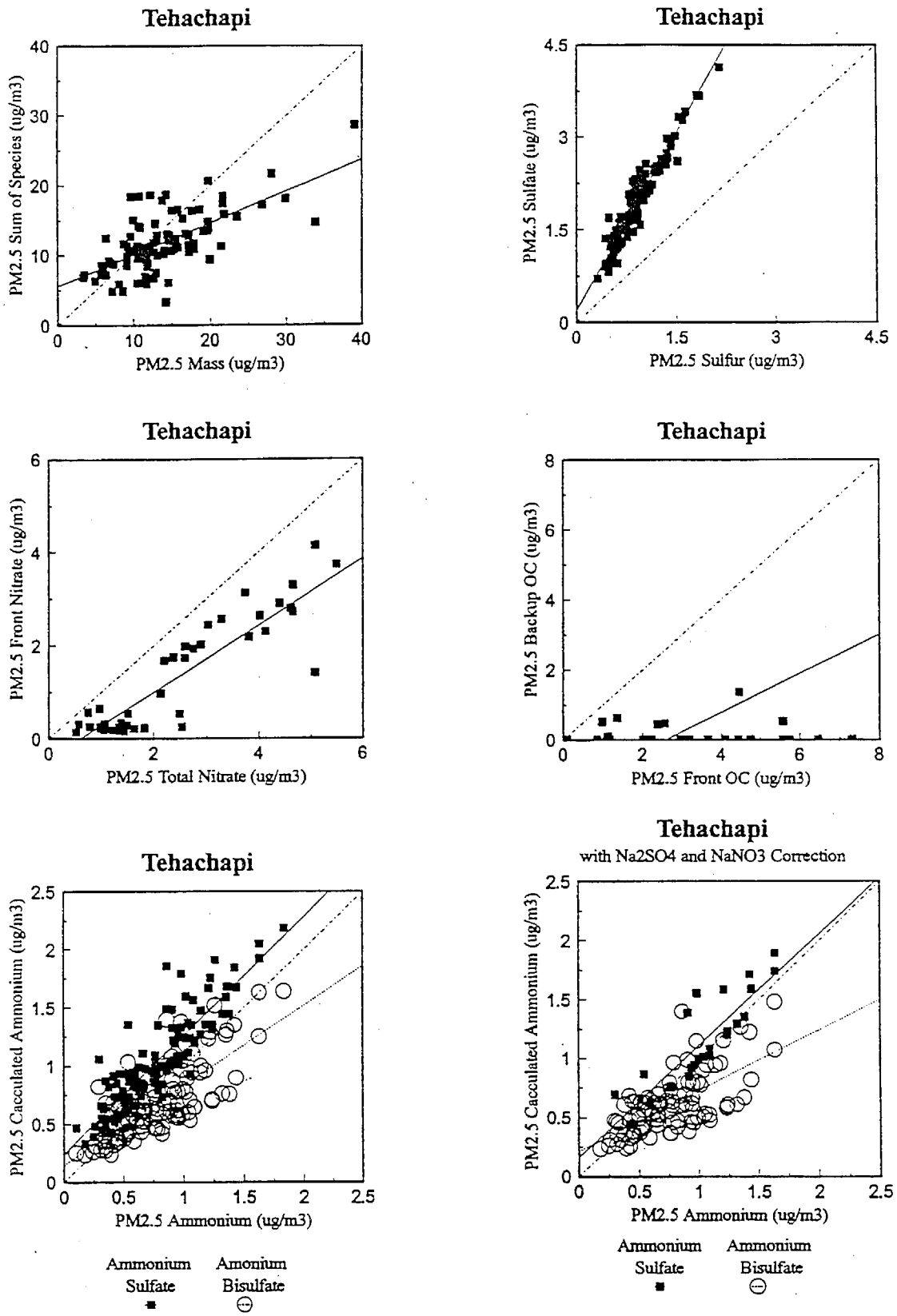

Figure 3-5. Scatterplots of $PM_{2.5}$ Sum of Species Versus Mass, Sulfate Versus Sulfur, Front Versus Backup Filter Nitrate and Carbon, and Calculated Versus Measured Ammonium at the Tehachapi Site.

3.3.3 Physical Consistency

Composition of chemical species concentrations measured by different methods can be examined for a few cases. Sulfate ($SO_4^=$) is acquired by ion chromatographic analysis on quartz-fiber filters and total sulfur (S) is obtained by x-ray fluorescence analysis on Teflon-membrane filters of the sequential filter samplers. The $SO_4^=$ to S ratio should equal "three" if all of the sulfur is present as soluble sulfate. Table 3-6 shows that the slopes of sulfate versus sulfur ranges from 1.9 at the Blodgett and Sequoia Lower Keweah sites, to 2.4 at the Yosemite site. Water insoluble sulfur may exist on these samples. Even though the sulfate versus sulfur ratios are 20% to 30% lower than expected, the correlations appear to be reasonable ($r^2 \geq 0.73$)

$PM_{2.5}$ nitrate (i.e., non-volatilized nitrate) from the front quartz-fiber filters is compared with $PM_{2.5}$ total particulate nitrate (i.e., non-volatilized plus volatilized nitrate, also termed nitric acid denuded nitrate) from the quartz/nylon filter packs which was preceded by a nitric acid denuder. The nylon backup filters were intended to capture the volatilized particulate nitrate from the front quartz-fiber filters. The $PM_{2.5}$ total nitrate should be greater than or equal to the $PM_{2.5}$ nitrate, depending on the extent of volatilization.

Figures 3-2 to 3-5 show scatterplots of $PM_{2.5}$ particulate nitrate versus $PM_{2.5}$ total nitrate for the four sites. Secondary ammonium nitrate is not a stable compound. Its equilibrium with gaseous ammonia and nitric acid is strongly influenced by temperature and relative humidity (Watson *et al.*,1993c). The dissociation of particulate nitrate from the front quartz filters is higher in the summer time when temperatures are higher. Figures 3-2 to 3-5 yield a slope of 0.33 for the Sequoia Lower Keweah site and 0.71 for the Tehachapi site, with an insignificant intercept. It indicates that approximately 30% to 60% of the particulate nitrate from the front

quartz filters volatilized during summer. The variations in volatilization are greater in the Yosemite and Sequoia Lower Keweah sites ($0.43 \leq r^2 \leq 0.62$) as compared to the Blodgett and Tehachapi sites ($0.82 \leq r^2 \leq 0.90$). Volatilized nitrate is not part of the measured $PM_{2.5}$ mass.

A backup quartz filter was installed behind the Teflon-membrane filter in the DRI sequential filter sampler to estimate the magnitude of artifact organic carbon. As shown in Figures 3-2 to 3-5, the magnitude of gaseous organic carbon on the quartz-fiber backup filters varied significantly from site to site. The slope of front versus backup organic carbon were 0.11 at the Yosemite site to 0.56 at the Tehachapi site. The backup organic carbon are generally below the LQLs of 3.5 $\mu g/m^3$ at the Blodgett and Tehachapi sites. As expected, the correlations are poor at all sites. Gaseous organic carbon concentrations were also higher in the forested region such as Yosemite and Sequoia Lower Keweah sites, where volatile or semi-volatile organic carbon such as β-pinene and pinonaldehyde are suspected to be enriched (e.g., Simoneit and Mazurek, 1982; Pandis *et al.*, 1991).

3.3.4 Ion Balances

Ammonium nitrate (NH_4NO_3), sodium nitrate ($NaNO_3$), sodium sulfate (Na_2SO_4), ammonium sulfate ($(NH_4)_2SO_4$), and ammonium bisulfate (NH_4HSO_4) are the most likely nitrate and sulfate compounds in the Sierra Nevada. Ammonium (NH_4^+) can be calculated based on the stoichiometric ratios of the different compounds and compared with that which was measured.

Two cases were examined for the ammonium balance:

- Case I: where nitrate and sulfate or bisulfate are balanced by equivalent ammonium.

- Case II: where some of the sulfate, calculated from soluble or elemental sodium, is assumed to come from sea salt and some of the nitrate is associated with sea salt sodium (Na^+) in an amount equivalent to the reduction of chloride (Cl^-) from its seawater Cl^-/Na^+ ratio.

"Case I" assumes that sulfate is either ammonium sulfate or ammonium bisulfate, and that all of the particulate nitrate is in the form of ammonium nitrate. Measured ammonium concentrations should equal those calculated from ammonium bisulfate or ammonium sulfate and ammonium nitrate on a molar to molar basis. The following steps were applied in these calculations:

- Assuming all sulfate is ammonium sulfate:

$$\text{calculated ammonium} = 0.38 \times \text{sulfate} + 0.29 \times \text{nitrate}$$

- Assuming all sulfate is ammonium bisulfate:

$$\text{calculated ammonium} = 0.192 \times \text{sulfate} + 0.29 \times \text{nitrate}$$

The ammonium, nitrate, and sulfate concentrations used in these comparisons are those measured on the front quartz-fiber filters for the $PM_{2.5}$ fraction. The above comparisons assume that nitrate lost by volatilization of ammonium nitrate from the front quartz-fiber filter depletes both particulate ammonium and nitrate.

Measured and calculated ammonium are plotted in the lower left-hand corner of Figures 3-2 to 3-5 for the four sites. Each figure contains calculated ammonium based for both the ammonium sulfate and ammonium bisulfate cases. Three types of ion balances are exhibited in these figures:

- The majority of ammonium bisulfate points are on the 1:1 line. This suggests that ammonium bisulfate is the dominant species and most of the sulfuric acid was not completely neutralized by ammonia. The $PM_{2.5}$ ion balance at the Edison site (Figure 3-3) shows this tendency, at least when ammonium concentrations were low.

- The majority of ammonium sulfate points are on the 1:1 line. This suggests that ammonium sulfate is the dominant species at the sampling site. The $PM_{2.5}$ ion balance at the Tehachapi site (Figure 3-5) shows this tendency, at least when ammonium concentrations were low.

- The 1:1 line lies between the ammonium sulfate and ammonium bisulfate points. This suggests a mixture of both ammonium sulfate and ammonium bisulfate in the environment. The $PM_{2.5}$ ion balance at the Sequoia Lower Keweah site (Figure 3-4), shows this tendency.

In "Case II", the ammonium balance is refined by subtracting sulfate and nitrate which might occur as sodium sulfate (Na_2SO_4) or sodium nitrate ($NaNO_3$) . This can occur by reaction of sulfuric and nitric acids with sodium chloride (NaCl). If this is the case, the sulfate (i.e., Na_2SO_4) concentration is equal to $0.25 \times Na^+$ (Pytcowicz and Kester, 1971). The following steps were applied to re-calculated ammonium by subtracting for sodium sulfate:

- Calculate sulfate in sodium sulfate as $0.25 \times Na^+$;

- Convert the sulfate as sodium sulfate to equivalents of ammonium, as ammonium bisulfate or ammonium sulfate according to the relationships given in "Case I"; and

- Subtract this ammonium equivalent from the total calculated ammonium.

Steps were also taken to estimate the amount of nitrate associated with sodium nitrate:

- Calculate the chloride deficit (Cl_d^-) for sodium chloride as $1.8 \times Na^+$ minus Cl^-;

- If Cl_d^- is less than zero, sodium nitrate is zero; if Cl_d^- is greater than zero, calculate an equivalent nitrate concentration corresponding to the chloride deficit as $2.6956 \times Cl_d^-$, where 2.6956 is the stoichiometric ratio of nitrate to sodium in sodium nitrate;

- Convert this sodium nitrate to an ammonium equivalent using the relationships given in "Case I; and

- Subtract this ammonium equivalent from the total calculates ammonium.

For comparison, the lower right-hand corner of Figures 3-2 to 3-5 display the calculated ammonium (less sodium sulfate and sodium nitrate) versus measured ammonium for $PM_{2.5}$ size

fraction at the three sites. These figures show that subtracting the calculated ammonium for sodium nitrate and sodium sulfate has two effects: 1) it reduces the scatter in the ion balance; and 2) it shifts the points downward so than the ammonium sulfate points line up along the 1:1 line. The effects are least evident for $PM_{2.5}$ at the Tehachapi site (Figure 3-5) where some of the estimated ammonium was still lower than the measured values. Figures 3-2 to 3-5 thus suggest that ammonium sulfate is the dominant species in most cases and that sulfate and nitrate from marine aerosol exist, but not at significant levels.

These cation/anion balances support the accuracy and precision of the nitrate, sulfate, and ammonium measurements on $PM_{2.5}$ front quartz-fiber filters, since such close agreement would not be found if these analyses were invalid. This balance also demonstrates that most of the nitrate and sulfate present in these particle samples occurs as ammonium nitrate and ammonium sulfate.

3.4 Statistical Summary of 24-hour Mass and Chemical Concentrations

Tables 3-7 and 3-8 present averages, standard deviations and maximum concentrations for 24-hour average $PM_{2.5}$ concentrations at the Blodgett and Tehachapi sites as well as $PM_{2.5}$ and PM_{10} concentrations at the Yosemite and Sequoia Lower Keweah sites. A sample-volume weighted average of the four diurnal samples (i.e., 0000 to 0700, 0700 to 1200, 1200 to 1700, 1700 to 2400 PDT) taken during the 14 SJVAQS/AUSPEX episode days was calculated to obtain the 24-hour concentrations. The diurnal averages in these tables are useful for comparison with results from other studies and they can be related to the 24-hour federal PM_{10} standard. The particulate nitrate and ammonium concentrations reported in this table represent those measured

Table 3-7
Statistical Summary of 24-hour $PM_{2.5}$ Measurements Between 7/13/90 and 8/24/90
During the Fourteen SJVAQS/AUSPEX Episode Days

Chemical Species	Sequoia Lower Keweah Average (μg/m³)	Std. Dev. (μg/m³)	Maximum (μg/m³)	No. in Average	Tehachapi Average (μg/m³)	Std. Dev. (μg/m³)	Maximum (μg/m³)	No. in Average
Mass	10.74	2.26	15.19	14	11.21	4.99	18.31	12
Chloride (Cl^-)	0.0103	0.0075	0.0301	14	0.0388	0.0304	0.1055	12
Nitrate (NO_3^-)	0.2432	0.0824	0.3844	14	1.2859	1.0647	3.0616	12
Sulfate ($SO_4^=$)	2.0072	0.5311	3.0848	14	2.1032	0.7456	3.0730	12
Ammonium (NH_4^+)	0.7117	0.2014	1.1334	14	0.8997	0.3178	1.2248	12
Soluble Sodium (Na^+)	0.0830	0.0360	0.1354	14	0.1029	0.0496	0.2402	12
Soluble Potassium (K^+)	0.0756	0.0344	0.1441	14	0.0848	0.0779	0.3081	12
Organic Carbon (OC)	5.3238	1.1927	7.0036	14	2.0654	2.3245	7.8050	12
Elemental Carbon (EC)	1.6410	0.4798	2.9638	14	1.0270	0.8879	2.3184	12
Aluminum (Al)	0.1209	0.0828	0.3962	14	0.1103	0.0500	0.2204	12
Silicon (Si)	0.2006	0.0721	0.4191	14	0.3675	0.1472	0.7348	12
Phosphorus (P)	0.0000	0.0001	0.0003	14	0.0007	0.0012	0.0038	12
Sulfur (S)	0.8572	0.2634	1.4562	14	1.0014	0.3758	1.5249	12
Chlorine (Cl)	0.0041	0.0069	0.0261	14	0.0113	0.0258	0.0959	12
Potassium (K)	0.1388	0.0403	0.2300	14	0.1402	0.0409	0.2023	12
Calcium (Ca)	0.0355	0.0068	0.0470	14	0.0850	0.0348	0.1486	12
Titanium (Ti)	0.0037	0.0020	0.0066	14	0.0081	0.0042	0.0153	12
Vanadium (V)	0.0006	0.0005	0.0015	14	0.0008	0.0006	0.0023	12
Chromium (Cr)	0.0005	0.0004	0.0013	14	0.0001	0.0002	0.0005	12
Manganese (Mn)	0.0015	0.0008	0.0034	14	0.0023	0.0012	0.0043	12
Iron (Fe)	0.0742	0.0180	0.1185	14	0.1416	0.0437	0.2290	12
Cobalt (Co)	0.0006	0.0005	0.0020	14	0.0003	0.0002	0.0007	12
Nickel (Ni)	0.0005	0.0004	0.0013	14	0.0018	0.0007	0.0029	12
Copper (Cu)	0.0030	0.0016	0.0069	14	0.0042	0.0026	0.0114	12
Zinc (Zn)	0.0103	0.0061	0.0261	14	0.0075	0.0039	0.0154	12
Gallium (Ga)	0.0007	0.0005	0.0016	14	0.0006	0.0007	0.0022	12
Arsenic (As)	0.0005	0.0004	0.0016	14	0.0006	0.0003	0.0012	12
Selenium (Se)	0.0005	0.0004	0.0015	14	0.0005	0.0004	0.0012	12
Bromine (Br)	0.0045	0.0010	0.0064	14	0.0071	0.0026	0.0117	12
Rubidium (Rb)	0.0006	0.0004	0.0014	14	0.0002	0.0001	0.0004	12
Strontium (Sr)	0.0008	0.0004	0.0016	14	0.0003	0.0002	0.0009	12
Yttrium (Yt)	0.0003	0.0003	0.0011	14	0.0002	0.0003	0.0009	12
Zirconium (Zr)	0.0007	0.0006	0.0020	14	0.0008	0.0004	0.0015	12
Molybdenum (Mo)	0.0014	0.0006	0.0026	14	0.0001	0.0002	0.0006	12
Palladium (Pd)	0.0064	0.0043	0.0148	14	0.0014	0.0017	0.0049	12
Silver (Ag)	0.0059	0.0037	0.0120	14	0.0061	0.0029	0.0113	12
Cadmium (Cd)	0.0042	0.0043	0.0125	14	0.0100	0.0033	0.0146	12
Indium (In)	0.0028	0.0018	0.0058	14	0.0031	0.0024	0.0083	12
Tin (Sn)	0.0091	0.0063	0.0222	14	0.0123	0.0054	0.0238	12
Antimony (Sb)	0.0057	0.0049	0.0157	14	0.0116	0.0064	0.0236	12
Barium (Ba)	0.0477	0.0227	0.0864	14	0.0347	0.0215	0.0667	12
Lanthanum (La)	0.0154	0.0120	0.0332	14	0.0230	0.0127	0.0438	12
Gold (Au)	0.0014	0.0008	0.0027	14	0.0003	0.0005	0.0018	12
Mercury (Hg)	0.0013	0.0006	0.0023	14	0.0004	0.0003	0.0010	12

Table 3-7 (continued)
Statistical Summary of 24-hour $PM_{2.5}$ Measurements Between 7/13/90 and 8/24/90
During the Fourteen SJVAQS/AUSPEX Episode Days

Average Chemical Species (μg/m³)	Sequoia Lower Keweah Average Standard (μg/m³)	Std. Dev. Maximum (μg/m³)	Maximum No. in (μg/m³) Average	No. in Average	Tehachapi Average (μg/m³)	Std. Dev. (μg/m³)	Maximum (μg/m³)	No. in Average
Thallium (Tl)	0.0001	0.0001	0.0004	14	0.0002	0.0002	0.0007	12
Lead (Pb)	0.0042	0.0010	0.0065	14	0.0038	0.0021	0.0071	12
Uranium (Ur)	0.0006	0.0005	0.0018	14	0.0004	0.0005	0.0015	12
Nylon Backup NO_3^-	0.3055	0.1501	0.5350	14	1.0625	0.4884	1.9852	12
Nitric Acid plus NO_3^-	2.3852	0.4051	2.9915	14	5.6597	2.0995	8.3683	12
Nitric Acid	1.8664	0.3744	2.4366	14	4.6720	1.8763	7.4746	12
Sulfur Dioxide (SO_2)	1.2682	0.5948	2.0972	14	2.9213	1.0208	4.4943	12
Ammonia (NH_3)	3.3216	0.5298	4.4654	14	3.5028	1.1983	5.3942	12
Absorption by Particles (b_{sp})[a]	0.0[b]	0.0[b]	0.0[b]	0[b]	25.4303	6.8830	34.8668	12

[a] Unit in Mm^{-1}
[b] Measurement not available

Table 3-7
Statistical Summary of 24-hour $PM_{2.5}$ Measurements Between 7/13/90 and 8/24/90
During the Fourteen SJVAQS/AUSPEX Episode Days

	Blodgett				Yosemite			
Chemical Species	Average (μg/m³)	Std. Dev. (μg/m³)	Maximum (μg/m³)	No. in Average	Average (μg/m³)	Std. Dev. (μg/m³)	Maximum (μg/m³)	No. in Average
Mass	5.99	3.07	12.12	14	15.73	9.79	38.012	14
Chloride (Cl^-)	0.0391	0.0934	0.3694	14	0.0590	0.0515	0.1651	14
Nitrate (NO_3^-)	0.3903	0.1905	0.9101	14	0.2264	0.1000	0.4567	14
Sulfate ($SO_4^=$)	1.0631	0.4862	1.9557	14	1.7943	0.4967	2.5275	14
Ammonium (NH_4^+)	0.3431	0.1976	0.7287	14	0.4880	0.1996	0.8198	14
Soluble Sodium (Na^+)	0.0893	0.0985	0.3501	14	0.0936	0.0653	0.2354	14
Soluble Potassium (K^+)	0.0295	0.0924	0.3606	14	0.0622	0.0313	0.1362	14
Organic Carbon (OC)	0.6502	0.4951	1.5848	14	11.8572	6.1158	25.8188	14
Elemental Carbon (EC)	0.3858	0.2631	1.0782	14	1.8285	0.8083	3.5152	14
Aluminum (Al)	0.1707	0.0774	0.2788	14	0.1540	0.0574	0.2418	14
Silicon (Si)	0.2882	0.1357	0.5432	14	0.3806	0.1255	0.6091	14
Phosphorus (P)	0.0038	0.0035	0.0110	14	0.0003	0.0007	0.0027	14
Sulfur (S)	0.5569	0.2186	0.9644	14	0.7511	0.2026	1.0344	14
Chlorine (Cl)	0.0036	0.0041	0.0121	14	0.0111	0.0176	0.0713	14
Potassium (K)	0.0852	0.0406	0.1906	14	0.1458	0.0393	0.2263	14
Calcium (Ca)	0.2179	0.1926	0.8324	14	0.0806	0.0282	0.1723	14
Titanium (Ti)	0.0114	0.0063	0.0246	14	0.0091	0.0054	0.0199	14
Vanadium (V)	0.0037	0.0011	0.0055	14	0.0007	0.0008	0.0027	14
Chromium (Cr)	0.0008	0.0003	0.0015	14	0.0001	0.0002	0.0006	14
Manganese (Mn)	0.0036	0.0019	0.0066	14	0.0031	0.0012	0.0053	14
Iron (Fe)	0.1297	0.0623	0.2448	14	0.1562	0.0393	0.2419	14
Cobalt (Co)	0.0013	0.0006	0.0024	14	0.0005	0.0003	0.0011	14
Nickel (Ni)	0.0011	0.0005	0.0019	14	0.0004	0.0002	0.0007	14
Copper (Cu)	0.0014	0.0006	0.0027	14	0.0011	0.0009	0.0036	14
Zinc (Zn)	0.0005	0.0005	0.0016	14	0.0086	0.0028	0.0160	14
Gallium (Ga)	0.0015	0.0008	0.0034	14	0.0005	0.0006	0.0017	14
Arsenic (As)	0.0002	0.0003	0.0013	14	0.0007	0.0005	0.0019	14
Selenium (Se)	0.0016	0.0006	0.0022	14	0.0003	0.0003	0.0010	14
Bromine (Br)	0.0019	0.0008	0.0030	14	0.0028	0.0010	0.0044	14
Rubidium (Rb)	0.0001	0.0001	0.0003	14	0.0006	0.0004	0.0013	14
Strontium (Sr)	0.0017	0.0006	0.0028	14	0.0014	0.0010	0.0040	14
Yttrium (Yt)	0.0004	0.0002	0.0008	14	0.0002	0.0002	0.0006	14
Zirconium (Zr)	0.0008	0.0007	0.0027	14	0.0006	0.0004	0.0014	14
Molybdenum (Mo)	0.0004	0.0004	0.0010	14	0.0012	0.0008	0.0031	14
Palladium (Pd)	0.0074	0.0037	0.0154	14	0.0041	0.0031	0.0128	14
Silver (Ag)	0.0088	0.0052	0.0175	14	0.0053	0.0039	0.0129	14
Cadmium (Cd)	0.0081	0.0046	0.0174	14	0.0044	0.0035	0.0132	14
Indium (In)	0.0008	0.0017	0.0050	14	0.0050	0.0039	0.0141	14
Tin (Sn)	0.0126	0.0067	0.0257	14	0.0115	0.0072	0.0290	14
Antimony (Sb)	0.0037	0.0043	0.0147	14	0.0072	0.0047	0.0152	14
Barium (Ba)	0.0008	0.0017	0.0051	14	0.0515	0.0182	0.0813	14
Lanthanum (La)	0.0133	0.0133	0.0376	14	0.0174	0.0110	0.0363	14
Gold (Au)	0.0036	0.0010	0.0054	14	0.0014	0.0009	0.0028	14
Mercury (Hg)	0.0013	0.0009	0.0033	14	0.0007	0.0005	0.0016	14

Table 3-7 (continued)
Statistical Summary of 24-hour $PM_{2.5}$ Measurements Between 7/13/90 and 8/24/90
During the Fourteen SJVAQS/AUSPEX Episode Days

Average Chemical Species (μg/m³)	Blodgett Average Standard (μg/m³) (μg/m³)	Blodgett Std. Dev. Maximum (μg/m³) (μg/m³)	Blodgett Maximum No. in (μg/m³) Average	Blodgett No. in Average	Yosemite Average (μg/m³)	Yosemite Std. Dev. (μg/m³)	Yosemite Maximum (μg/m³)	Yosemite No. in Average
Thallium (Tl)	0.0001	0.0002	0.0006	14	0.0002	0.0003	0.0009	14
Lead (Pb)	0.0054	0.0016	0.0075	14	0.0032	0.0016	0.0054	14
Uranium (Ur)	0.0009	0.0004	0.0018	14	0.0006	0.0004	0.0015	14
Nylon Backup NO_3^-	0.1145	0.1516	0.6064	14	0.1045	0.0745	0.2359	14
Nitric Acid plus NO_3^-	0.9079	0.3056	1.4658	14	3.5830	3.6672	14.1746	14
Nitric Acid (HNO_3)	0.8063	0.2771	1.3432	14	3.3131	3.7594	14.1736	14
Sulfur Dioxide (SO_2)	0.2967	0.2535	0.8681	14	0.6680	0.5500	1.5696	14
Ammonia (NH_3)	0.3381	0.1477	0.6194	14	1.6415	1.1752	3.0741	14

Table 3-8
Statistical Summary of 24-hour PM_{10} Measurements Between 7/13/90 and 8/24/90

Chemical Species	Yosemite Average (µg/m³)	Yosemite Std. Dev. (µg/m³)	Yosemite Maximum (µg/m³)	Yosemite No. in Average	Sequoia Lower Keweah Average (µg/m³)	Sequoia Lower Keweah Std. Dev. (µg/m³)	Sequoia Lower Keweah Maximum (µg/m³)	Sequoia Lower Keweah No. in Average
Mass	23.29	13.23	49.73	14	21.14	3.45	25.91	14
Chloride (Cl^-)	0.0786	0.0819	0.3320	14	0.0012	0.0027	0.0096	14
Nitrate (NO_3^-)	0.3142	0.2207	0.8164	14	0.6872	0.2572	1.1906	14
Sulfate ($SO_4^=$)	1.8653	0.4635	2.5996	14	1.8892	0.6349	3.1373	14
Ammonium (NH_4^+)	0.6368	0.1694	0.8615	14	0.7807	0.2371	1.2354	14
Soluble Sodium (Na^+)	0.1282	0.1174	0.4158	14	0.1083	0.0504	0.2240	14
Soluble Potassium (K^+)	0.0860	0.0529	0.2009	14	0.1115	0.0366	0.1703	14
Organic Carbon (OC)	10.2319	5.3599	22.2803	14	5.2116	1.2930	7.3106	14
Elemental Carbon (EC)	1.7237	1.0922	4.2126	14	1.9607	0.5695	3.2606	14
Aluminum (Al)	1.1203	0.3256	1.8214	14	1.1355	0.2599	1.7672	14
Silicon (Si)	2.6386	0.6958	4.0380	14	2.9233	0.7102	4.6309	14
Phosphorus (P)	0.0016	0.0039	0.0143	14	0.0018	0.0037	0.0119	14
Sulfur (S)	0.8555	0.1924	1.1619	14	1.1024	0.2973	1.6094	14
Chlorine (Cl)	0.0426	0.1430	0.5580	14	0.0086	0.0123	0.0456	14
Potassium (K)	0.3797	0.1030	0.5832	14	0.4525	0.0898	0.5819	14
Calcium (Ca)	0.2733	0.1012	0.5526	14	0.2994	0.0634	0.4396	14
Titanium (Ti)	0.0472	0.0142	0.0794	14	0.0434	0.0169	0.0712	14
Vanadium (V)	0.0019	0.0011	0.0038	14	0.0010	0.0006	0.0020	14
Chromium (Cr)	0.0004	0.0004	0.0017	14	0.0008	0.0004	0.0015	14
Manganese (Mn)	0.0130	0.0037	0.0212	14	0.0137	0.0027	0.0176	14
Iron (Fe)	0.5539	0.1419	0.8350	14	0.5270	0.1117	0.7874	14
Cobalt (Co)	0.0003	0.0004	0.0012	14	0.0004	0.0003	0.0011	14
Nickel (Ni)	0.0006	0.0003	0.0012	14	0.0009	0.0006	0.0025	14
Copper (Cu)	0.0021	0.0012	0.0045	14	0.0130	0.0048	0.0227	14
Zinc (Zn)	0.0115	0.0020	0.0148	14	0.0143	0.0038	0.0251	14
Gallium (Ga)	0.0005	0.0006	0.0022	14	0.0006	0.0006	0.0020	14
Arsenic (As)	0.0014	0.0007	0.0027	14	0.0013	0.0005	0.0020	14
Selenium (Se)	0.0004	0.0002	0.0010	14	0.0006	0.0003	0.0011	14
Bromine (Br)	0.0038	0.0011	0.0059	14	0.0062	0.0013	0.0091	14
Rubidium (Rb)	0.0014	0.0005	0.0022	14	0.0013	0.0003	0.0020	14
Strontium (Sr)	0.0034	0.0016	0.0074	14	0.0031	0.0009	0.0048	14
Yttrium (Yt)	0.0004	0.0003	0.0008	14	0.0005	0.0003	0.0013	14
Zirconium (Zr)	0.0010	0.0005	0.0023	14	0.0009	0.0006	0.0018	14
Molybdenum (Mo)	0.0007	0.0004	0.0016	14	0.0009	0.0006	0.0017	14
Palladium (Pd)	0.0053	0.0032	0.0097	14	0.0048	0.0021	0.0088	14
Silver (Ag)	0.0089	0.0051	0.0176	14	0.0077	0.0041	0.0159	14
Cadmium (Cd)	0.0068	0.0051	0.0176	14	0.0056	0.0031	0.0112	14
Indium (In)	0.0054	0.0061	0.0240	14	0.0061	0.0039	0.0152	14
Tin (Sn)	0.0081	0.0062	0.0252	14	0.0050	0.0045	0.0146	14
Antimony (Sb)	0.0060	0.0044	0.0136	14	0.0064	0.0047	0.0151	14
Barium (Ba)	0.0531	0.0179	0.1052	14	0.0326	0.0230	0.0757	14
Lanthanum (La)	0.0286	0.0202	0.0774	14	0.0221	0.0195	0.0734	14
Gold (Au)	0.0009	0.0009	0.0033	14	0.0017	0.0010	0.0036	14
Mercury (Hg)	0.0004	0.0004	0.0013	14	0.0003	0.0003	0.0008	14

Table 3-8 (continued)
Statistical Summary of 24-hour PM_{10} Measurements Between 7/13/90 and 8/24/90

Chemical Species	Yosemite Average (µg/m³)	Yosemite Std. Dev. (µg/m³)	Yosemite Maximum (µg/m³)	Yosemite No. in Average	Sequoia Lower Keweah Average (µg/m³)	Sequoia Lower Keweah Std. Dev. (µg/m³)	Sequoia Lower Keweah Maximum (µg/m³)	Sequoia Lower Keweah No. in Average
Thallium (Tl)	0.0012	0.0007	0.0026	14	0.0011	0.0007	0.0023	14
Lead (Pb)	0.0022	0.0013	0.0042	14	0.0036	0.0018	0.0069	14
Uranium (Ur)	0.0005	0.0004	0.0011	14	0.0004	0.0003	0.0013	14
Nylon Backup NO_3^-	0.1328	0.1102	0.3690	14	0.3191	0.2190	0.6695	14
Nitric Acid plus NO_3^-	0.0000	0.0000	0.0000	14	0.0000	0.0000	0.0000	14
Nitric Acid (HNO_3)	0.0000	0.0000	0.0000	14	0.0000	0.0000	0.0000	14
Sulfur Dioxide (SO_2)	0.0000	0.0000	0.0000	14	0.0000	0.0000	0.0000	14
Ammonia (NH_3)	0.0000	0.0000	0.0000	14	0.0000	0.0000	0.0000	14

on the quartz-fiber filters so that the values will be comparable to those found in the other monitoring network. Volatilized nitrate form the nylon backup filters, as well as gaseous concentrations of nitric acid, ammonia, and sulfur dioxide are also presented in Table 3-7.

The maximum 24-hour average PM_{10} concentration was 49.7 $\mu g/m^3$ found at the Yosemite site on August 23, 1990, with the highest diurnal concentration (77.4 $\mu g/m^3$) occurring during the morning period (0700 to 1200 PDT) and the second highest concentrations (70.6 $\mu g/m^3$) occurring after midnight (0000 to 0700 PDT).

Organic carbon, elemental carbon, sulfate, aluminum, and silicon are the major components of PM_{10} which account for 75% of the average PM_{10} mass at the Yosemite site and 62% of the average PM_{10} mass at the Sequoia site. PM_{10} organic carbon is the single largest component and accounts for 43% of the average PM_{10} mass at the Yosemite site and 25% of the average PM_{10} mass at the Sequoia site. These averages are biased high at the Yosemite site owing to the occurrence of the forest fire during August 22 to 24, 1990.

Maximum 24-hour average PM_{10} organic carbon of 22.3 $\mu g/m^3$ was found at the Yosemite site on August 23, 1990; with the highest diurnal concentration (39.9 $\mu g/m^3$) occurring during the morning (0700 to 1200 PDT) and the second highest concentrations (30.1 $\mu g/m^3$) occurring after midnight (0000 to 0700 PDT). Besides the organic carbon, PM_{10} average concentrations for other species appear to be similar between the two sites.

Table 3-7 shows that the maximum 24-hour average $PM_{2.5}$ mass concentration of 38.0 $\mu g/m^3$ was also found at the Yosemite site on August 22, 1990; with the highest diurnal concentration (66.1 $\mu g/m^3$) occurring during the morning (0700 to 1200 PDT) and the second highest concentration (58.7 $\mu g/m^3$) occurring after midnight (0000 to 0700 PDT).

The average $PM_{2.5}$ concentrations were highest (15.7 ± 9.8 $\mu g/m^3$) at the Yosemite site, which is 40 to 50% higher than the averages at the Tehachapi and Sequoia sites, and nearly a factor of 2.6 higher than the average at the Blodgett site.

As expected, organic carbon, elemental carbon, sulfate, nitrate, and ammonium are the major components of $PM_{2.5}$ fraction. The largest variation was found for average PM_{10} organic carbon concentrations. It varied from 0.7 ± 0.5 $\mu g/m^3$ at the Blodgett site, to 2.1 ± 2.3 $\mu g/m^3$ at the Tehachapi site, to 5.3 ± 1.2 $\mu g/m^3$ at the Sequoia site, and to 11.9 ± 6.1 $\mu g/m^3$ at the Yosemite site.

Average and maximum $PM_{2.5}$ mass and chemical compositions at the Blodgett site were at least a factor of 2 lower than the other sites. During the study, the maximum 24-hour $PM_{2.5}$ concentrations were found: at the Tehachapi site for nitrate (3.1 $\mu g/m^3$); at the Tehachapi and Sequoia Lower Keweah site for sulfate (3.1 $\mu g/m^3$) and ammonium (1.2 $\mu g/m^3$), and at the Yosemite site for organic carbon (25.8 $\mu g/m^3$) and elemental carbon (3.5 $\mu g/m^3$).

Table 3-7 also reports a statistical summary for gaseous sulfur dioxide, ammonia, and nitric acid concentrations. Average sulfur dioxide concentrations varied form 3.5 ± 1.2 $\mu g/m^3$ at the Tehachapi site, to 3.3 ± 0.5 $\mu g/m^3$ at the Sequoia Lower Keweah site, to 1.6 ± 1.2 $\mu g/m^3$ at the Yosemite site, and to 0.34 ± 0.15 $\mu g/m^3$ at the Blodgett site.

Similar trends were found for ammonia at these four sites. While the average ammonia concentrations at the Tehachapi site (3.5 ± 1.2 $\mu g/m^3$) were similar to the average in the Sequoia Lower Keweah site (3.3 ± 0.5 $\mu g/m^3$); it is a factor of 2 to 10 higher than the averages found at the Yosemite and Blodgett site.

Average nitric acid concentrations also rank highest at the Tehachapi site (4.7 ± 1.9 $\mu g/m^3$), which was 30% and 60% higher than averages observed at the Yosemite and Sequoia Lower Keweah site, respectively, and a factor of 6 higher than the averages at the Blodgett site.

3.5 Temporal and Spatial Variations in $PM_{2.5}$ and PM_{10}

Figures 3-6a and 3-6b illustrated the sample-to-sample variation in $PM_{2.5}$ and PM_{10} at the Yosemite and Sequoia sites, and in $PM_{2.5}$ at the Blodgett and Tehachapi sites during the 14 episode days. The first noticeable feature is that PM_{10} particle concentrations from August 22 to 24, 1990, are two to three times higher at the Yosemite site with respect to the other sites. These elevated concentrations, especially in the $PM_{2.5}$ fraction, resulted from the forest fire in the Yosemite National Park during that period. The second noticeable features is that more than 50% of PM_{10} mass is in the $PM_{2.5}$ fraction at the Yosemite and Sequoia sites. Excluding the fire episode, the $PM_{2.5}$ and coarse particle (PM_{10} minus $PM_{2.5}$) concentrations are generally low at both sites.

With a few exceptions, $PM_{2.5}$ masses at the Yosemite site followed a diurnal cycle during the summer. The highest $PM_{2.5}$ mass concentrations were found during the morning period (0700 to 1300 PDT), and decreased in the afternoon (1200 to 1700 PDT). Coarse particle concentrations were elevated during daytime with respect to nighttime, especially in the afternoon. The diurnal cycles are most significant during the August episode, while concentrations in the early morning (0000 to 0700 PDT) samples are three to four times higher than the afternoon (1200 to 1700 PDT) and nighttime (1700 to 2400 PDT) samples. It is suspected that the surface radiation inversion are pronounced after midnight and last through the

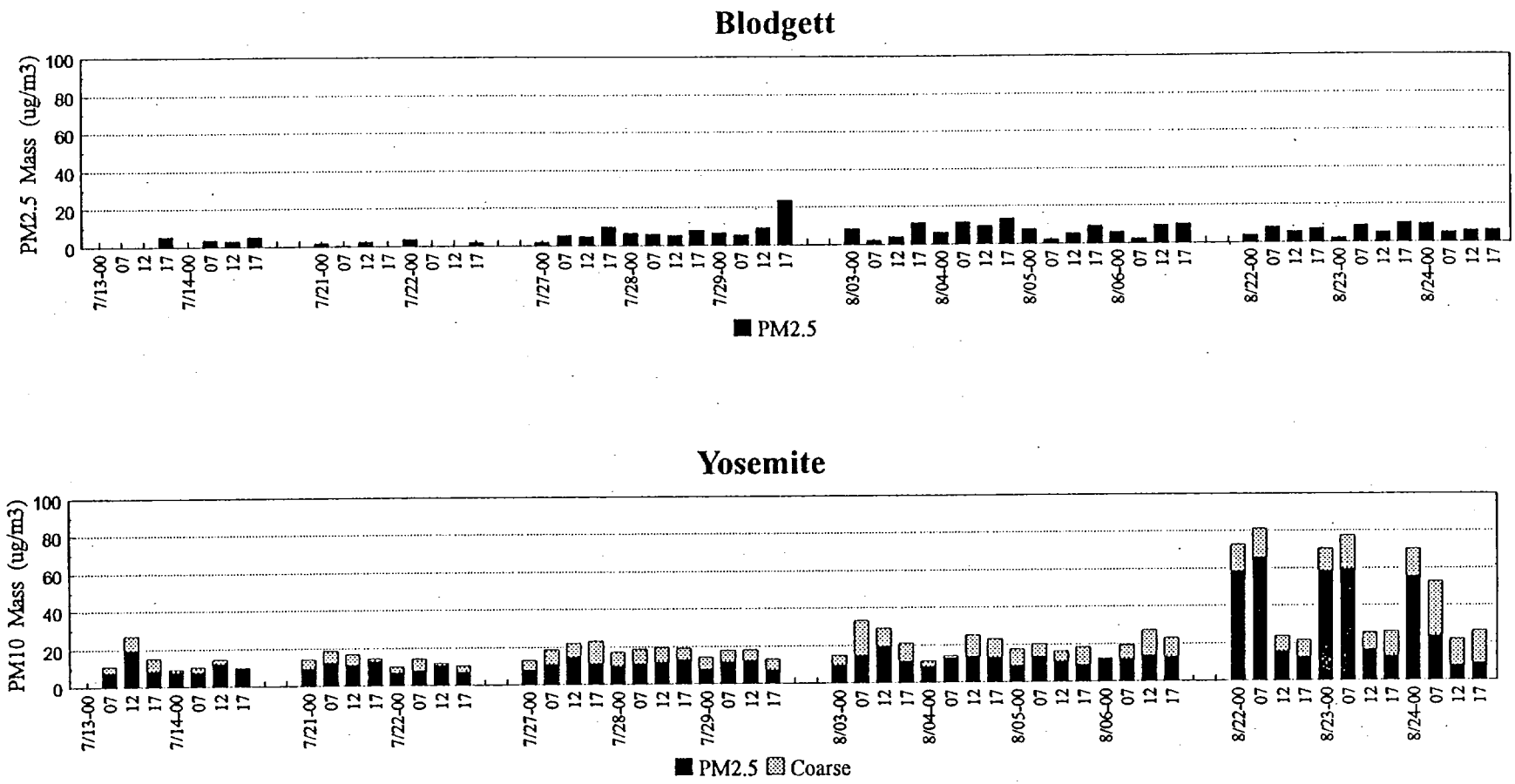

Figure 3-6a. Time Series Plot of $PM_{2.5}$ and PM_{10} Mass at the Blodgett and Yosemite Sites.

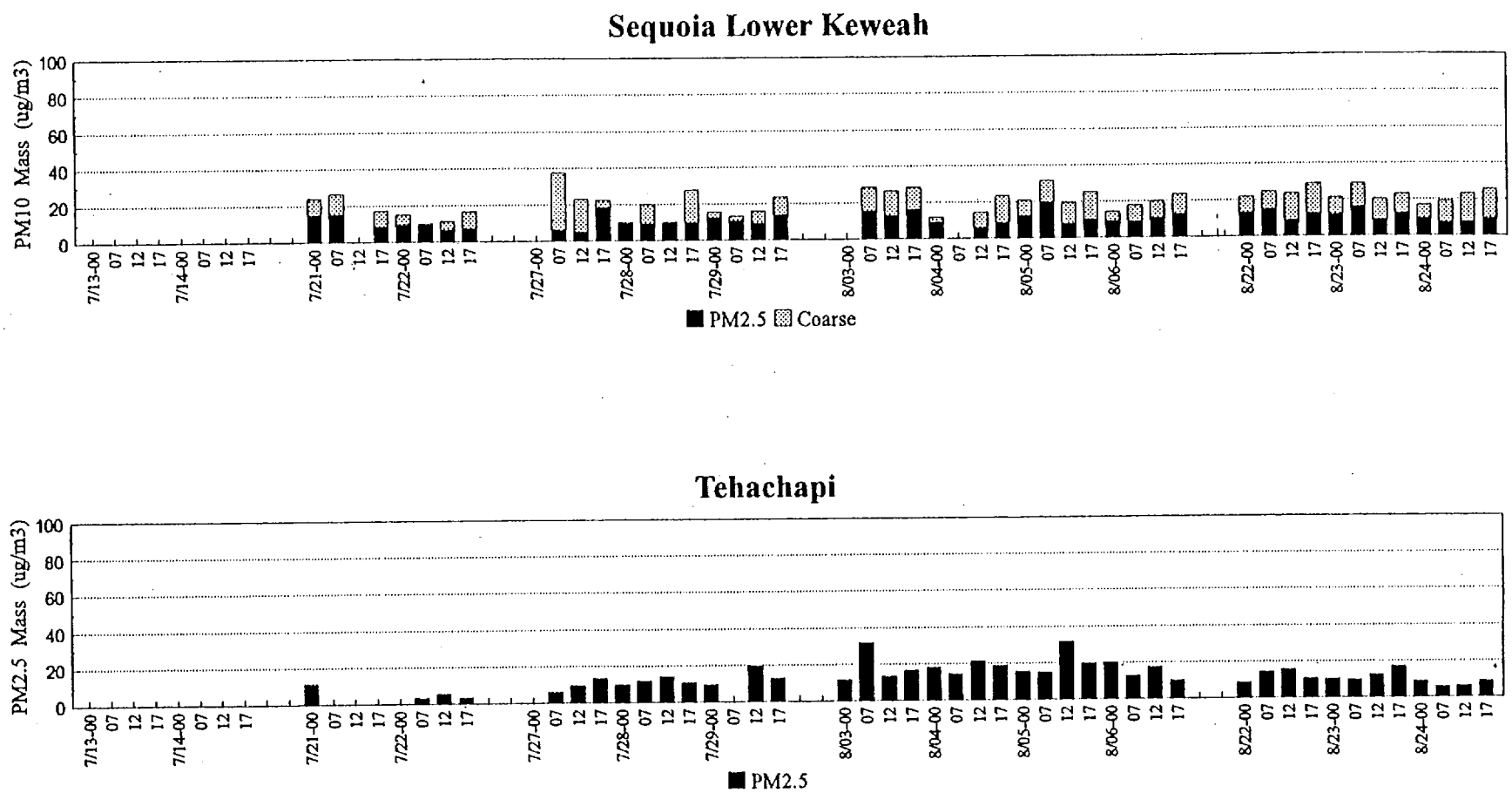

Figure 3-6b. Time Series Plot of $PM_{2.5}$ and PM_{10} Mass at the Sequoia Lower Keweah and Tehachapi Sites.

morning period. Less prevalent diurnal variations of the $PM_{2.5}$ and PM_{10} mass were found at the Sequoia Lower Keweah site, with slightly higher concentrations observed during the morning (0700 to 1200 PDT) samples.

$PM_{2.5}$ mass concentrations are generally very low through the 14 episode days with a few excursions found after dawn (1700 to 2400 PDT). Variations in $PM_{2.5}$ mass concentrations are less pronounced at the Tehachapi site with respect to other sites.

3.6 Temporal Variations of Particulate Nitrate, Nitric Acid, Particulate Ammonium, and Ammonia

Figures 3-7a and 3-7b show how three types of nitrate compounds vary form sample to sample. The bottom bar represents the $PM_{2.5}$ nitrate (non-volatilized nitrate) on quartz-fiber filters, the height of the middle bar represents $PM_{2.5}$ total particulate nitrate (non-volatilized plus volatilized nitrate), and the height of all the bars represents the sum of gaseous nitric acid and $PM_{2.5}$ total particulate nitrate. Note that most of the samples consist of a combination of nitric acid, volatilized, and non-volatilized particulate nitrate, but their relative proportions vary among sampling sites and time of day.

The outstanding feature of these plots is the variation in the sum of the gaseous nitric acid and $PM_{2.5}$ total particulate nitrate. With a few exceptions at the Yosemite site, this sum was much greater at the Tehachapi site, with respect to the other sites. The sum of the nitric acid and nitrate concentrations are generally low ($< 4\ \mu g/m^3$) at the Sequoia and Blodgett sites. Nitric acid concentrations increased form midnight to the morning period (0700 to 2400 PDT) and peaked during daytime, and gradually decreased after dawn (1700 to 2400 PDT). Large excursions of nitric acid concentrations were found during daytime at the Yosemite site on July

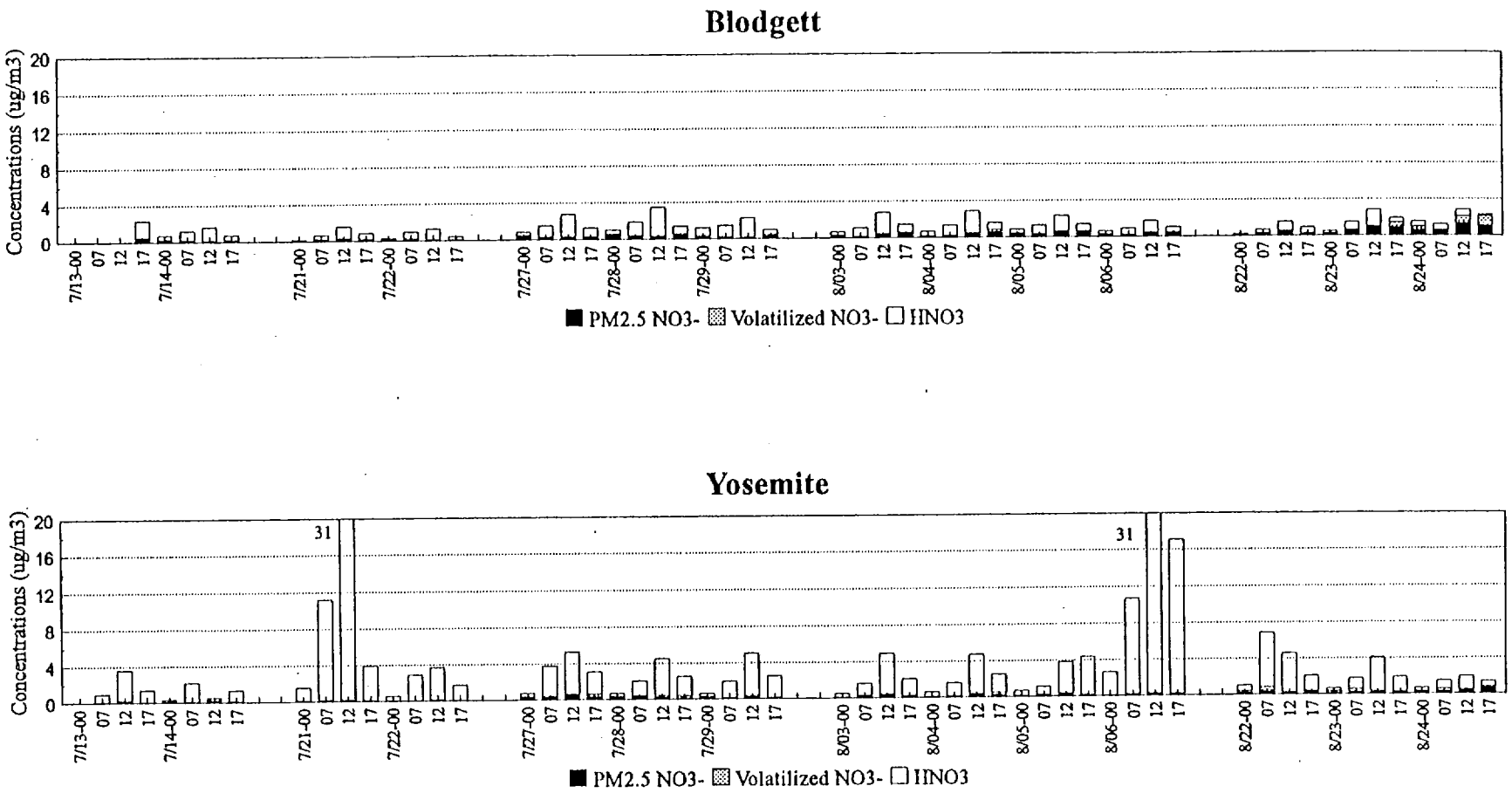

Figure 3-7a. Time Series Plot of $PM_{2.5}$ Nitrate, Volatidized Nitrate, and Nitric Acid at the Blodgett and Yosemite sites.

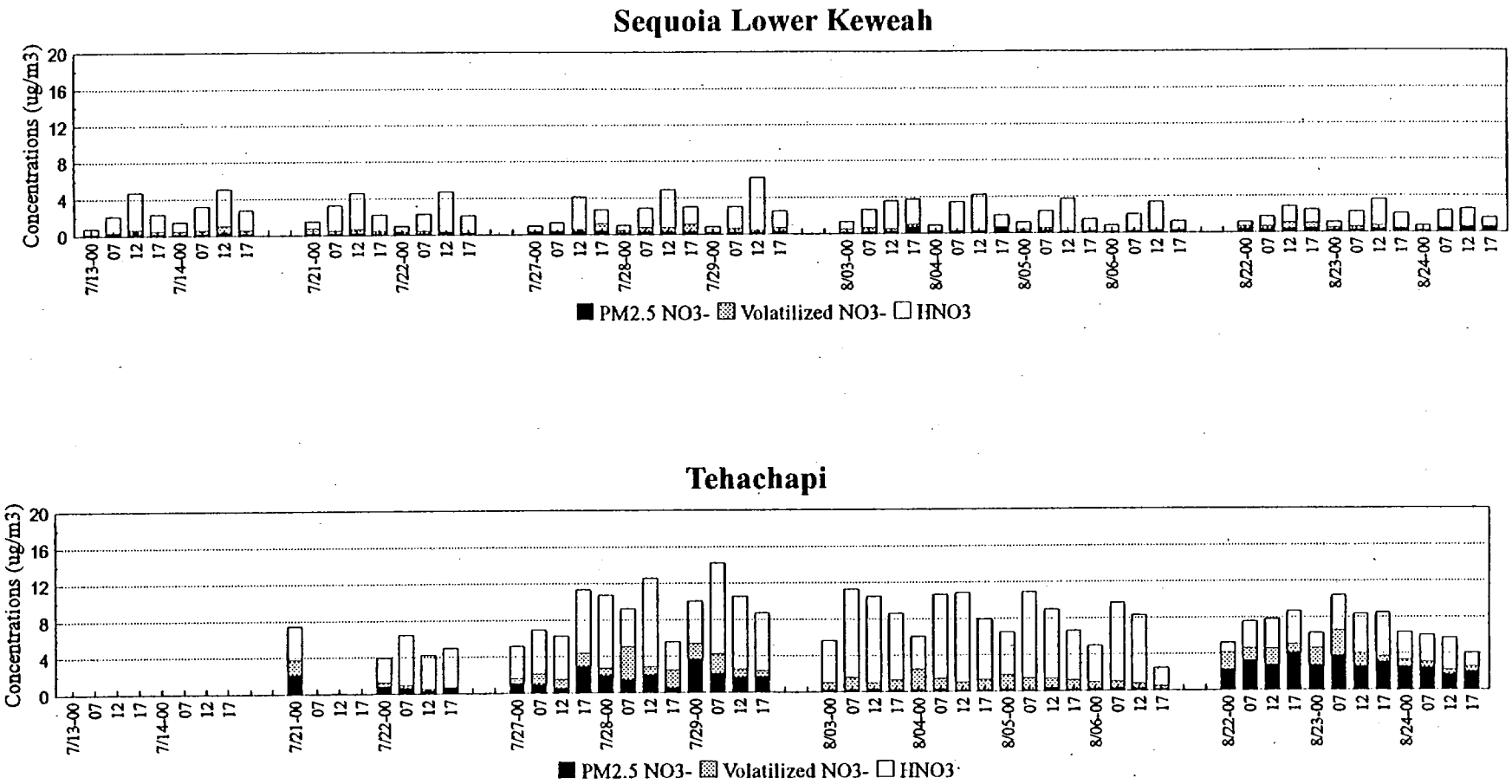

Figure 3-7b. Time Series Plot of $PM_{2.5}$ Nitrate, Volatidized Nitrate, and Nitric Acid at the Sequoia Lower Keweah and Tehachapi Sites.

21 and August 6, 1990, while afternoon nitric acid concentrations reached 31 and 30$\mu g/m^3$. $PM_{2.5}$ volatilized and non-volatilized nitrate are only less than 25% of the corresponding nitric acid concentrations at all three sites. Volatilized nitrate levels are mostly higher during the daytime whereas non-volatilized nitrate concentrations (generally in 1 to 3 $\mu g/m^3$ range) varied from sample to sample. Nitrate compounds tend more toward volatilized nitrate and nitric acid phases during the daytime and toward the particulate phase during the nighttime. This is consistent with the diurnal changes in equilibrium which correspond to diurnal changes in temperature.

Analogous time series were found for gaseous ammonia and $PM_{2.5}$ ammonium in Figure 3-8a and 3-8b. Both ammonia and ammonium concentrations were low at the Blodgett site ($<$ 1$\mu g/m^3$) throughout the study period. While the particulate ammonium concentrations were low ($\leq$ 1$\mu g/m^3$) at the Yosemite, Sequoia Lower keweah, and Tehachapi sites, ammonia concentrations reached 10 $\mu g/m^3$ during afternoon (1200 to 1700 PDT) on August 5, 1990 at the Tehachapi site. Ammonia concentrations followed the similar pattern with respect to nitrate compounds, with higher gaseous ammonia and $PM_{2.5}$ ammonium concentrations at the Tehachapi site. Diurnal patterns of ammonia concentrations were not as distinguished as nitric acid levels, usually low in the early morning, and peaks from mid-morning to afternoon.

3.7 Temporal Variations of Organic and Elemental Carbon

Time series plot of $PM_{2.5}$ organic and elemental carbon are shown in Figures 3-9a and 3-9b for the four sites during the 14 episode days. The height of the bar in this figure represents the total carbon (i.e., total non-carbonate carbon, sum of organic and elemental carbon). Total

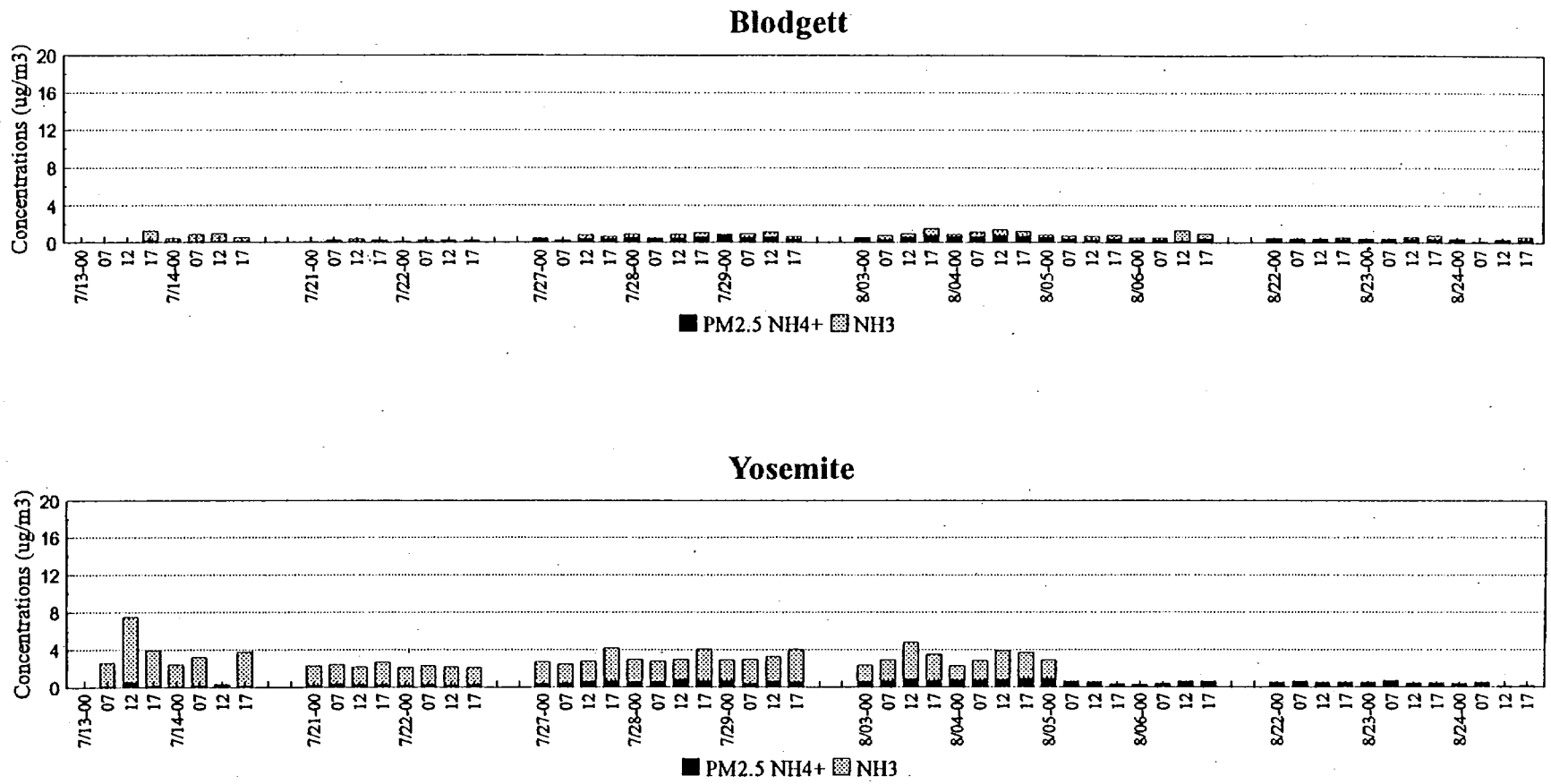

Figure 3-8a. Time Series Plot of $PM_{2.5}$ Ammonium and Ammonia at the Blodgett and Yosemite Sites.

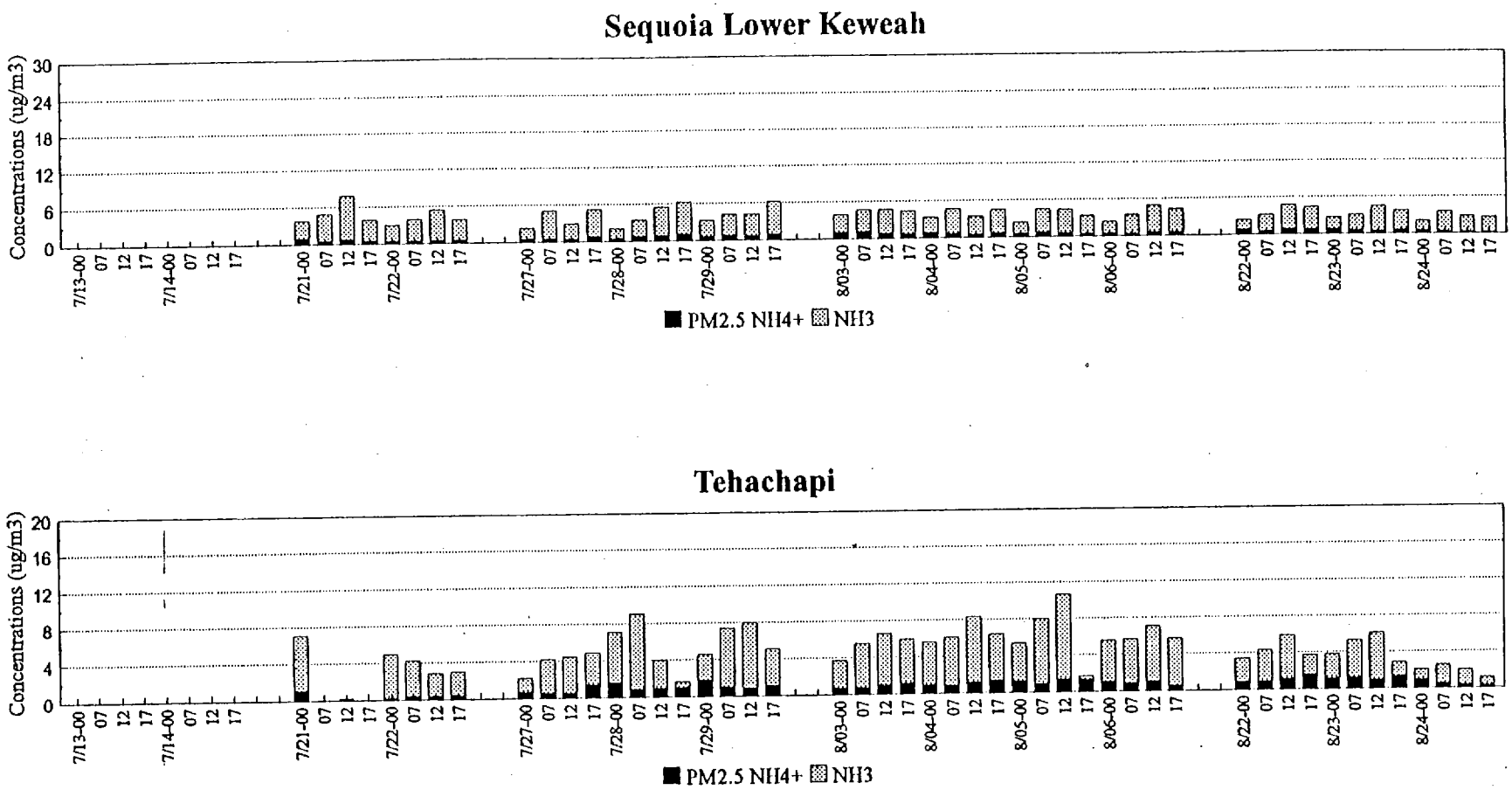

Figure 3-8b. Time Series Plot of $PM_{2.5}$ Ammonium and Ammonia at the Sequoia Lower Keweah and Tehachapi Sites

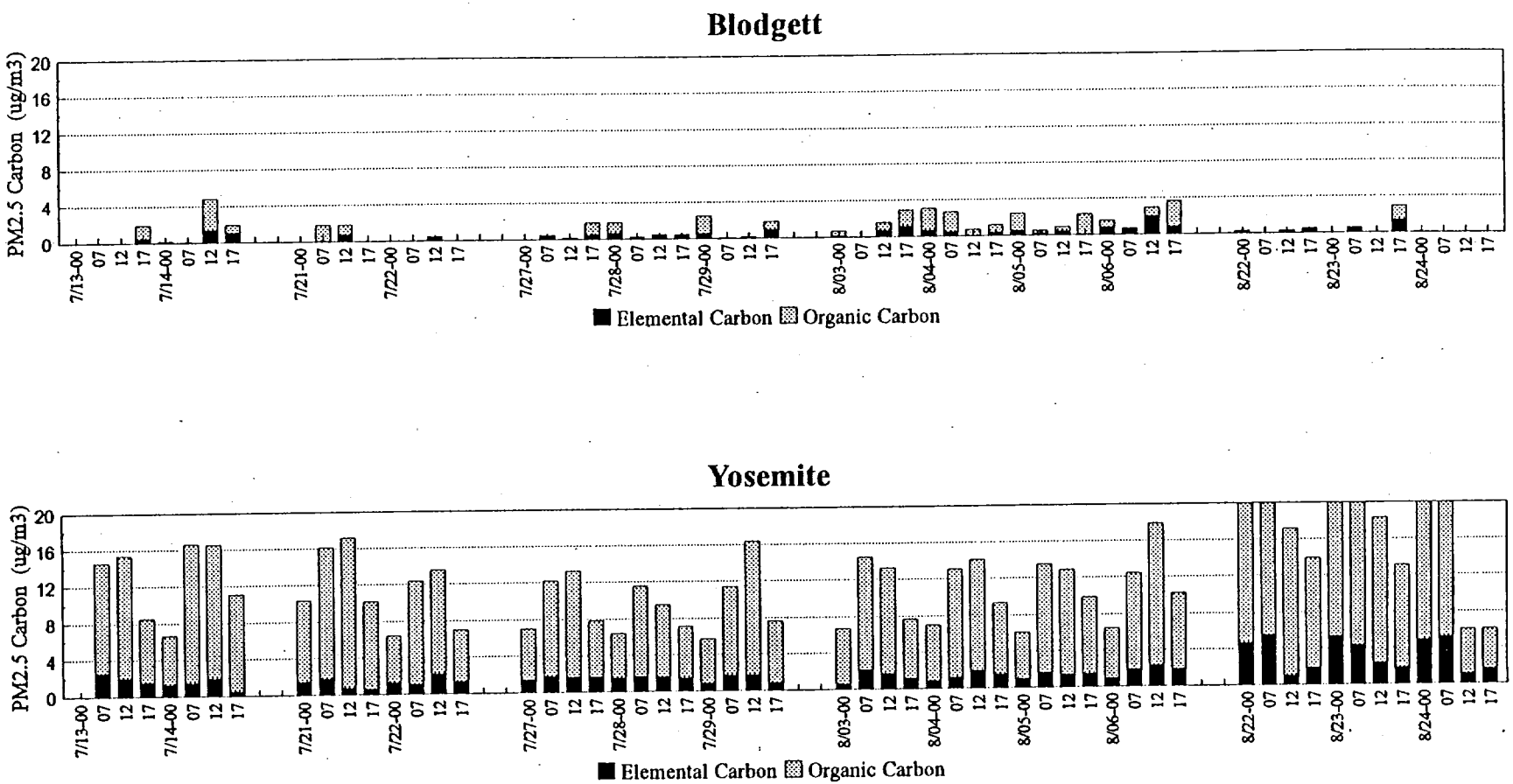

Figure 3-9a. Time Series of $PM_{2.5}$ Organic and Elemental Carbon at the Blodgett and Yosemite Sites.

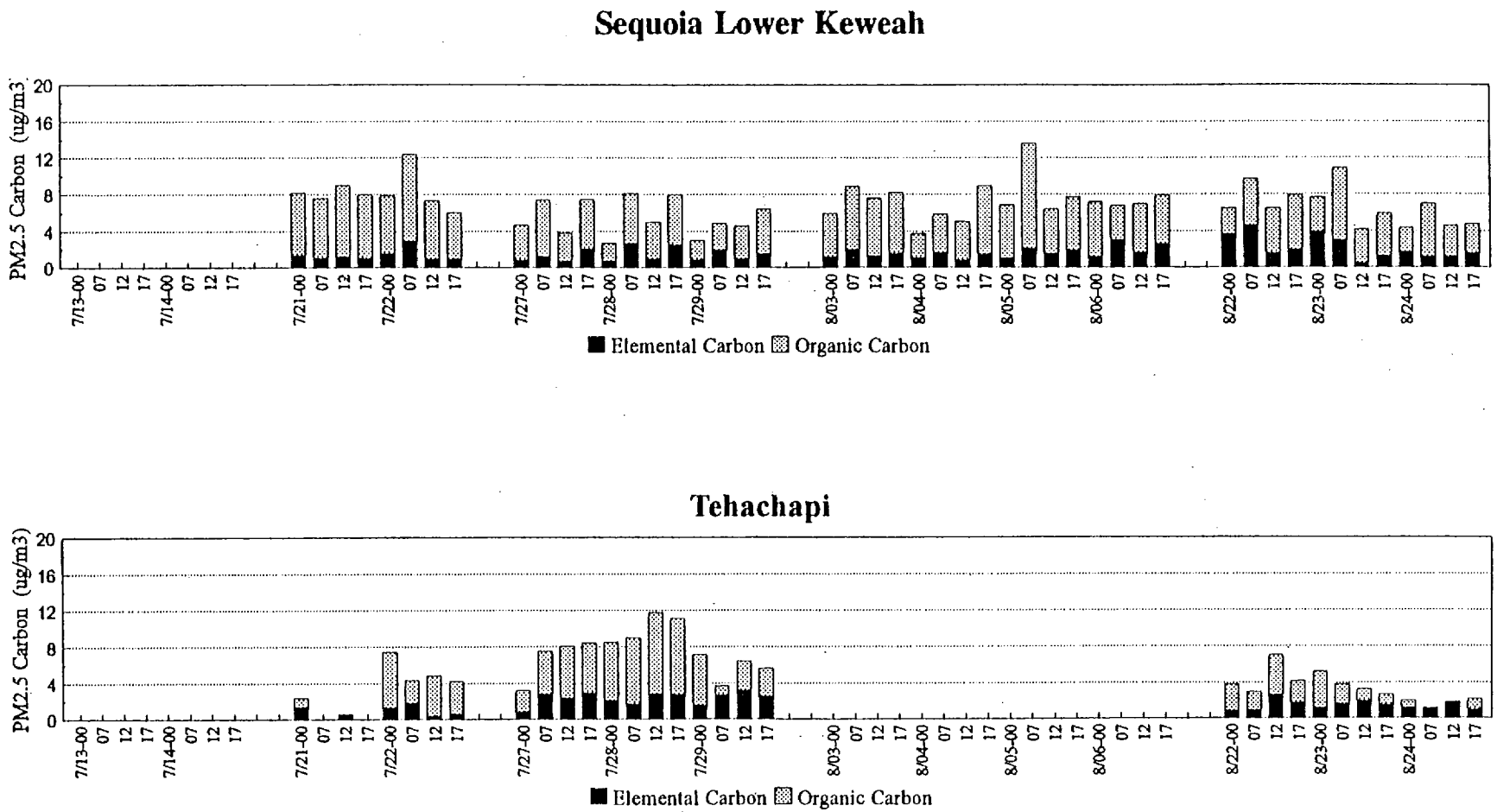

Figure 3-9b. Time Series of $PM_{2.5}$ Organic and Elemental Carbon at the Sequoia Lower Keweah and Tehachapi Sites.

carbon levels at the Yosemite site were 25% to 50% higher than the Sequoia Lower Keweah and Tehachapi sites site, and 3 to 4 times higher than the Blodgett site. Elemental carbon, (i.e., light absorbing carbon) constituted less than 15% of the total carbon among all three sites. While organic carbon concentrations tended to increase during the day, peaked during daylight samples, elemental carbon tended to vary less significantly between the day and night. This phenomenon was mostly pronounced at the Yosemite site where forest fires significantly increased the carbon concentrations. The highest carbon concentrations (49.2 $\mu g/m^3$) occurred during the morning (0700 to 1200 PDT) of August 22, 1990.